Role of Neuropilin-1 in CD8+ T cells



Mike Bogetofte Barnkob

Linacre College

University of Oxford

A thesis submitted for the degree of

Doctor of Philosophy

Trinity 2018

To Hannah and Helle.

Acknowledgements

”If your career as a scientist fails, you can always become a comedian.”
Professor Wendy Bickmore, Director of the MRC Human Genetics Unit, University of Edinburgh.

This sound advice was given to me following a talk I gave, and I have since taken Professor Bickmore’s words to heart. Science should be fun, and luckily, I have been extremely fortunately to be surrounded by entertaining, lively and amusing colleagues and friends throughout my DPhil and time in Oxford.

First and foremost, I would like to thank Professor Vincenzo Cerundolo for taking me onboard. The academic freedom and intellectual challenges allowed in the Cerundolo lab is incredibly liberating and has given me opportunities that I will cherish for the rest of my life. In his book, The Periodic Table, Primo Levi describes the exalting feeling of conducting experiments: “Ours are the two experiences of adult life of which Pavese spoke, success and failure, to kill the white whale or wreck the ship; one should not surrender to incomprehensible matter, one must not just sit down. We are here for this – to make mistakes and to correct ourselves, to stand the blows and hand them out”. Of failures, there have been multiple, but Enzo has guided me through most – importantly, I have been allowed to make them, repeatedly, and always been meet with understanding and support. For that I am extremely grateful. I am also quite happy to have been allowed to put up a large inflatable shark, alien, spaceship, monkey and a dinosaur in the lab.

Secondly, my time in Oxford has been shaped by the wonderful students and researchers in the Cerundolo lab: to Violaine, Andreas, Lauren, Margarida, Uzi, Corinna, Rosie, Melissa, Gennaro, Victoria, Rui and Nazish, thanks for all the laughs, your intellectual input and for your friendship. I must also thank Mariolina, Jili, Uzi and Giorgio for continuously answering my many questions about experiments and reagents: your combined wisdom is truly amazing. Anne Farmer for always knowing what to do. Prathiba, Claudia and Laura for helping to bringing some structure to an often chaotic work-

place.

This thesis would have been impossible without valuable input and help from multiple collaborators: primarily Violaine and Yale, who taught me about CRISPR/Cas9 and how to have a good time. Friendship is a strong HDR donor and I have truly enjoyed our camaraderie which I hope will continue many years still. Tudor A. Fulga for our many chats about life in science and for coming up with exciting new ideas. Simon Davis for always having an open door, answering my questions and forcing me to decide if this project had legs or not. Marco Fritzsche and Huw Colin-York for teaching me about actin and the extremely small. Philip Macklin for teaching me about pathology and the large. Chris Lagerholm for being the most helpful person alive and teaching me how to use a microscope. Mike Dustin for his sense of detail and allowing me into his lab. Salvo for being an amazing friend and fellow YouTube star. Yvonne Jones for continued guidance and invaluable input concerning semaphorins and reagents without which the work presented here would have been impossible. Youxin and Vitul for introducing me to structural biology and to Chinese science fiction. Marella de Bruijn for believing in me. Lars R. Olsen for teaching me about bioinformatics and specialty coffee.

Outside the lab, I have been incredibly lucky to have been supported by my family and close friends. My old mentor Pete Bak, who first taught me about immunology, science and how to enjoy an IPA, has been with me throughout the PhD through his many words of wisdom. Courtney and Tyler for amazing times in our little hippie-collective. To Mum and Dad for accepting that moving to another country was something I needed to do and understanding when I couldn't make it to all the family events.

Finally, for providing immense support, friendship and love throughout the entire DPhil, I cannot thank my wife Helle enough. She has kept me sane, helped me crystallize my thinking, distracted me when necessary and always accepted the frenzied lifestyle of a lab monkey. Our time in Oxford has been an amazing journey that you accepted from the beginning and for that I am eternally grateful. I am particularly excited about our at-home single-cell experiment which started in Oxford, and now, approximately 10^{15} cells later[1], seems to be turning out quite well.

[1] This is based on the assumption that one cell weighs approximately 10^{-11} gram.

Abstract

Role of Neuropilin-1 in CD8+ T cells

Mike Bogetofte Barnkob, Linacre College

Submitted for the degree of Doctor of Philosophy, Michaelmas 2018.

A major limiting factor in anti-tumour immunity is the ability of T cells to infiltrate and function in the suppressive tumour microenvironment.

Semaphorins are a family of secreted and membrane-bound proteins that act as guidance cues in neurons and endothelial cells during development. By multimerizing heterodimers of neuropilin-1 (NRP1):plexin A receptors semaphorins strongly affect the F-actin cytoskeleton. Since many developmental programs are up-regulated in cancer cells, we hypothesized that tumours would hijack this physiological process to hamper immune responses.

In tumour-specific T cells, we found that NRP1 was up-regulated *in vitro* and *in vivo* upon activation. To directly interrogate the role of Semaphorin 3A (Sema3A) in modulating T cell functions, we performed two complementary lines of research:

1. *In vivo*, we evaluated the role of NRP1 in T cell—tumour immunity by generating a T cell conditional knockout of NRP1
2. *In vitro*, we assessed the ability of Sema3A to modulate T cell survival, migration, adhesion and immunological synapse formation.

We demonstrated that mice lacking expression of NRP1 on T cells control the growth of transplantable tumours cell-lines. We showed that addition of Sema3A affects T cell migration and adhesion. Additionally, we showed an inhibitory effect of Sema3A on peptide MHC:TCR synapse formation. Experiments suggested that these effects were mediated through Myosin IIA hyper-activation.

Finally, we extended these findings to humans, demonstrating that in renal cell cancer a subset of tumour-infiltrating T cells express NRP1. These T cells are most likely newly activated T cells, in the sense that they were more clonal and expressed T cell antigen receptors (TCRs) specific for cancer testis (CT)-antigens. They were also found in close proximity to Sema3A-rich areas.

Taken together, our results provide novel insights into the NRP1/Plexin/Sema3A axis as an important tumour evasion mechanism.

Statement of Authorship

Statement of authorship

I declare that this thesis represents my own work, except where stated below. It has not been submitted for any other degree. The following parts of this thesis have been conducted in collaboration with other researchers:

- Analysis of TCGA data and other publicly available datasets were done in collaboration with Dr. Lars Rønn Olsen[2].
- Corrina Kulicke[3] helped perform Plexin-A1 and Plexin-A2 western blots.
- Recombinant Sema3A and mutant Sema3A reagents were made by Dr. Vitul Jain[4]and Dr. Youxin Kong[3].
- Generatation of S-Flu H7N1 was made by Professor Alain R Townsend[2] and prepared for intranasal infection by Dr. Pramila Rijal[2].
- B16.F10.Ova cell-line was made by Dr. Uzi Gilead[2].
- Lentivirus design, guide design and reagents for CRISPR-Cas9 experiments were made by Yale Michaels[5]. Knockout of cell-lines was performed with Violaine André[2] in collaboration with Yale Michaels[4].

[2]Center for Biological Sequence Analysis, Department of Systems Biology, Technical University of Denmark, Lyngby, Denmark

[3]Medical Research Council Human Immunology Unit, Weatherall Institute of Molecular Medicine, University of Oxford, Oxford, United Kingdom

[4]Division of Structural Biology, Wellcome Centre for Human Genetics, University of Oxford, Oxford, United Kingdom

[5]Weatherall Institute of Molecular Medicine, Radcliffe Department of Medicine, University of Oxford, Oxford, United Kingdom

- The Oxford Biobank collected blood and tumour tissue from renal cell carcinoma patients. Dr. Lisa Browning[6] selected tissue for immunohistochemistry. Autostaining was optimized and done by Leticia Campo[7]. Dr. Philip Macklin[8] performed pathological assessment of images and helped scan them and image analysis was done using a bioinformatic pipeline developed by Joshua A. Bull[9].
- Dr. Salvatore Valvo[10] prepared the reagents, plates and microscope used in supported lipid bilayer experiments. Subsequent image analysis was done using a bioinformatics pipeline developed by Dr. Viveka Mayya[8].
- Dr. Victoria Woodcock[2] and Dr. Margarida Rei[2] made HLA-A2 CT antigen tetramers and helped with staining of cells.

[6]Department of Cellular Pathology, John Radcliffe Hospital, Oxford, United Kingdom
[7]GCP Lab, Department of Oncology, University of Oxford, Oxford, United Kingdom
[8]Nuffield Department of Medicine, University of Oxford, Oxford, United Kingdom
[9]Mathematical Institute, University of Oxford, Oxford, United Kingdom.
[10]Kennedy Institute of Rheumatology, Nuffield Department of Orthopedics, Rheumatology and Musculoskeletal Sciences, University of Oxford, Oxford, United Kingdom.

Contents

Abstract **iv**

Statement of Authorship **vi**

Contents **viii**

List of Figures **xii**

List of Tables **xiv**

List of Abbreviations **xv**

1 Introduction **1**
1.1 There are no more than five musical notes, yet... 2
1.2 T cell response to cancer cells 3
1.3 Cancer cell response to T cells 11
1.4 Neuropilin-1 and class 3 semaphorins 19
1.5 Aim of this thesis 22

2 General Material and Methods **23**
2.1 Cell-lines and their culture 23
2.2 Analysis of publicly available transcriptional data 25
2.3 OT-I T cell protocols 26
2.4 Flow cytometry protocols 28
2.5 Mouse husbandry and handling 31
2.6 RT-qPCR protocol 33
2.7 Western blot protocol 33
2.8 CRISPR/Cas9 editing of cells 34
2.9 Lentiviral transduction of cells 35

2.10 Immunofluorescence staining . . . 35
2.11 Live-cell imaging of cells . . . 36
2.12 Transwell chemotaxis assay . . . 37
2.13 Immunological synapses analysis on supported lipid bilayers . . . 38
2.14 T cell—cancer cell coculture assay . . . 39
2.15 IHC staining of ccRCC sections . . . 40
2.16 CT-tetramer staining . . . 41
2.17 Statistical analysis . . . 42

3 NRP1 is Upregulated on Tumour-specific CD8+ T cells 43
3.1 Introduction . . . 43
3.2 NRP1 is upregulated on OT-I T cells following activation . . . 45
3.3 NRP1 is expressed on tumour-specific OT-I T cells *in vivo* . . . 47
3.4 Activated and tumour-specific OT-I T cells expressed the NRP1 co-receptor Plexin-A1 . . . 49
3.5 NRP1-positive OT-I T cells can bind recombinant Sema3A . . . 52
3.6 Discussion . . . 54

4 NRP1 Deficiency Enhances Anti-tumour Activity of CD8+ T cells 56
4.1 Introduction . . . 56
4.2 NRP1-conditional knockout mice develop normally . . . 57
4.3 NRP1-conditional knockout mice respond similarly to activation . . . 61
4.4 Tumour growth is stunted in mice with NRP1-deficient T cells . . . 66
4.5 Tumour growth is unaffected in NRP1-deficient mice with depleted CD8+ cells . . . 69
4.6 NRP1-deficient CD8+ cells infiltrate tumours more readily . . . 71
4.7 Generation of Sema3A knockout and over-expressing B16.F10.Ova cell lines . . . 72
4.8 Mixed chimera mice with $NRP1^{Flox/+}$ and $NRP1^{Flox/Flox}$ bone-marrows have same phenotype as conditional NRP1-knockout mice . . . 76
4.9 Tumour-specific T cells are inhibited from entering Sema3A-rich tumours 77
4.10 Discussion . . . 79

5 Sema3A is Expressed by Vasculature and Lymphatics in Tumours 81
5.1 Introduction . . . 81
5.2 Sema3A is not expressed by CD4+ or CD8+ effector T cells . . . 82
5.3 Sema3A is weakly expressed by regulatory CD4+CD25+FoxP3+ T cells . 83
5.4 Sema3A is not expressed by B cells, monocytes, DC's or macrophages . . 84

5.5 Sema3A is expressed by vasculature and lymphatics in tumours but not in lymph nodes . . . 85
5.6 Discussion . . . 86

6 Sema3A is a Negative Regulator of T cell Adhesion and Migration 88
6.1 Introduction . . . 88
6.2 T cells are in close proximity to Sema3A rich areas in tumours . . . 90
6.3 Sema3A is a negative regulator of integrin-mediated adhesion . . . 91
6.4 Sema3A negatively affects T cell migration through NRP1 . . . 94
6.5 Sema3A decreases T cell ability to adhere under physiological levels of flow . . . 96
6.6 Sema3A negatively affects T cells chemotaxis through NRP1 . . . 98
6.7 Discussion . . . 99

7 Sema3A Inhibits T cell Synapse Formation by Affecting Actin Dynamics Through Actomyosin II Activity 102
7.1 Introduction . . . 102
7.2 Sema3A decreases cell adhesion and spreading on an activating surface . 105
7.3 Sema3A-bound CD8+ T cells form poor immunological synapses on supported lipid bilayers . . . 106
7.4 Sema3A negatively affects T cell—cancer cell conjugation . . . 110
7.5 Sema3A decreases tumour-specific T cell cytotoxicity . . . 111
7.6 Sema3A immobilizes the F-actin cytoskeleton through actomyosin II activity . . . 113
7.7 Discussion . . . 119

8 NRP1 and Sema3A Expression in Clear Cell Renal Carcinoma 122
8.1 Introduction . . . 122
8.2 Clear cell renal cell carcinoma cohort . . . 123
8.3 Sema3A is located in glomeruli in healthy tissue and on CD31+ cells in clear cell renal cell carcinoma (ccRCC) . . . 125
8.4 A propotion of tumour-infiltrating T cells are NRP1+ . . . 129
8.5 Discussion . . . 130

9 Conclusion 132
9.1 Results from this thesis . . . 132
9.2 Outstanding questions . . . 135
9.3 Concluding remarks . . . 138

Bibliography **140**

List of Figures

3.1 NRP1 is upregulated on OT-I T cells following activation 46

3.2 NRP1 is expressed on tumour-specific OT-I T cells 48

3.3 Plexin-A1 is expressed on OT-I T cells following *in vitro* activation 50

3.4 Plexin-A1 and transforming growth factor beta receptor II (TGFβRII) is expressed on tumour-specific OT-I T cells 52

3.5 Stimulated, but not naive, OT-I T cells can bind Sema3A 54

4.1 NRP1-conditional knockout mice develop normally 58

4.2 NRP1-conditional knockout mice generate similar output of T cells from thymus and spleen 60

4.3 NRP1-conditional knockout CD8+ T cells produce similar levels of effector cytokines 61

4.4 NRP1-conditional knockout mice react similarly to challenge with influenza A/PR/8/34 H7N1 64

4.5 Sema3A is not expressed in lung or draining lymph node (dLN) before or during S-flu H7N1 infection 65

4.6 Sema3A is expressed by B16.F10 cells under different conditions 67

4.7 B16.F10 and Lewis lung carcinoma (3LL) cancer growth is stunted in $NRP1^{Flox/Flox}$ mice 69

4.8 Tumour growth is not stunted in NRP1-deficient mice with depleted CD8+ cells 71

4.9 NRP1-deficient CD8+ cells infiltrate into tumours more readily 72

4.10 Generation of Sema3A knockout (KO) and over-expression (OE) B16.F10.Ova cell lines . . . 75
4.11 Mixed bone-marrow chimeras have same phenotype as NRP1-knockout mice 77
4.12 Tumour-specific T cells are inhibited from entering Sema3A-rich tumours . . 78

5.1 Sema3A is not expressed by CD4+ or CD8+ effector T cells . . . 83
5.2 Sema3A is weakly expressed by regulatory CD4+CD25+FoxP3+ T cells . . . 84
5.3 Sema3A is not expressed by B cells, monocytes, DC's or macrophages . . . 85
5.4 Sema3A is expressed by vasculature and lymphatics in tumours . . . 86

6.1 T cells are in close proximity to Sema3A rich areas in tumours . . . 91
6.2 Sema3A does not affect integrin-receptor levels on stimulated T cells . . . 92
6.3 Sema3A is a negative regulator of integrin-mediated adhesion . . . 94
6.4 Sema3A negatively affects T cell migration through NRP1 . . . 96
6.5 Sema3A decreases T cell ability to adhere under physiological levels of flow . 97
6.6 Sema3A negatively affects T cell chemotaxis through NRP1 . . . 99

7.1 Sema3A decreases cell adhesion and spreading . . . 106
7.2 Sema3A-bound CD8+ T cells do not form immunological synapses on supported lipid bilayers . . . 108
7.3 Analysis of thousands of cells show strong effect of Sema3A on adherence and quality of immunological synapses . . . 110
7.4 Cell-cell conjugation is inhibited when Sema3A is present . . . 111
7.5 Sema3A decreases tumour-specific T cell cytotoxicity . . . 113
7.6 IRM shadow and F-actin signal overlap . . . 115
7.7 Sema3A immobilizes the F-actin cytoskeleton . . . 116
7.8 Sema3A increases myosin II activity in activated T cells . . . 118

8.1 Sema3A expression inversely associated with survival in ccRCC . . . 124
8.2 Sema3A expression in healthy and cancerous kidney . . . 126
8.3 Sema3A and CD31 are co-expressed . . . 128

8.4 Vasculature and Sema3A are variables in determining T cell infiltration . . . 129
8.5 A propotion of tumour-infiltrating T cells in ccRCC are NRP1+ 130

List of Tables

1.1 Tumour antigen categorization and examples. 6

2.1 List of antibodies used in this study. 29

2.2 List of CT-antigens used in staining cocktail. 42

8.1 Baseline characteristics for clear cell renal cell carcinoma cohort used in this study. 125

List of Abbreviations

List of abbreviations

3LL Lewis lung carcinoma

AF647 Alexa fluorophore 647

APC antigen-presenting cell

APCs antigen-presenting cells

BEC blood endothelial cells

c-SMAC central supramolecular activation cluster

CAFs carcinoma-associated fibroblasts

CASP8 Caspase 8

CCL2 CC-chemokine ligand 2

CCL3 CC-chemokine ligand 3

CCL5 CC-chemokine ligand 5

CCL21 CC-chemokine ligand 21

CCR5 CC-chemokine receptor 5

CCR7 CC-chemokine receptor 7

ccRCC clear cell renal cell carcinoma

CRISPR clustered, regularly interspaced, short palindromic repeats

CRMP2 collapsin response mediator protein 2

CT cancer testis

CTLA4 cytotoxic T-lymphocyte-associated protein 4

CXCL9 C-X-C motif chemokine 9

CXCL10 C-X-C motif chemokine 10

CXCL12 C-X-C motif chemokine 12

CXCR3 C-X-C chemokine receptor type 3

CXCR4 C-X-C chemokine receptor type 4

CYTOF cytometry by time of flight

d-SMAC distal supramolecular activation cluster

DC dendritic cells

dLN draining lymph node

DNA deoxyribonucleic acid

EAE experimental autoimmune encephalitis

EC endothelial cells

EMT epithelial-mesenchymal transition

ER endoplasmic reticulum

FasL Fas ligand

FRC fibroblastic reticular cells

GAGs glycosaminoglycans

GAP GTPase-activating protein

GDP guanosine diphosphate

GFP green fluorescent protein

GTP guanosine triphosphate

HA hemagglutinin

HLA human leukocyte antigen

HEVs high endothelial venules

ICAM-1 intercellular adhesion molecule 1

IDO indoleamine 2,3-dioxygenase

IF immunofluorescence

IFNγ interferon gamma

IHC immunohistochemistry

IL-2 interleukin 2

IL-10 interleukin 10

IRM interference reflection microscopy

LAG3 Lymphocyte-activation gene 3

LCMV lymphocytic choriomeningitis virus

LEC lymphatic endothelial cells

LFA-1 lymphocyte function-associated antigen 1

LN lymph node

MDSCs myeloid-derived suppressor cells

MET hepatocyte growth factor receptor

MHC major histocompatibility complex

MLCK myosin light chain kinase

ndLN non-draining lymph node

NP nuclear protein

NRP1 neuropilin-1

OVA ovalbumin

p-SMAC peripheral supramolecular activation cluster

PAMPs pathogen-associated molecular patterns

PBMCs peripheral blood mononuclear cells

PD-1 programmed cell death protein 1

PDL1 programmed death-ligand 1

PHA phytohaemagglutinin P

PIK3CA phosphatidylinositol 4,5-bisphosphate 3-kinase catalytic subunit alpha isoform

PMA phorbol myristate acetate

pMHC peptide MHC

PSGL-1 P-selectin glycoprotein ligand-1

RT-qPCR reverse transcription quantitative polymerase chain reaction

Sema3A Semaphorin 3A

Sema3E Semaphorin 3E

Sema3F Semaphorin 3F

SMACs supramolecular activation clusters

STING stimulator of interferon genes

TAA tumour-associated antigens

TAP transporter associated with antigen processing

TCGA The Cancer Genome Atlas

TCR T cell antigen receptor

TCRs T cell antigen receptors

TGFβ transforming growth factor beta

TGFβRI transforming growth factor beta receptor I

TGFβRII transforming growth factor beta receptor II

TIGIT T cell immunoreceptor with Ig and ITIM domains

TILs tumour-infiltrating leukocytes

TIM3 T cell immunoglobulin and mucin-domain containing-3

TIRF total internal reflection fluorescence

TNFα tumor necrosis factor alpha

TLRs Toll-like receptors

TME tumour-microenvironment

TRAIL TNF-related apoptosis-inducing ligand

TSA tumour-specific antigens

VEGFα vascular endothelial growth factor alpha

VEGFαRII vascular endothelial growth factor alpha receptor II

WB western blot

WT wild type

Chapter 1

Introduction

Studying the interaction between malignant cells and their healthy counterparts continues to be one of the most scientifically rewarding and important enterprises we can embark on today. Cancer is estimated to kill 8-9 million people each year[1], and although great strides have been made in increasing our understanding of and ability to treat the disease, most forms still remain deadly.

In this chapter I will introduce three aspects of cancer biology that will form the basis of the rest of the thesis: how CD8+ effector T cells respond to and control cancer cells; how tumours reciprocate against the immune system; and finally, I will introduce the NRP1, Plexin and Semaphorin signalling-system. However, I will start with a brief preface on cancer.

1.1 There are no more than five musical notes, yet...

In the last decades our understanding of cancer as a disease of the cell has transformed our understanding of the illness. We know that cancers arise from genetic mutations affecting driver oncogenes and tumour suppressor genes, which enable cells to proliferate, differentiate and mutate in an unregulated manner[2, 3]. These mutations can arise as point-mutations, indels, copy-number variations, genomic fusions or methylation events[4–6] and form the basis of cancer evolution.

However, it is not the growth of a single mutated clone that make tumours lethal: instead it is the heterogeneity of both cancer cells[1, 7, 8], and the cell types surrounding them[9–11], that enable tumours to thrive in a constrained microenvironment, metastases and withstand attacks from the immune system and medical therapies[1, 12–14]. The genetic heterogeneity of cancer cells provides "the substrate upon which selection can act"[15] and engage in cooperative behavior[1, 8], while the heterogeneity of cell types in the tumour-microenvironment (TME) is increasingly recognized as providing important support for cancer development and progression[11, 16]. Together this diversity of both cancer cells and stromal cells increase tumours fitness and ability to survive[8, 13].

Exactly how important the stromal compartment of tumours are has only recently become clear[17–20]. Consisting of immune cells, fibroblasts, endothelial cells and a complex extracellular matrix[16], this compartment often outweighs the number of cancer cells in a tumour[11]. Together they enable niches for tumour-development[1], offer therapeutic resistance[21] and of special interest here, generate an overall immunosuppressive environment[22]. While therapies that have focused on changing the makeup

and activity of immune cells have revolutionized cancer treatment over the last decade, there is now an increasing focus on targeting other cell types in this microenvironment as well.

This thesis is set at the interface between two important components of the TME, namely cytotoxic T cells and endothelial cells. We found that neovasculature and lymphatic vessels in tumours secrete the protein Sema3A, which is normally only present during embryonic development. Due to its known effect on endothelial cells, Sema3A has been suggested as an anti-tumour agent[23, 24], but using murine and human models, we here show that the protein also negatively regulates key aspects of anti-tumour T cell function through a surface receptor called NRP1.

1.2 T cell response to cancer cells

The immune system's capacity to react to and shape cancer development is well established. The process has been described as cancer immunoediting[25, 26], in which T cell—cancer interactions proceed along three general paths: elimination, in which the immune system actively eliminates cancer cells; equilibrium, in which tumour expansion in inhibited[27]; and finally, escape, in which cancer cells attenuate the attack from the immune system.

In this section I will focus on how CD8+ effector T cells, detect, infiltrate and react to cancer cells, while the next section will concentrate on how tumours escape this attack.

This is a rather narrow approach: it should be noted that the immune system has been associated not only with preventing cancer, but also shown to promote oncogenesis in several settings[28]. Additionally, it is clear that different immune cell types are not per

se tumour promoting or inhibitory. Instead the phenotypes of individual immune cells, the composition of the entire immune infiltrate, and their shared interactions within tumours, all determine whether or not they enable or inhibit tumour growth[29]. Using sequencing data from The Cancer Genome Atlas (TCGA), it was recently suggested that tumours could be classified in six "immune subtypes"[30], and new methods such as single cell RNA-seq, CITE-seq and cytometry by time of flight (CYTOF) are now revealing exactly how complex this infiltrate is[31–33]. However, a certain platonic idealism - a black and white view of the world - is better suited to establishing the basic facts on which one can then later elaborate, and so that is what I will do here.

1.2.1 Tumour antigens

CD8+ T cells recognize and kill cells if they express foreign proteins, known as antigens, and these are presented as small 8-10-mer peptides loaded into major histocompatibility complex (MHC) class I molecules on the cell surfaces. Also called epitopes, these peptides are generated in the proteasome, transported into the endoplasmic reticulum (ER) by the transporter associated with antigen processing (TAP) protein and loaded into MHC-complexes which contain β2 microglobulin. This peptide MHC (pMHC) complex then traffic to the cell membrane, where T cells use a surface receptor-complex called the T cell antigen receptor (TCR) to survey the presented epitopes[34]. If strong enough binding occurs between the TCR and pMHC[35], T cells initiate a complex sequence of events that eventually lead to cytotoxic killing of the presenting cell (this will be described in more detail in chapter 8). As T cells expressing TCRs that can bind self-antigens, i.e. from endogenous proteins, are removed during their development, this

system allows for T cells to react to and destroy cells infected with viral or bacterial pathogens.

For T cells to recognize cancer cells the latter therefore needs to express antigens that are somehow different from endogenous proteins, or at least antigens for which there exists TCRs amongst circulating T cells. A large number of tumour-antigens that can elicit a response from T cells have now been described (for examples see Table 1.1)[34, 36]. They can be divided into two broad categories, tumour-specific antigens (TSA) and tumour-associated antigens (TAA)[36].

The majority of TSAs consists of point and missense mutations that give rise to changes in the amino acid sequence of proteins and are often simply called cancer neoantigens. Not surprisingly, tumours with a high mutational load generate a larger number of neoantigens[37]. Tumours associated with a viral aetiology, such as cervical cancers caused by human papilloma-virus, give rise to another class of TSAs. Finally, protein fusions, such as BCR-ABL in leukemias, give rise to a third class. Of the TAAs, cancer-testis antigens are the biggest class with over 60 different genes having been identified[34]. These antigens are normally only expressed by cells in the reproductive organs, but are often re-expressed in cancer cells[38]. Another important class are differentiation antigens, which are only found in the tissue of the tumour.

While TSAs are generally thought to be more immunogenic, most of them arise from passenger mutations, meaning they differ from tumour to tumour. This makes it challenging to target these antigens therapeutically[36]. TAAs on the other hand can be found shared among different tumours, although TCRs targeting them are often of low affinity[39].

Table. Categories of tumour antigens		
Type	Description	Examples
Tumour-specific antigen		
Neoantigens	Arising from mutations in the cancer genome	CASP8[52], RAS[53], CDK4[54]
Protein fusions	Arising due to chromosomal translocations	BCR-ABL[55], RUNX1[56]
Viral antigens	Arising from virally encoded proteins	HPV E6[57], HBsAg[58]
Tumour-associated antigens		
Cancer-testis	Normally expressed in germline tissue	NY-ESO-1[59], MAGE-A1[60]
Oncofetal	Normally expressed during development	CEA[61], SSEA-3[62]
Differentiation	Only expressed in one tissue	GP100[63], Melan-A[64]
Overexpressed	Arising from proteins highly expressed in cancer cells	ERBB2 (Her2/Neu)[65], WT1[66]

Table 1.1: Tumour antigen categorization and examples.

How many antigens are available for T cells to act upon? Peptide abundance, MHC affinity and amino acid composition all affect the immunogenicity of an antigen[40]. *In silico* analysis of TCGA data are estimating approximately 0.8-45 mutations per megabase deoxyribonucleic acid (DNA), depending on patient age and tumour type[41]. Since TCR diversity among tumour-infiltrating leukocytes (TILs) correlates with the number of mutations[42], it is tempting to equate mutational load to antigenicity of a tumour. Indeed recent studies have found that survival in patients receiving anti-cytotoxic T-lymphocyte-associated protein 4 (CTLA4) and programmed cell death protein 1 (PD-1) therapies increases with higher mutational load of the tumours[43, 44]. However it is important to remember, that while most mutations might be immunogenic, some also attenuate T cell mediated immune responses[45], for example by inhibiting antigen presentation (see more below). For cancer-testis antigens, expression can vary substantially from patient to patient, as their expression are strongly dependent on transcriptional factors and methylation events[34, 38]. Finally, it is clear that the antigen landscape evolves rapidly following T cell-mediated attack[46, 47]. Antigen expression is therefore a highly dynamic process, and methods that can increase their release and presentation to the immune system is an active research area[48–51].

1.2.2 T cell priming and activation

While the presence of tumour antigens is a prerequisite for anti-tumour T cell immunity, if and how these antigens are presented to naive T cells is essential. However, unlike acute viral infections, cancer development is a slow, often years-long process which leads to poor activation of T cells[67].

Investigations using mouse models now point to dendritic cells (DC) as the master regulators of T cell priming and activation in tumours. These bone-marrow derived cells have been shown to increasingly cross-present antigens as tumours grow in size[68]. Conversely, in *Batf3*-knockout mice which lack the ability to cross-present antigens through DCs, highly immunogenic tumours grew unperturbed[69]. For DCs to become activated in viral or bacterial infections, they must be stimulated by pathogen-associated molecular patterns (PAMPs), often through Toll-like receptors (TLRs). However in cancers, which can be thought off as "sterile infections", emerging evidence is now pointing to DC activation occurring through DNA-sensing pathways such as stimulator of interferon genes (STING) instead. Indeed STING knockout mice have defective T cell priming and lack anti-tumour control[70]. Uric acid, heat shock proteins and ATP released from dying cancer cells have all been shown to mature and activate DCs[71–73]. It has therefore been suggested that a strong type I interferon signal among DCs is a prerequisite for proper T cell priming[74].

Recently it was shown that within tumours a DC subset defined by CD103 and CC-chemokine receptor 7 (CCR7)-receptors plays important roles in activating T cells by effectively phagocytosing dying cancer cells and trafficking to dLNs[75, 76]. Here DCs form long-lasting synapses with naive T cells[77] and provide critical "second signal"

activation to T cells (through CD28), after which T cells proliferate and start to migrate. T cells and DC interactions also occur within the tumour itself, but in murine cancer models priming here does not seem to properly activate T cells[78, 79].

While T cell—DC interactions in the lymph node (LN) lead to up-regulation of stimulatory receptors and ligands (such as CD28 and CD80) and cytokines (such as IL-15)[80], DCs can also be a negative regulator of T cell priming. It was recently shown that programmed death-ligand 1 (PDL1)-expression by DCs is a major determining factor in how well mice control tumours[81, 82]. Indeed, activation by DCs that were themselves not properly activated has been shown to suboptimally prime T cells[83].

Although DCs are fundamental for activating T cells, CD4+ helper T cells also play important roles in amplifying the magnitude and quality of CD8+ T cell responses to cancer[84]. Upon encounter with its cognate antigen on DCs, CD4+ T cells increase DC activation through CD40:CD40L interactions, which then boosts CD8+ T cell activation in a process called licensing[85]. In this process CD4+ T cells also produce pro-stimulatory cytokines such as IL-2, which help CD8+ T cell proliferation[86]. Recent work has shown that licensing is dependent on CD27 on CD8+ T cells and CD70 on DCs as well[87].

An important question is how T cell priming is affected by their affinity to tumour epitopes presented to them. TCRs that recognize TAAs have been shown to be low-affinity[39, 88], and only a low number of high affinity TCRs have been found against neoantigens in lung and skin cancers[89]. However, experiments using model antigens have shown that while reduced ligand potency slowed down activation of T cells, all eventually became fully primed[90, 91]. Intriguingly, preliminary data have shown that

T cells with low affinity TCRs might actually be less likely to enter states of T cell dysfunction in tumours[92].

1.2.3 Trafficking and infiltration into tumours

Following priming, activated T cells must traffic out of the lymph node and into tumours to detect and kill cancer cells. Not surprisingly, a high density of TILs correlates with favourable clinical outcomes[93–95]. However, the number of TILs in a tumour does not correlate with mutational burden[95–97], indicating that infiltration is a major obstacle T cells have to overcome. Unlike acute infections in which inflammatory cues help guide T cells, tumours are not always conducive to T cell infiltration, although the exact mechanism behind this restriction is not well established.

Based on the number of TILs and their localization, tumours have been classified in three different subtypes: immune dessert, in which no T cells are present at all; immune excluded, in which T cells infiltrate the tumour mass, but are immobilized in the stroma; and immune inflamed, in which T cells readily infiltrate both tumour mass and into cancerous tissue as well. In the following paragraphs I will briefly outline factors that determine T cells ability to infiltrate into tumours[98].

T cell trafficking is a choreographed event, in which chemokines, endothelial cells (EC):T cell interactions, and T cell receptors, are important factors[99]. Following activation, T cells down-regulate receptors such as CD62L and CCR7, thereby losing their ability to home to LNs. Instead up-regulation of E- and P-selectins and chemokine receptors such as CC-chemokine receptor 5 (CCR5) and C-X-C chemokine receptor type 3 (CXCR3) ensures their migration into inflamed organs[100]. E- and P-selectins enable

attachment and rolling across the endothelium, while chemokine binding to chemokine receptors causes activation of lymphocyte function-associated antigen 1 (LFA-1), allowing for intercellular adhesion molecule 1 (ICAM-1)-mediated adhesion to ECs and transmigration (for a more detailed explanation see chapter 6)[101, 102]. These steps are thought to happen primarily on ECs in postcapillar regions called high endothelial venules (HEVs), which themselves are activated through cytokines such as tumor necrosis factor alpha (TNFα). Chemokines produced by activated ECs and underlying stromal cells are immobilized via binding to heparin sulphate glycosaminoglycans (GAGs) and serve as powerful exit cues for migrating T cells[101].

In melanoma patients, expression of ligands for CCR5 (CC-chemokine ligand 2 (CCL2), CC-chemokine ligand 3 (CCL3) and CC-chemokine ligand 5 (CCL5)) and CXCR3 (C-X-C motif chemokine 9 (CXCL9) and C-X-C motif chemokine 10 (CXCL10)) is associated with increased T cell infiltration[103, 104], although CCR5 has been reported to be redundant for T cell infiltration[105]. However, whether different tumour types express the same chemokine signatures is unknown[102]. While it is well described that memory T cells have a specific set of chemokine-receptor patterns that will ”imprint” their homing to specific tissues[106], little is known about what, if any, chemokine-receptors and ligands are associated with immune desert, excluded and inflammed tumour-types, although preliminary work has started to tease apart this complexity[107].

1.2.4 Recognition and killing of cancer cells

Once transmigration into the tumour tissue has occurred, T cells migrate around in search for cells that express their cognate antigens. Besides being affected by

chemokines, the physical environment, such as the collagen content, play important roles in determining T cell movement within the tumour[108].

In order to kill cancer cells, T cells must recognize pMHC that present the same epitope against which they were first primed and activated. This TCR-triggering causes profound changes in the T cells, leading them to form an immunological synapse against the target cell into which they can direct secretion of cytotoxic molecules such as Granzyme B and perforin[109] (a more detailed explanation of synapse formation will be provided in chapter 7). These molecules lead to apoptotic cell death through activation of Caspases and other molecules involved in apoptosis within the cancer cell[110]. Another way T cells can kill target cells is through so-called death ligands, such as FasL or TNF-related apoptosis-inducing ligand (TRAIL)[110]. While this T cell:target cell interaction concludes over minutes in *in vitro* model systems, T cells can be seen to be in close contact with cancer cells over hours *in vivo*[111].

Finally, T cells are known to produce interferon gamma (IFNγ) upon re-activation within the tumour. This cytokine has been shown to play an important role in T cell control of tumours[112], probably through its ability to up-regulate MHC class I expression on cancer cells[113] and its anti-proliferative effects[114].

1.3 Cancer cell response to T cells

Following this idealized description of how CD8+ T cells detect and control cancer growth, I will now outline some of the multiple way's cancer cells respond to and circumvent this attack. Broadly speaking, tumours evolve to present an immuno-suppressive environment. This process happens across multiple tumour types and even though their

starting points are different, they converge on certain immune-evasive phenotypes. To quote Darwin: ”the common rule thoughout nature is infinite diversity of structure for gaining the same ends”[1]. The ”ends” I will be focusing on here are acquired resistance; immunological ignorance; inhibition of T cell infiltration; immune suppression by the TME; and T cell dysfunction.

1.3.1 Resistance to immune-mediated control of cancer

Because cancer cells are genomic and epigenetically unstable, a major type of evasion to T cell mediated control of tumour growth is acquired immune resistance via Darwinian evolution of the cancer cell clones[115]. These immunoresistant clones are selected via the selective pressure applied by T cells and other immune cells.

Most obviously, loss of antigen or simply culling of antigen-positive cells, will result in lack of T cell attack. There is good evidence this is an ongoing process in tumours[46, 47] with cancer cells constantly being pruned by the immune system. Mutations within the antigen-presentation apparatus is also a well described resistance mechanism. For example it was recently shown that one gene, β2-microglobulin, was mutated in 10% to 30% of melanoma patients[116]. Across a wide range of cancers, β2-microglobulin and human leukocyte antigen (HLA)-A, -B and -C mutations were associated with immune evasive cancer cells[30, 117]. Defects in the proteosome and peptide transporters are also well-described[115]. Together these findings indicating that loss of antigen presentation is a key phenotype for resistance development.

Loss of function mutations are also often seen in apoptotic signaling pathways. Caspase 8 (CASP8), hepatocyte growth factor receptor (MET) and phosphatidylinositol

4,5-bisphosphate 3-kinase catalytic subunit alpha isoform (PIK3CA) are involved in extrinsic activation of apoptosis[110], for example through Fas ligand (FasL) and TRAIL-induced killing, and were seen to be heavily mutated in a wide range of cancers[117].

Finally, resistance can also be seen when cancer cells utilize proteins that are normally used in the termination of an immune response or in re-creating tissue homeostasis. For example, cancer cells often up-regulate the immune-regulator PDL1, which inhibits T cell mediated attack through the receptor PD-1, when subjected to IFNγ[118]. Immune-modulatory receptors expressed by tumour cells for other co-inhibitory proteins on T cells include Galectin-9 (for the receptor T cell immunoglobulin and mucin-domain containing-3 (TIM3)), LSECtin (for Lymphocyte-activation gene 3 (LAG3)) and CD155 (for T cell immunoreceptor with Ig and ITIM domains (TIGIT))[119].

1.3.2 Immunological ignorance

Immunological ignorance describes situations in which antigens are never noticed by T cells and so no cytotoxic attack is initiated[120]. This is due a lack of or poor priming of T cells in draining lymph nodes.

A number of mechanism have been described that inhibit priming and cross-presentation of tumour antigens. For DCs to be attracted to tissue and become activated, dying cancer cells must release a number of immunogenic compounds, such as ATP or heat-shock proteins[121]. Failure to do so, can lead to ”tolerogenic” cell death, which does not result in uptake by antigen-presenting cell (APC)s and cross-presentation of antigens[121]. The cytokine interleukin 10 (IL-10) which is frequently found in cancer patients, has additionally been shown to inhibit DC differentiation[115]. DCs from can-

cer patients are indeed often impaired and immature, which leaves them with low levels of co-stimulatory ligands such as CD80 and CD40, and therefore poor stimulators of T cells[122]. Methods to increase immunogenic cell death within tumours is an active research area, sought to be combined to checkpoint immunotherapy[123].

Finally, it has been suggested that certain epitopes might dominate over others within the antigen-repertoire of a tumour. This ”immunodominance” phenomenon is thought to lead to preferential detection of few antigens, as opposed to other, perhaps more immunogenic, antigens. Additionally, a cancer clone that has lost MHC-expression might still cross-present this antigen, effectively diverting T cell mediated responses away from other epitopes[115].

1.3.3 Inhibition of T cell infiltration

A major rate-limiting step in the anti-tumour response of T cells, is their restriction from either the entire tumour or from entering into the cancerous cells within the TME itself[93, 124]. It is becoming increasingly clear that this restriction inhibits the effect of checkpoint blockade[125] and even adoptive transfer therapies, where millions of tumour-specific T cells are injected into patients[126, 127].

As mentioned above, tumours can be thought of as either immune desert, immune restricted or immune inflamed. Most likely, immune desert tumours are immunological ignorant, lack antigens or have heavily mutated antigen-presentation. In immune restricted and inflamed tumours, a combination of inhibitory events might be taking place. I will outline some here.

Tumour vasculature and T infiltration

The architecture of the vasculature is essential to T cell infiltration. Broadly speaking it has been noticed that tumour vasculature is often immature, fragmentary and leaky, and this disorganization has been associated with poor immune cell infiltration. However, the molecular and physical mechanisms behind these effects are still being elucidated.

Functionally, blood flow through tumours can be chaotic. Because the vasculature grows in a disorganized manner in tumours, the result is insufficient blood flow, hypoxia, and high interstitial fluid pressure in places[128]. Perhaps counter-intuitively, vasculature leakiness does not promote T cell infiltration. Instead therapies that aim to "normalize", as oppose to outright destroy, the tumour vasculature by inhibiting vascular endothelial growth factor alpha (VEGFα) or providing low doses of TNFα, have been shown to promote T cell infiltration[129, 130], and this approach is actively researched in combination with checkpoint blockade[128]. Interestingly, a recent report highlighted how initial normalization might also lead to up-regulation of PDL1 on the vasculature through an IFNɣ feedback loop. Combination therapy with both αPDL1- and antiangiogenic therapy helped normalize the vasculature, which lead to formation of HEVs, and increased T cell infiltration[131].

Lack of EC activation can also be a limiting factor. Absent or down-regulated adhesion molecules such as ICAM-1 inhibit T cell adhesion and transmigration[132, 133]. ICAM-1 expression have been seen to be regulated directly by tumours via the endothelin B receptor in ovarian cancer[134]. It has also been shown that tumour-derived molecules, such as VEGFα, IL-10 and prostaglandin G2, strongly affect the vasculature

and induces a so-called “death barrier” by up-regulating FasL on the ECs which inhibit T cell infiltration[135].

Chemokines, secreted molecules and infiltration

Another major hurdle to T cell infiltration is a lack of expression of chemoattractive chemokines such as CXCL10 within the tumour[107]. Alternatively, chemo-attractive signals might only be expressed by the surrounding stroma, not within the cancer parenchyma itself, thereby actively misdirecting T cells away from the cancer cells. Stromal cells such as carcinoma-associated fibroblasts (CAFs) can actively secret C-X-C motif chemokine 12 (CXCL12) and attract T cells[136]. Additionally, high expression of certain chemokine signatures is now known to attract immune-suppressive cells, as opposed to APCs that would promote immunogenicity[137].

A number of other molecules are also known to specifically inhibit T cell homing. transforming growth factor beta (TGFβ)-signatures have been strongly associated with lack of infiltration in both *in silico* analysis[30], mouse and human models[138]. Additionally, a number of neuro-trophic factors have been associated with effects on T cell migration[139–141].

Inhibition of infiltration by other cell-types

It is now clear that multiple other immune cells also control the level of T cell infiltration.

In murine models of pancreatic cancer, CAFs are known to produce desmoplastic stroma by secreting ECM components that physically trap T cells within the stroma and

inhibit T cell infiltration[22]. In human tissue the production of extra-cellular matrix fibers severely inhibited and control T cell motility[142].

Suppressive immune cells such as CD4+ regulatory T cells and myeloid-derived suppressor cells (MDSCs) are able to alter CD8+ T cell infiltration by regulating L-selectin on T cells, and producing reactive nitrogen species that reduce the effects of chemokines[143, 144].

1.3.4 Immune suppression by the TME

Most tumours evolve to become highly immunosuppressive environments[22]. This happens in part due to the growth requirements of tumours leading to inhibitory effects on the immune system, and most likely also through Darwinian selection.

As mentioned above, tumours are characterized by having aberrant and immature vasculature, which results in nutrient-poor, acidic and hypoxic regions within the tumour. In these environments there is competition for nutrients, which cancer cells constantly battle to grab, for example by up-regulating nutrient transporters or rewiring metabolic pathways. T cells are known to rely on aerobic glycolysis for proliferation and cytotoxic killing[145, 146] and are therefore inhibited in these anaerobic environments.

Furthermore, CD8+ T cells have been shown to require glucose for TCR-triggering, proliferation and cytokine production, and limited availability within the TME therefore severely inhibits these effector functions[147–149]. There is evidence that cancer cells are actively able to out-compete T cells by up-regulating glucose-transporters: in ccRCC patients, high expression of the glucose-transporter 1 was associated with low levels of

TILs[150].

A number of metabolites and their enzymes have also been associated with suppressive immune functions, the most explored being indoleamine 2,3-dioxygenase (IDO). High expression is seen in a number of cancers and has been correlated with poor CD8+ T cell infiltration and patient survival. IDO converts tryptophan into kynurenines, which inhibit both T cell proliferation and TCR-triggering[22]. Additionally, IDO has been shown to actively recruit regulatory T cells into the TME[151].

As mentioned earlier, mismatched chemokine signatures selectively recruit immunosuppressive cells into the tumour environment. These include CD4+ regulatory T cells, MDSCs and certain macrophages[152]. These cells are also attracted by growth factors secreted by cancer cells[153]. Cytokines, such as TGFβ, within the tumour can also reprogram myeloid-cells and macrophages into suppressive phenotypes[154]. These cells inhibit CD8+ T cell function in a plethora of ways, among others, by expressing co-inhibitory receptors such as PDL1[155], by producing arginase-1[152], by sequestering cystitine[156] and producing cytokines that attract regulatory T cells[157].

1.3.5 T cell dysfunction

Finally, I will briefly touch on T cell dysfunction within tumours.

It is now clear that persistent antigen exposure can drive severe dysfunction and ”exhaustion” of T cell functions[158]. Dysfunctional TILs are known to express a number of co-inhibitory molecules on their cell surface including PD-1, CTLA4, TIM3 and LAG3, and are found to have impaired effector functions, for example lacking the ability to express cytotoxic molecules following re-stimulation and the capacity to proliferate[159–

161]. This loss of function is imprinted on T cells through transcriptional and epigenetic programming[161, 162].

This dysfunction can be modulated by co-inhibitory receptors. Most well explored is the effects of PD-1 signaling, which, through it's ligand PDL1, cause modulation of signals down-stream of TCR-triggering[158]. Signaling through PD-1 leads to phosphorylation of two tyrosines in it's cytoplasmic domain, which allows for recruitment of the tyrosine phosphotases Shp1 and Shp2. Recently it was suggested that Shp2 dephosphorylates the co-stimulatory molecule CD28[163, 164], thereby inhibiting important "signal 2" stimulation of the cell. Importantly, this has provided a rational for using antibodies that target and block PD-1, thereby allowing for modulation of T cell dysfunction[162, 165].

1.4 Neuropilin-1 and class 3 semaphorins

1.4.1 Overview

NRP1 is a co-receptor that plays a pivotal role in regulating the binding of a number of extracellular ligands. Among these are the Semaphorins and VEGFα, which are involved in a number of essential cellular functions. By affecting the binding of these ligands, through selective dimerization with members of the plexin or VEGF receptor families, NRP1 is able to fine-tune their cellular responses. While the role of NRP1 is well explored in the central nervous and cardiovascular system, little is known about its effects in the immune system and even less about its role in the tumour-microenvironment.

1.4.2 Neuropilin-1

Neuropilin-1 (also called CD304; NRP1) is a 120-130 kD single transmembrane spanning glycoprotein, which has been shown to be involved in neural development, especially in neuronal cell guidance and angiogenesis[166]. Recently, it's role within the immune system has gathered attention[167]. NRP1 knockouts are embryonic lethal due to chaotic vascular and neuronal growth[168, 169].

In humans, neuropilin-1 is encoded by 17 exons located on chromosome 10p12[170]. It consists of a large (835 amino acids) extracellular region, a single transmembrane spanning domain (23 amino acids) and a small cytoplasmic domain (44 amino acids). The extracellular region consists of two N-terminal CUB domains (designated a1 and a2), two coagulation factor V/VIII homology domains (b1 and b2) and a membrane-proximal MAM domain (c)[171]. The a1-a2 domains mediate binding to semaphorin-3A, while the glycosylated b1-b2 domains are responsible for heparin and VEGF-A isoform 165 binding[171]. The transmembrane region contains a GxxxGxxxG motif which, together with the MAM domain[172], is important for dimerization[173].

Within the immune system, NRP1 has most thoroughly been described as a marker for CD4+CD25+FoxP3+ Regulatory T cells[174]. Using conditional knockout mice Delgoffe et al have shown that the receptor plays an important role in enhancing regulatory T cells ability to suppress immune responses in tumours[175].

1.4.3 Class 3 Semaphorins, Plexins and Their Signalling

NRP1 acts as a co-receptor for a number of soluble ligands, including class 3 Semaphorins, and as such helps integrate and modulate their signalling[171].

Class 3 Semaphorins

Semaphorins are a family of evolutionary conserved membrane-bound and secreted proteins, important for chemotactic response in the developing central nervous and cardiovascular system, mainly thought to affect cell adhesion and migration through plexin receptors[176].

In vertebrates five different classes of Semaphorins exist, class 3 through 7, while an additional class 8 is encoded by viruses. Class 1-2 only exist in invertebrates. All contain a so-called sema-domain, followed by a plexins, semaphorin and integrins (PSI) domain. For class 3 semaphorins this is followed by an immunoglobulin-like domain. Class 3 and viral semaphorins are secreted[176], and, in the case of class 3, can affect migration of developing neurons across long ranges[177].

Plexins

The receptors for Semaphorins are mainly the plexin receptor family, a homogenous family of transmembrane proteins, each consisting of an extracellular Sema-domain, three PSI and three Ig-like, plexins and transcription factor (IPT) domains. Intracellularly plexins are highly homologous, each containing a juxtamembrane segment followed by GTPase activating protein (GAP) domain with a RhoGTPase binding domain (RBD) insert[178]. Plexins are grouped in 4 categories, A-D, in vertebrates[176]. Class 3 semaphorins bind plexinA1-4 and plexinD1. While Sema3A can bind PlexinD1 directly, plexin dimerization with NRP1 is required for binding to PlexinA1-4 and to initiate downstream signaling[171].

How Semaphorin binding is converted into cell signaling, has been eloquently de-

scribed in recent papers[171, 179, 180]: Specifically, NRP1 and plexins form dimers, which can then be further stabilized by Sema3A binding, allowing for plexin-NRP1-plexin-NRP1 dimerization[171]. These complexes confer a conformational change intracellularly, causing the otherwise kinked juxtamembrane segment of the plexins to straighten, opening up the active sites of a GTPase-activating protein (GAP)-domain, which in turn allows for hydrolysis of the active guanosine triphosphate (GTP)-bound GTPase to their inactive guanosine diphosphate (GDP)-bound form, thereby inactivating Rap, a key activator of cell-matrix adhesion[179, 180].

Whether class 3 semaphorins attract or repulse cells, seems to be dependent on cell-type[176], but it has also been suggested that the switch from attraction to repulsion can be mediated by different Neuropilins[181], or by the level of guanylate cyclases, as both are able to create different effects in the same cell-type[182]. For example, it has been shown that Sema3A can act as a chemorepellant for the axon and an attractant for the apical dendrite in the same neuron. Finally, signalling through Plexin is dependent on whether other NRP1 co-receptors and ligands are available, such as the VEGF-A isoform 165[183].

1.5 Aim of this thesis

In this thesis, I will explore the role of NRP1 in CD8+ T cells, specifically what function it plays during T cell—tumour immunity.

Chapter 2

General Material and Methods

2.1 Cell-lines and their culture

2.1.1 General cell culture

Cell culture was performed using antiseptic techniques in HEPA filtered culture cabinets. Cell lines were grown at $37\,^{\circ}\mathrm{C}$ in a 5% CO_2 atmosphere. For some experiments, cells were cultured for 24 hours in a 1% O_2 hypoxic chamber. All cell-lines were screened for Mycoplasma. Adherent cells where split by Trypsin-EDTA detachment and serially passaged and their viability regularly checked using a Countess automated cell counter (Life Technologies). Cells were stored in 10% DMSO + 20% FCS media in liquid nitrogen storage tanks for long term storage.

2.1.2 Cell-lines used in this study

B16.F10 and B16.F10.Ova cell-lines were provided by Uzi Gileadi (Cerundolo Lab, RDM, University of Oxford). The latter was generated by transducing B16.F10 with

a modified Ovalbumin-IRES-GFP construct, containing a start codon and amino-acid 47 to 386 of the full-length ovalbumin, which ensures that Ovalbumin is not secreted by the cell-line. 3LL cells were a gift from Chris Pugh (NDM, University of Oxford). B16.F10.Ova Sema3A knockout (KO) cells were generated using CRISPR/Cas9 genome-editing (see below). B16.F10.Ova Sema3A overexpressing (OE) were generated by transduction the cells (see below) with a EFS-Sema3A cDNA-mCherry lentivirus, cloned by VectorBuilder. HEK293T cells were a gift from Tudor A. Fulga (RDM, University of Oxford).

2.1.3 Media and reagents for cell-line culture

R10

For non-adherent cells. RPMI-1640, 10% FCS, 2 mM Glutamine, 1 mM Sodium Pyruvate, 1x Non-essential amino acids, 100 U/ml penicillin + 100 µg/ml streptomycin, 10 mM HEPES, 50 µM β-mercaptoethanol.

D10

For adherent cells. DMEM, 10% FCS, 2 mM Glutamine, 1 mM Sodium Pyruvate, 100 U/ml penicillin + 100 µg/ml streptomycin.

T cell media

For culturing T cells. IMDM, 10% FCS, 2 mM Glutamine, 1 mM Sodium Pyruvate, 1x Non-essential amino acids, 100 U/ml penicillin + 100 µg/ml streptomycin, 10 mM HEPES, 50 µM β-mercaptoethanol. 10 IU IL-2 was added from frozen stock just before use.

2.2 Analysis of publicly available transcriptional data

2.2.1 Protocol

We downloaded raw expression data collected from mice from the "Immunological Genome Project data Phase 1" via the Gene Expression Omnibus (series accession: GSE15907). We specifically focused on naïve CD8+ T cells (accessions: GSM605909, GSM605910, GSM605911), CD8+ effector T cells (accessions: GSM538386, GSM538387, GSM538388, GSM538392, GSM538393, GSM538394), and CD8+ memory T cells (accessions: GSM538403, GSM538404, GSM538405). The raw expression array files were processed by Lars R. Olsen using the affy package[184] and differential expression of selected genes (CD72, NRP1, NRP2, PLXNA1, PLXNA2, PLXNA3, PLXNA4, PLXNB1, PLXNB2, PLXNB3, PLXNC1, PLXND1, SEMA3A, SEMA3B, SEMA3C, SEMA3D, SEMA3E, SEMA3F, SEMA3G, SEMA4A, SEMA4B, SEMA3C, SEMA4D, SEMA4F, SEMA4G, SEMA5A, SEMA5B, SEMA6A, SEMA6B, SEMA6C, SEMA6D, SEMA7A, TIMD2, HPRT, OAZ1, RPS18, NFATC2, TBX21, EOMES, CD28, PDCD1, CTLA4, LAG3, BTLA, TIM3, ICOS, TNFRSF14, TNFSF14, CD160, CD80, LAIR1, CD244, CXCR1, CXCR2, CXCR3, CXCR4, CXCR5, CCR1, CCR2, CCR3, CCR4, CCR5, CCR5, CCR6, CCR7, CCR8, CCR9, CCR10) between naïve and effector and memory cells was examined using the limma package[185] in R[186].

2.3 OT-I T cell protocols

2.3.1 Harvesting and preparing splenocytes

Mice were euthanized using CO_2, and spleens were harvested and stored in T cell media on ice. A single cell suspension was created by straining the spleen through a $70\,\mu m$ nylon mesh using the blunt end of a syringe. Cells were washed off the mesh by applying 5 mL T cell media, following by mixing of the solution by aspiration. Cells were then washed and resuspended in 3 mL red blood-cell (RBC) lysis buffer for 5 minutes on ice. Cells were washed again in T cell media, counted and resuspended at 2×10^6 cells pr. mL in T cell media.

2.3.2 Stimulation using peptides

Into single splenocyte solution, 10 IU IL-2 (Cat. 212-12, PeproTech) pr. mL and 25-100nM SIINFEKL peptide (Cambridge Peptides) pr. mL was added and mixed. Approximately $200\,\mu L$ cells were then plated onto a 96-well U-bottom plate and allowed to expand for 48 hours.

2.3.3 Stimulation using CD3/CD28 beads

Into single splenocyte solution, 10 IU IL-2 (Cat. 212-12, PeproTech) pr. mL was added and mixed. CD3/CD28 Dynabeads (Thermo Fisher) was washed in PBS, and added to cell at a cell-to-bead ratio of 2:1. Cells were then plate unto a 96-well U-bottom plate and allowed to expand for 24-48 hours. Before downstream use, beads were removed by briefly washing the cells and allowing them to settle on a magnet for 2 minutes, and

then aspirating only the cells in solution.

2.3.4 Stimulation using plate-bound CD3 antibodies

Approximately 2 hours before harvest of splenocytes, a flat 96-well plate was prepared by adding CD3 (Clone 145-2C11, Biolegend) at 5 ug/mL in $30\,\mu L$ PBS to each well, and incubating enture plate at $37\,^{\circ}C$ until use. When single splenocyte solution is prepared, and 10 IU IL-2 added, the solution is removed from the plate and $200\,\mu L$ splenocytes added to each well.

2.3.5 ”Chronic” stimulation using peptide and CD3 antibodies

Cells first prepared using peptide stimulation protocol for 48 hours, then sorted using magnetic beads (see below), re-stimulated using plate-bound CD3 antibodies for 24 hours, washed, sorted, and re-stimulated again using CD3 again.

2.3.6 Sorting CD8+ T cells using magnetic beads

CD8a+ Negative T Cell Isolation Kit (Order no. 130-104-075, Miltenyi Biotec) was used to sort T cells and was done according to protocol from the company. Briefly, cell were washed in MACS buffer (0.5% bovine serum albumin and 2 mM EDTA in PBS), incubated with antibody cocktail, followed by magnetic beads for 10 minutes each on ice. Cells were then loaded into a prewetted LS column (Order no. 130-042-401, Miltenyi Biotec) inserted into a magnet in approximately 3-5 mL MACS buffer.

2.4 Flow cytometry protocols

FACS buffer

For washing and staining cells for flow cytometry. PBS with PBS, 2% BSA, 0.1% NaN3 sodium azide.

Single stain controls

Single colour controls were either cells or OneComp Compensation Beads (Cat. no 01-1111-41, Thermo Fisher). One drop of beads was incubated with the same amount of antibody as one well of cells, incubated for 5 minutes, and washed in PBS.

Flow cytometers and data analysis

Cells were analysed on either Attune NxT (Life Technologies) or an LSR Fortessa X20 or X50 (BD Biosciences) in the WIMM Flow Cytometry Facility and data were analysed using FlowJo v10 (FlowJo) and R[186].

2.4.1 Table of antibodies used for flow cytometry in this study

Table. List of antibodies used in this study.			
Name	**Fluorophore(s)**	**Company**	**Clone**
CD3e	BV650	BioLegend	17A2
CD4	APC710	Tonbo Bioscience	GK1.5
CD4	BUV810	BD	GK1.5
CD8a	BV711	BioLegend	53-6.7
CD11a	PE	BioLegend	M17/4
CD11b	APC	BioLegend	M1/70
CD19	BV425	BioLegend	6D5
CD24	APC710	BD	M1/69
CD25	PerCP/Cy5.5	BioLegend	3C7
CD31	BV510	BD	MEC13.3
CD44	APC/Cy7, PE/Cy7	BioLegend	IM7
CD45.1	FITC	eBioscience	A20
CD45.2	PerCP/Cy5.5	BioLegend	104
CD49d	BUV395	BD	9C10
CD62L	BV610, FITC	BioLegend	Mel-14
CD69	BUV737	BD	H1.2F3
CD103	PE/Cy7	BioLegend	2E7
CD105	PE-CF594	BD	MJ7/18
CD162	BV421	BD	2PH1
EpCAM	APC/Cy7	BioLegend	G8.8
F4/80	BV610	BioLegend	BM8
FoxP3	BV421	BioLegend	MF-14
IFNy	PE	BioLegend	XMG1.2
Granzyme B	FITC	BioLegend	GB11
Ly6C	BV780	BioLegend	HK1.4
MHC-II	PerCP/Cy5.5	BioLegend	AF6-120.1
NRP1	BV421	BioLegend	3E12
NRP1	PE	BioLegend	3E12
PlexinA1	PE	R&D Systems	FAB4309P
PlexinA2	APC	R&D Systems	FAB5486A
PlexinA4	PE	R&D Systems	FAB58561P
Podoplanin	APC	BioLegend	8.1.1
TCRb	APC/Cy7	BioLegend	H57-597
TCRb	PE-CF594	BD	H57-597
TGFbRI	PE	R&D Systems	FAB5871P
TGFbRII	PE	R&D Systems	FAB532P
TNFa	PerCP/Cy5.5	BioLegend	MP6-XT22
Sema3A	FITC, PE	R&D Systems	IC1250P
VEGFR2	PE	BioLegend	Avas12
Zombie Violet Dye	BV421	BioLegend	
Zombie Aqua Dye	BV525	BioLegend	
Zombie Near-infrared	APC-780	BioLegend	

Table 2.1: List of antibodies used in this study.

2.4.2 Surface staining

Cells were harvested and pipetted into 96 U well plate, followed by wash in FACS buffer and centrifugation at 1500 rpm for 3 min. All subsequent wash step were per-

formed the same way.

For surface staining, cells were washed with 200 µl FACS Buffer and blocked in 100 µl Fc block (diluted 1:100) in FACS Buffer for 10 min on ice and washed. Antibody cocktail was added on top of cells and the two mixed by pipetting. Cells were stained on ice for at least 20 min, in the dark and washed twice. When applicable cells were fixed in 2% PFA for at least 10 min at RT before acquisition.

2.4.3 Intracellular staining

For intracellular staining, cells were fixed in 100 µl/well of FoxP3 IC Perm/fix Buffer (Cat. no 00-8222-49, Thermo Fisher) for 20 min at RT. Cells were pelleted, the fixative removed, and 200 µl/well of 1x Perm Buffer added for 20 min at RT and washed. Antibody mix were added and cells stained for at least 20 min on ice in Perm buffer and washed twice.

2.4.4 Preparation of tissue from mice for flow cytometry

When staining cells in B16.F10 and 3LL tumours, or from lungs or thymus, the following protocol was used. Mice were euthanized using CO_2, and tumours were harvested and stored in T cell media on ice. Organs were cut into smaller pieces with a scalpel and incubated for 30 minutes with reagents from a tumour dissociation kit (Order no. 130-096-730, Miltenyi Biotec). A single cell suspension was then created by straining the cells through a $70\,\mu\mathrm{m}$ nylon mesh using the blunt end of a syringe. Cells were washed off the mesh by applying 5 mL T cell media, following by mixing of the solution by aspiration. After a wash, the cells were resuspended in approximately 2 mL of

100% Percoll solution (Cat. no. 17-0891-01, GE Healthcare), and layered carefully on top of 3 mL of 80% and 40% Percoll solution, and spun for 30 minutes at 2000g. Cells at the 80-40% interphase was pipetted out and washed, and stained using protocols outlined above.

2.5 Mouse husbandry and handling

2.5.1 Mouse strains used in this thesis

All mice were sex-matched and aged between 6 and 12 weeks at the time of the first experimental procedure. All studies were carried out in accordance with Animals (Scientific Procedures) Act 1986, and the University of Oxford Animal Welfare and Ethical review Body (AWERB) under project licence 40/3636.

CD4-Cre mice were a gift from Katja Simons (NDM, University of Oxford). LifeAct mice were a gift from Shankar Srinivas (DPAG, University of Oxford). C57BL/6, OT-I and CD45.1 mice were purchased from Biomedical services, University of Oxford. NRP1-floxed mice were purchased from Jackson Laboratories (Stock No: 005247).

The following strains were created and used in this thesis: CD45.1×OT-I, CD4-Cre×NRP1, LifeAct×CD45.1×OT-I, CD45.1×CD4-cre×NRP1.

2.5.2 Injection of tumour cells into mice

Cells where split at 1:3 ratio 24 hours before injection into mice in order to keep cells in log-phase. 1-2 days before injection, mice were shaved on their flanks. On the day of injection, cells where trypsinized and washed 3 times in PBS to remove residual

FBS. Preparation of 1.5 $\times$ 10^5 cells in 100 uL PBS were prepared and kept on ice until injection. Mice were anesthetized using isoflurane and cells injected intradermally.

2.5.3 Adoptive transfer of T cells into mice

OT-I splenocytes were stimulated using peptides and sorted as described above, washed 2 times in PBS and injected i.v. via the tail vein.

2.5.4 Infection of mice with S-Flu H7N1

Mice were infected intranasally with 10^6 infectious units S-Flu H7N1 in 50uL viral growth media (DMEM with 2 mM Glutamine, 10 mM HEPES, 100 U/ml penicillin + 100 µg/ml streptomycin and 0.1% BSA) under anesthesia.

2.5.5 Injection of antibodies into mice

Anti-CD8a (cat. no. BE0061, clone 2.43, BioXcell) or IgG2b isotype control (cat. no. BE0090, clone LTF-2, BioXcell) were resuspended in PBS and injected intraperitoneally.

2.5.6 Mixed bone-marrow chimeras

To generate mixed bone marrow chimeric mice, male C57BL/6 host mice were lethally irradiated at 4.5 Gy for 300 seconds, followed by a 3 hour rest, and a subsequent 4.5 Gy dose for 300 seconds. Mice were injected i.v. with a 1:1 mixture CD45.1+ $NRP1^{Flox/+}$ and CD45.1+CD45.2+ $NRP1^{Flox/Flox}$ bone marrow. Recipient mice received drinking water containing antibiotics (0.16mg/mL Enrofloxacin (Baytril), Bayer Copo-ration). Mice were rested for 10 weeks before use.

2.6 RT-qPCR protocol

2.6.1 Protocol

RNA was extracted from cells using RNeasy kit (QIAGEN), followed by quantification on Nanodrop (Thermo Scientific). RNA was reverse transcribed using QuantiTect Reverse Transcription Kit (QIAGEN). Both controls without RNA or reverse transcription were included, and all experiments were performed in minimum technical triplicates and biological duplicates. cDNA was diluted to 10-20 ng in 5 ul/well and added to qRT-PCR plates. Taqman probes were combined with 2x Fast Taqman Master Mix and 5 ul/well added to the cDNA. qRT-PCRs were run on a QuantStudio7 qRT-PCR machine (Life Technologies). Expression was normalized to the house keeping gene HPRT.

The following TagMan probes were used in this thesis: BNIP3 (Mm01275600-g1), HPRT (Mm03024075-m1), PDK1 (Mm00554300-m1), PDL1 (Mm00452054-m1), SEMA3A (Mm00436469-m1) and VEGFA (Mm00437306-m1).

2.7 Western blot protocol

2.7.1 Protocol

Cells were washed in PBS and pelleted, before being resuspended in lysis buffer with a EDTA protease inhibitor for 30 minutes on ice to extract protein. Cell-debris was removed by centrifugation at 4°C. Supernatant containing protein was collected and quantified using Pierce BCA protein assay using diluted albumin as a standard.

Samples were mixed with 1x Loading Buffer (Life Technologies) and 1x Reducing

Agent (Life Technologies) and heated to 95°C for 5 minutes. 4-12% Bis-Tris gels and MES SDS Buffer (Life Technologies) were used for proteins with a molecular weight below 200 kDa, while proteins above 200 kDa were blotted on a 3-8% Tris-Acetate gels in MOPS Buffer (Life Technologies). Proteins were separated at 200V for approximately one hour and transferred onto either PVDF or nitrocellulose membrane using the TransBlot Turbo Transfer (BioRad) system. Gels were blocked in 5% milk PBS solution (blocking buffer) for 30 minutes at RT. Membranes were washed and stained with primary antibody in fresh blocking buffer and incubated at 4°C overnight on a shaker, washes five times in PBS with Triton-X followed by incubation with fluorescent secondary antibodies (LI-COR) diluted 1:20000 in blocking buffer for 1 hour on a shaker. Membrane were dried and imaged using the Odyssey Near-Infrared imaging system (LI-COR).

2.8 CRISPR/Cas9 editing of cells

A sgRNA targeting Sema3a was cloned into Cas9-2A-EGFP expression vector pX458. This vector was electroporated into $1x10^6$ B16.F10.Ova cells suspended in Solution V (Lonza) using the Amaxa 2B nucleofector (Lonza) with settings P-020. After 48 hours, single cells were sorted using the SH800 cell sorter (SONY) and expanded. Clones were genotyped by high-throughout sequencing. Briefly, the targeted locus was PCR amplified from each clone and subsequently indexed with a unique combination of i5 and i7 adaptor sequences. Indexed amplicons were sequencing on the MiSeqV2 (Illumina) and demultiplexed reads from each clone were compared to the wildtype Sema3a reference sequence using the CRISPResso webtool.

2.9 Lentiviral transduction of cells

A lentiviral Sema3A overexpression vector was purchased from VectorBuilder. To generate viral particles, this transfer vector was co-tranfected into HEK-293T cells along with the packaging and envelope plasmids pCMV-dR8.91 and pMD2.G using polyethylenimine. Crude viral supernatant was filtered and used to transduced B16.F10.Ova cells. Transduced cells were selected by FACS using the SH800 cell sorter (SONY) to create a Sema3A overexpression cell line.

2.10 Immunofluorescence staining

Immunofluorescence staining was performed on frozen sections of tumour, that had been flash frozen in OCT (Tissue Tek). Sections were cut at 10 uM thickness using a cryostat.

For immunofluorescence, sections were acetone fixed, background peroxidase was quenched with H_2O_2, and stained as follows: 1 hour nonspecific blocking from Vectastain Mouse on Mouse Kit (Vector Laboratories) in 0.3% Triton-X in PBS, wash, 30 min endogenous mouse immunoglobulin block (Vector Laboratories), wash, 2 hour incubation with primary antibodies anti-Sema3A PE (R&D Systems) and TCRb AF647 (BioLegend), in 0.1% Triton-X in PBS. Staining was conducted at room temperature in the dark. Nuclei were visualized with ProLong Diamond Antifade Mountant with DAPI (Invitrogen).

Images were acquisitioned using a Zeiss LSM780 confocal microscope, using a Zeiss Plan-Neofluar 63x (1.3 NA) lens and analyzed in Fiji/ImageJ.

2.11 Live-cell imaging of cells

2.11.1 Preparation of plates and chambers

u-Slide I 0.4 Luer (Cat. no. 80172, Ibidi), u-Slide 8 well (Cat. no. 80826, Ibidi) and u-Slide Angiogenesis (Cat. no. 81506, Ibidi) were used for live-cell imaging of T cell motility and synapse formation.

Proteins were immobilized on the plates by resuspension in PBS and allowing them to adhere either overnight at $5\,^{\circ}\mathrm{C}$ or for 2 hours as room-temperature, followed by three washes in PBS with 1-2% BSA. The following proteins and concentrations were used: ICAM-1-Fc (Cat. 553006, BioLegend, at 10ug/mL), CD3 (clone 145-2C11, BioLegend, at 10ug/mL), CXCL12 (Cat. 578702, BioLegend, at 0.4 ug/mL, BioLegend), Sema3A and Sema3A-mutant[171] (at 10-50 ug/mL). Plates were used immediately after preparation.

2.11.2 Analysis of cell motility and synapse formation on 2D surfaces

T cells were activated for 48 hours using peptide stimulation, sorted and washed. In cases were αNRP1 or isotype control treatment was applied, T cells were incubated with these antibodies for 15 minutes at $37\,^{\circ}\mathrm{C}$, before an additional wash. T cell media without phenol red was prewarmed and used with no IL-2 added to resuspend cells. Cells were added to plates placed in stage in environmental chamber set at $37\,^{\circ}\mathrm{C}$ directly at the microscope. DeltaVision Elite Live cell imaging microscope, Zeiss LSM 780 or 880 confocal microscopes were used with a Zeiss Plan-Neofluar 10x (0.3 NA), 40x (0.6 NA)or 63x (1.3 NA) lens.

In cases where T cells were tested under shear stress, cells were loaded into Hamilton syringes, and installed on an Harvard Apparatus PHD 2000 pump, and connected to chambered slides through 0.4 luer tubes. Flow rates and control of directionality of flow (ie, that it was laminar) were measured using fluorescent beads over set distances.

In cases were T cells were treated with drugs, these were first resuspended in T cell media and carefully added on top of solution while images were being acquired. Care was taken always to take into consideration the correct concentration under growing levels of media. The following drugs were used: Jasplakinolide (Cat. J4580, Sigma, used at 5uM) and Blebbistatin (Cat. 203390, EMD Millipore, used at 100 uM), as well as Sema3A (at 10-50 ug/mL).

Data was acquired at 20 sec to 1 minute pr. frame and analyzed in Fiji/ImageJ[187] using the Trackmate package[188]. Subsequent tracks were analyzed in R[186] and visualized using the ggplot2 package[189]. For cell contours, IRM and LifeAct, data was thredsholded and collected in Fiji/ImageJ, exported to R and analyzed there.

2.12 Transwell chemotaxis assay

Trans-migration was assessed in 24-well transwell plates with 3-μm pore size (Corning Life Sciences). The lower chamber was loaded with 500 μl T cell medium with 10 IU IL-2 and with or without 50 ng/mL CXCL10. 10^5 CD8+ T cells cells (Stimulated and sorted OT-I CD8+ cells) were added in a volume of 100 μl of T cell medium to the upper chamber, in either the presence of a blocking αNRP1 antibody or an isotype control, and 50ug/mL Sema3A. As a positive control, effector cells were placed directly into the lower chamber. As a negative control, migration medium alone was placed in the upper

chamber. Plates were incubated for 3 h at 37 °C in a 5% CO_2 atmosphere. Thereafter, the Transwell inserts were removed and the contents of the lower compartment were carefully recovered. Cells from the lower chamber were stained and the cells were quantified by flow cytometry.

2.13 Immunological synapses analysis on supported lipid bilayers

2.13.1 Generation of supported lipid bilayers (SLB)

The concentrations of the ligands used were as follows: 5 µg/ml to achieve 10 molecules/µm2 of biotinylated H2Kb-SIINFEKL, 68 ng/ml to achieve 100 molecules/µm2 of 12x-His-tagged CD80 (AF488-labelled), and 122 ng/ml to achieve 200 molecules/µm2 of 12x-His tagged ICAM-1 (AF405-labelled). These concentration were arrived at based on titrations on bead supported bilayers analyzed by flow cytometry.

2.13.2 Protocol

For live cell imaging, SLB presenting H2Kb-SIINFEKL (made by Uzi Giliadi and Jili Chen, Vincenzo Cerundolo group, University of Oxford), CD80, and ICAM-1 were assembled in sticky-Slide VI 0.4 luer (Ibidi) channels. The entire channel was filled with a liposome suspension to form bilayer all along the channel. Live cells on SLBs were imaged using the Olympus FluoView FV1200 confocal microscope that was enclosed in an environment chamber at 37 °C and operating under standard settings. 60x oil im-

mersion objective (1.4 NA) was used with 2x digital zoom for time-lapse imaging at 20 second intervals.

For fixed cell imaging, SLBs presenting H2Kb-SIINFEKL, CD80, and ICAM-1 were assembled in 96-well glass-bottom plates (MGB096-1-2-LG-L, Brooks). 50,000 cells were introduced into the wells at 37 °C and fixed 10 minutes later by adding 8% PFA in 2x PHEM buffer. After 3 washes with 0.1% BSA (in HBS) the fixed cells were imaged on the InCell 6000 wide-field fluorescence high-throughput imaging station using a 40x air objective (0.75 NA). The imaging station was programmed to visit specific equivalent locations in each of the desired wells in the 96-well plate.

2.13.3 Analysis of images

Analysis of fixed cell images was carried out by the MATALB based TIAM_HT package[190]. The source-code is available on the github repository: https://github.com/uvmayya/TIAM_HT.

2.14 T cell—cancer cell coculture assay

T cells were stimulated using peptides for 48 hours, sorted and allowed to rest for an additional 48 hours in fresh T cell media with 100 IU IL-2 added every day. B16.F10.Ova Sema3A KO and Sema3A OE cell-lines were washed three times in PBS, mixed 1:1 and re-plated in a flat 96-well plate at 20.000 cells pr. well, and allowed to settle for 2 hours at 37 °C in a 5% CO_2 atmosphere. Following this, T cells were added at effector:target ratios of 0, 1:1, 3:1, 9:1 or 18:1, in biological triplicates and technical duplicates. 24 hours later, cancer cells were removed from the plate, stained with live-dead markers and analyzed

on a flow cytometer in association with counting beads. Because Sema3A OE is mCherry positive and Sema3A KO is GFP positive, cells could be distinguished from each other.

2.15 IHC staining of ccRCC sections

Consecutive sections were cut by the Oxford Radcliffe Biobank and analyzed by trained patologists there.

Automated staining was carried out at the Experimental Cancer Medicine Centre, using the Leica BOND-MAX autostainer (Leica, Microsystem) using the following conditions: antigen retrieval at 100 °C for 20 min with Epitope Retrieval Solution 2 (AR9640, Leica Biosystems). Primary antibody incubation for 30mins with CD31 (clone MO823, DAKO, diluted 1/800), Sema3A (EPR19367, Abcam, diluted 1/100) and CD8 (clone M7103, DAKO, diluted 1/100) and detected using the BOND Polymer Refine Detection System (DS9800, Leica Biosystems) as per manufacturer's instructions.

Matching 2mm x 2mm regions were then selected by Dr. Philip Macklin from each three slides pr. patient, based on manually defined reference points. The image analysis was then performed by Joshua A. Bull, who briefly did the following to quantify cell numbers and staining: machine learning classifiers were trained using support vector machines using MATLAB and used to quantify CD8 T cell numbers as well as Sema3A and CD31 staining.

2.16 CT-tetramer staining

HLA-A2 monomers were made by Jili Chen (Cerundolo lab, RDM, University of Oxford), and loaded with CT-antigens through UV-directed ligand exchange using published protocols[191] by Margarida Rei and Victoria Woodcock.

Following ligand exchange, all monomers were tetramerized through binding to PE-Streptavidin, washed, and combined to allow for ”cocktail” staining of cells. Frozen veils of tumour tissue were thawed, dissociated, and CD45-positive sorted, followed by staining with 0.5 µg of each tetramer in 50 ul for one hour at RT. Otherwise staining happened like described previously.

2.16.1 List of CT-tetramers used in cocktail

Ligand	Antigen
MLMAQEALAFL	LAGE-1
SLLMWITQC	LAGE-1
SLLMWITQA	NY-ESO-1
KVLEYVIKV	MAGE-A1
GLYDGMEHL	MAGE-A10
YLQLVFGIEV	MAGE-A2
FLWGPRALV	MAGE-A3
KVAELVHFL	MAGE-A3
FLWGPRALV	MAGE-A3
ALKDVEERV	MAGE-C2
KVLEFLAKL	MAGE-C2
LLFGLALIEV	MAGE-C2
ELAGIGILTV	MART1
TLNDECWPA	Meloe-1
AMAPIKVRL	PRDX5 (OMT3-12)
LKLSGVVRL	RAGE-1
KASEKIFYV	SSX2
SVYDFFVWL	TRP2
YMDGTMSQV	Tyrosinase
CQWGRLWQL	BING4
VLPDVFIRCV	GnT-V

Table 2.2: List of CT-antigens used in staining cocktail.

2.17 Statistical analysis

Statistical analysis was performed in Prism software (GraphPad). Data was tested for Gaussian distribution. For multiple comparisons, either one-way or two-way analysis of variance (ANOVA) was used with Tukey's test to correct for multiple comparisons. For comparison between two groups, Students t test, Student's paired t test, or one-tailed or two-tailed Mann–Whitney test were used.

Chapter 3

NRP1 is Upregulated on Tumour-specific CD8+ T cells

3.1 Introduction

T cells are often restricted to certain areas in tumours or excluded from the tumour micro-environments completely[153]. Unfortunately, little is known about the molecular underpinnings of this restriction. We noticed that cell-based repulsion plays a major role during embryogenesis[176] and that a number of pathways normally associated with neuronal development have been described to affect leukocyte migration[139–141]. Typically these repulsion systems function via a range of secreted factors that bind to receptors on migrating cells, such as developing neurons or endothelial cells. When cells enter areas containing these secreted factors, the cellular cytoskeleton is affected in profound ways, often through Rho-family members, causing the cells to either arrest their migration or retract from the environment[176, 192].

One major cell repulsion system involved in vascular and neural development is the Semaphorin family [193]. Recently it has emerged that Semaphorins are also expressed in tumours [194]. We therefore hypothesized that Semaphorins could play a role in T cell-tumour interactions, specifically that Semaphorins could restrict T cells from migrating freely in tumours.

To explore this, we first conducted an *in silico* screen using publicly available data [195] to search for all known Semaphorin receptors on naive and activated T cells. While most semaphorin receptors had limited expression on naive T cells, one receptor, NRP1, was significantly upregulated following T cell activation. We confirmed that this was also the case at the protein level and that a majority of tumour-specific T cells retained high expression of the receptor *in vivo*. NRP1 is a promiscuous co-receptor with little signaling capacity itself. Instead the receptor increases the binding affinity of other receptors when they dimerize[171]. We tested for expression of known NRP1 co-receptors and identified Plexin-A1 as the major co-receptor present on CD8+ T cells. The ligand for the NRP1:Plexin-A1 receptor complex is the secreted protein called Sema3A. Using recombinant Sema3A, we confirmed that stimulated CD8+ T cells could indeed bind the ligand.

3.2 NRP1 is upregulated on OT-I T cells following activation

3.2.1 *In silico* screen reveals NRP1 as dominant Semaphorin receptor on activated CD8+ T cells

In order to identify possible Semaphorin receptors on T cells, we first performed an *in silico* analysis using publicly available data from the Immunological Genome Project Consortium, published in Best et al [195]. In this study OT-I T cells, which have transgenic expression of a TCR specific for the model antigen ovalbumin (OVA), were adoptively transferred into C57BL/6 mice and subsequently activated with an OVA-expressing strain of *Listeria monocytogenes*. Splenic CD8+ T cells were then collected 5, 8, 10, 15, 45 or 100 days later, bulk sorted and their mRNA sequenced alongside naive OT-I T cells. This allowed for comparison between naive and progressively activated T cells, which was useful, as many receptors involved in regulating T cell are up-regulated following activation. As can be seen from Figure 3.1A, the receptor NRP1 was significantly up-regulated in effector CD8+ T cells, similarly to the level of PD-1 (*Pdcd1*).

3.2.2 Expression level of NRP1 on the cell surface of CD8+ T cells is dependent on level of TCR engagement

We next explored whether this transcriptional upregulation also resulted in increased expression at the protein level and on the membrane of OT-I T cells. To this end we performed two complementary experiments. First we activated OT-I T cells

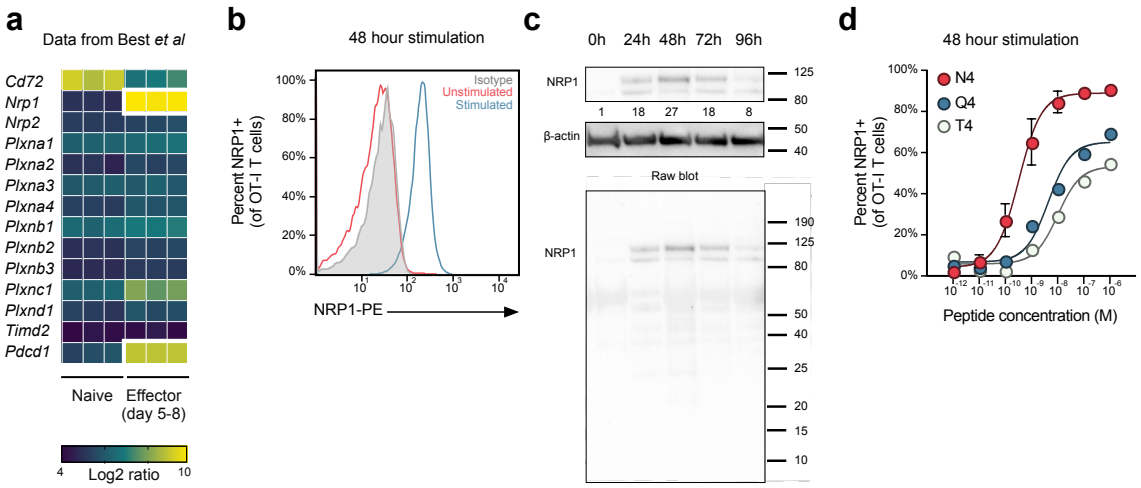


Figure 3.1: **NRP1 is upregulated on OT-I T cells following activation. A**. Analysis of transcript levels of Semaphorin-receptors on CD8+ OT-I T cells reveals NRP1 upregulation. PD-1 (*Pdcd1*) included as reference. Data from Best et al [195]. **B**. Flow cytometric analysis of surface NRP1 expression on OT-I T cells following 48 hours stimulation with SIINFEKL. Cells are gated on CD45.1, CD8 and TCRβ. Representative histogram of more than three biological repeats. **C**. Western blot confirms NRP1 upregulation in OT-I T cells is mainly of larger isoform, with peak expression 48 hours after stimulation start. Experiment was performed once. **D**. NRP1 upregulation is dependent on strength of peptide:MHC interaction, as revealed by flow cytometric analysis following OT-I T cell activation with peptides with varying TCR affinities. N4, SIINFEKL. Q4, SIIQFEKL. T4, SIITFEKL. Cells are gated on CD45.1, CD8 and TCRβ. N=3 per group, experiment was performed once. Data indicate mean ± SD.

with the OVA-derived peptide SIINFEKL for 48 hours, and performed flow cytometric analysis of the cells to quantify levels of NRP1. As can be seen from Figure 3.1B, NRP1 is uniformly upregulated on stimulated, but not naive T cells. This result was confirmed by western blot (WB) using a different antibody clone, which also revealed that the expression of NRP1 peaked 48 hours after stimulation start, with the larger isoform of the protein being dominant in CD8+ T cells (Figure 3.1C). Because of this, most subsequent *in vitro* experiments with OT-I T cells were done after 48 hours of stimulation, unless

otherwise stated.

We wanted to examine if the upregulation of NRP1 was dependent on the strength of TCR engagement. We selected two additional peptide ligands derived from the original OT-I ligand SIINFEKL (N4), namely SIIQFEKL (Q4) and SIITFEKL (T4) to stimulate OT-I T cells. All three ligands have the same affinity for the murine MHC H-2K^b, but differ in their ability to stimulate OT-I T cells, with N4 being approximately 18 and 71 times as potent as Q4 and T4, respectively [90]. This system allows for precise interrogation of the effects TCR engagement have on the expression of NRP1. Using varying concentrations of all three ligands, NRP1 was seen to correlate with both concentration and strength of T cell stimulation.

We also tested NRP1 expression following either phorbol myristate acetate (PMA) and calcium ionophore ionomycin, phytohaemagglutinin P (PHA) or CD3/CD28 activation. While CD3/CD28 activation consistently lead to upregulation of NRP1, PMA/ionomycin and PHA did not (data not shown).

Taken together, we conclude that the Semaphorin co-receptor NRP1 is upregulated in a TCR-dependent manner.

3.3 NRP1 is expressed on tumour-specific OT-I T cells *in vivo*

We wanted to explore whether the expression of NRP1 was retained on tumour-specific T cells. For this we turned to the B16.F10 melanoma model, which has been extensively used in tumour-immunology studies in the past [196]. The B16.F10 cell-

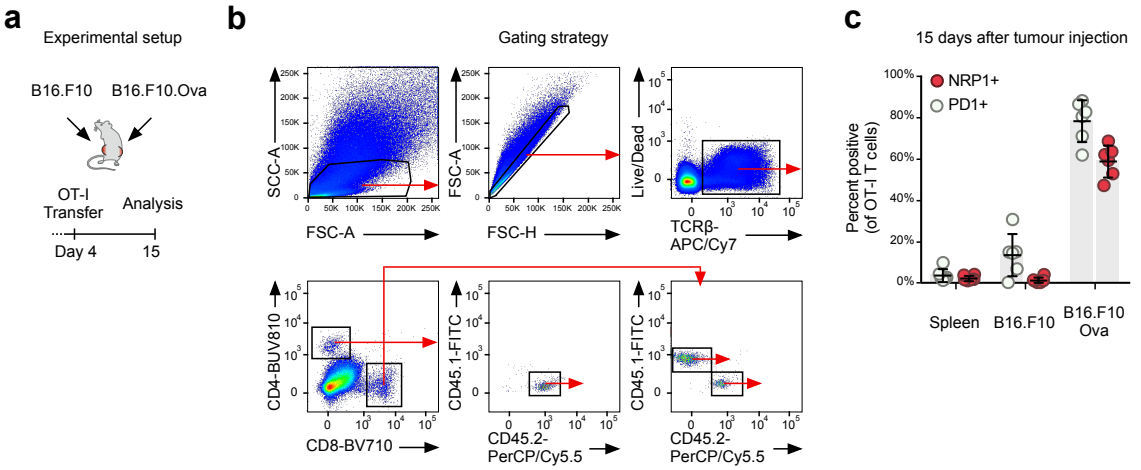


Figure 3.2: **NRP1 is expressed on tumour-specific OT-I T cells. A-B**. Experimental setup and gating strategy used to interrogate NRP1 expression on tumour-specific OT-I T cells. **C**. Expression PD-1 and NRP1 on OT-I T cells in spleen, non-antigen expressing tumour (B16.F10) and antigen-expressing tumour (B16.F10.Ova). N=6, experiment was performed twice. Data indicate mean ± SD.

line was first cultured from a spontaneously arising melanoma in C57BL/6 mice and is generally thought of as being hard to treat. A B16.F10 cell-line expressing the OVA-antigen was generated in such a way that the antigen was not secreted (see materials and methods). This allowed for dual injection of the B16.F10 and B16.F10.Ova cell-lines in opposing flanks of C57BL/6 mice, followed by adoptive transfer of 48 hour stimulated OT-I T cells, as outlined in Figure 3.2A. The OT-I mice were back-crossed onto a CD45.1 background, allowing for easy separation of adoptively transferred OT-I T cells and endogenous T cells by flow cytometry (see gating strategy in Figure 3.2B).

15 days post tumour injection, the OT-I T cells localized in the antigen-positive B16.F10.Ova tumour expressed NRP1 to a high degree (approximately 60% of cells) as well as PD-1 (approximately 80%). In the same mice however, on OT-I T cells found in either spleen or the antigen-negative B16.F10 tumour, NRP1 could not be detected.

3.4 Activated and tumour-specific OT-I T cells expressed the NRP1 co-receptor Plexin-A1

3.4.1 *In vitro* activated OT-I T cells express the NRP1 co-receptor Plexin-A1

NRP1 is a co-receptor for multiple other receptors, but due it's small cytoplasmic tail consisting of only 21 amino acids, does not convey any signaling itself. Instead it's downstream effects are determined by which co-receptor it dimerizes with and the availability of their shared ligand. When this study started, a number of known NRP1 co-receptors had been described, including Plexin-A1, -A2, -A3 and -A4 [171, 197], vascular endothelial growth factor alpha receptor II (VEGFαRII) [193, 198, 199] and transforming growth factor beta receptor I (TGFβRI) and TGFβRII [200] (Figure 3.3A). The PlexinA family mediate Semaphorin signaling, while VEGFαRII and TGFβRI/TGFβRII mediate VEGFα and TGFβ signaling, respectively.

Since both VEGFα and TGFβ have been shown to affect CD8+ T cell function in tumours [201–203], we wanted to explore whether these receptors were co-expressed on NRP1+CD8+ T cells, in addition to the Plexin-A receptors.

We attempted to avoid steric hindrance from NRP1 by choosing antibodies for the co-receptors that targeted regions of the protein outside known interaction-sites between NRP1 and the protein. While this was possible for TGFβRI, TGFβRII and VEGFαRII, most Plexin-A antibodies either targeted potential interaction regions or the company would not supply information about which part of the protein they had used for immunization. We therefore tested and titrated all antibodies against tissue known to express the pro-

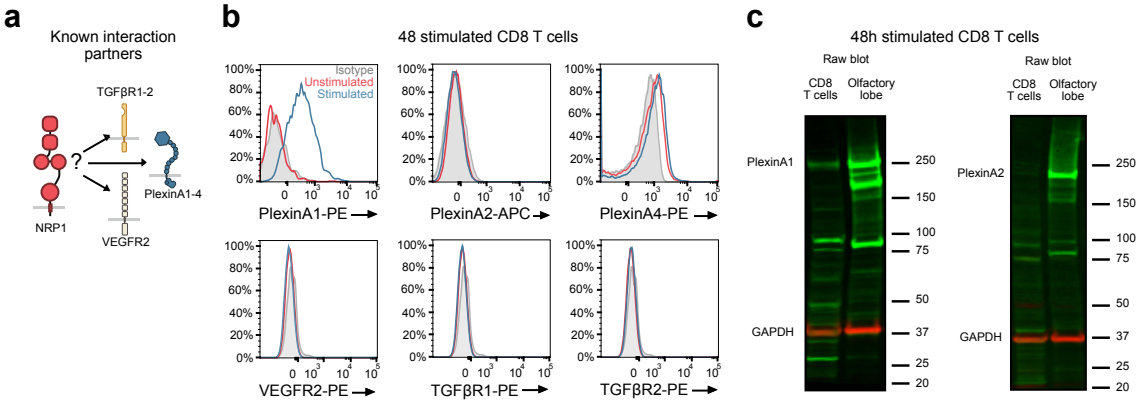


Figure 3.3: **Plexin-A1 is expressed on OT-I T cells following *in vitro* activation. A**. Schematic of known NRP1 interactions partners. **B**. Flow cytometric analysis of NRP1 interactions partners reveals upregulation of Plexin-A1, but not other co-receptors, on stimulated OT-I T cells. Cells are gated on CD45.1, CD8 and TCRβ. N=1, experiment was performed three times. **C**. WB confirms expression of Plexin-A1 in stimulated OT-I T cells. Olfactory lobe used as positive control. Experiment performed twice.

teins to ensure their specificity. For Plexin-A1, -A2 and -A4, neurons from the olfactory lobe and thalamus proved good positive controls as they also express NRP1; however, positive staining could not be seen for Plexin-A3 in olfactory lobe, thalamus, eye, spleen or gallbladder, and so this protein will not be described further. For both VEGFαRII, TGFβRI and TGFβRII, endothelial cells in heart and lung proved good controls.

Following this, we stimulated OT-I T cells with SIINFEKL for 48 hours and analyzed the cells by flow cytometry. The only protein that was significantly expressed on OT-I T cells at this time-point was Plexin-A1 (3.3B). We confirmed this result by WB, showing that indeed Plexin-A1, but not PlexinA2, was expressed after stimulation on OT-I T cells.

3.4.2 Tumour-specific OT-I T cells express Plexin-A1, and to a less extend, TGFβRII

Next we wanted to validate our *in vitro* findings using our B16.F10.Ova tumour model. Using the same experimental setup and gating as described in 3.2A-B, we repeated our screen of co-receptors, albeit in a smaller scale, focusing on Plexin-A1, A2, TGFβRI and TGFβRII.

15 days post tumour injection, we harvested tumours and analyzed both adoptively transferred OT-I T cells as well endogenous CD8+, CD4+ and regulatory CD4+CD25+FoxP3+ T cells. This experiment confirmed that tumour-specific OT-I T cells retained expression of Plexin-A1 (on an average of 80% of all cells), but also had an increased expression of the co-receptor TGFβRII (on an average of 20% of cells) (Figure 3.4A).

In a separate experiment, we co-stained TILs OT-I T cells with both NRP1 and Plexin-A1 antibodies, and saw good co-expression of the two receptors on these T cells (Figure 3.4B).

Interestingly, the expression on the endogenous CD4+ and CD8+ T cells that had infiltrated the B16.F10.Ova tumour, resembled the expression pattern we observed in our tumour-specific OT-I T cells (Figure 3.4C), with Plexin-A1 being upregulated on a subset of these cells. While this was also the case for regulatory CD4+CD25+FoxP3+ T cells, they also expressed high levels of both TGFβ-receptors.

Taken together with our *in vitro* data, we conclude that the main NRP1 co-receptor on CD8+ tumour-specific T cells is Plexin-A1.

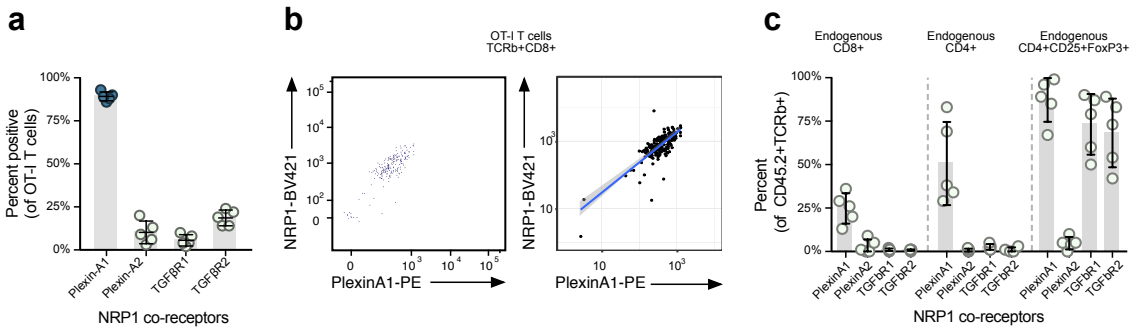


Figure 3.4: **Plexin-A1 and TGFβRII is expressed on tumour-specific OT-I T cells infiltrating B16.F10.Ova tumours. A**. Tumour-specific OT-I T cells express Plexin-A1, and to a less extent TGFβRII in B16.F10.Ova tumours. Cells are gated on CD45.1, CD8 and TCRβ. N=5, experiment was performed once. Data indicate mean ± SD. **B**. Representative scatter plot of NRP1 and Plexin-A1, which are co-expressed on tumour-specific OT-I T cells in B16.F10.Ova tumours. Cells are gated on CD45.1, CD8 and TCRβ. N=5. **C**. Analysis of NRP1 co-receptors on endogenous T cells show that a subset of CD8+ and CD4+ T cells express Plexin-A1, but that most CD4+CD25+FoxP3+ T cells express both Plexin-A1, TGFβRI and TGFβRII. N=5, experiment was performed once. Data indicate mean ± SD.

3.5 NRP1-positive OT-I T cells can bind recombinant Sema3A

The main ligand for Plexin-A1:NRP1 is the secreted protein Sema3A. Surface plasmon resonance experiments have previously shown that Sema3A binding requires both NRP1 and a PlexinA member to associate and dimerize[171]. Since we had found both NRP1 and Plexin-A1 on the cell surface of activated OT-I T cells we wanted to test if these cells indeed could bind Sema3A.

We used a murine recombinant Sema3A protein made in professor Yvonne Jones laboratory which contained the Sema-binding domain, the PSI-domain of the protein and a HIS-tag. The structure of this recombinant protein has been solved, and it has

been shown to fold correctly and be biologically active[171]. Analysis showed that the protein was found in both a dimerized and monomeric form (data not shown).

Cells were incubated with the protein for 15 minutes on ice, fixed with 4% PFA and analyzed using flow cytometry. As expected, 48 hour stimulated (NRP1/Plexin-A1 positive) cells, but not naive (NRP1/Plexin-A1-negative) OT-I T cells, bound Sema3A in a dose-dependent manner (Figure 3.5A). The cells that bound Sema3A could additionally be seen to be mainly NRP1 positive (Figure 3.5, left), confirming that this receptor is indeed important for Sema3A binding.

We also wanted to test Sema3A binding under more physiological conditions. To this end we labelled Sema3A with Alexa fluorophore 647 (AF647). Calculations showed a 1.5/1 fluorescent protein to protein ratio. Stimulated OT-I T cells were then incubated with Sema3A in a standard incubator (37 °C and 5% CO_2) in T cell media for 1 hour, washed and live cells visualized using confocal microscopy. As can be seen in Figure 3.5B, Sema3A bound to the membrane of cells, but also that some cells had internalized the protein. Most likely the punctate dots seen in these cells, is Sema3A being degraded in autophagosomes.

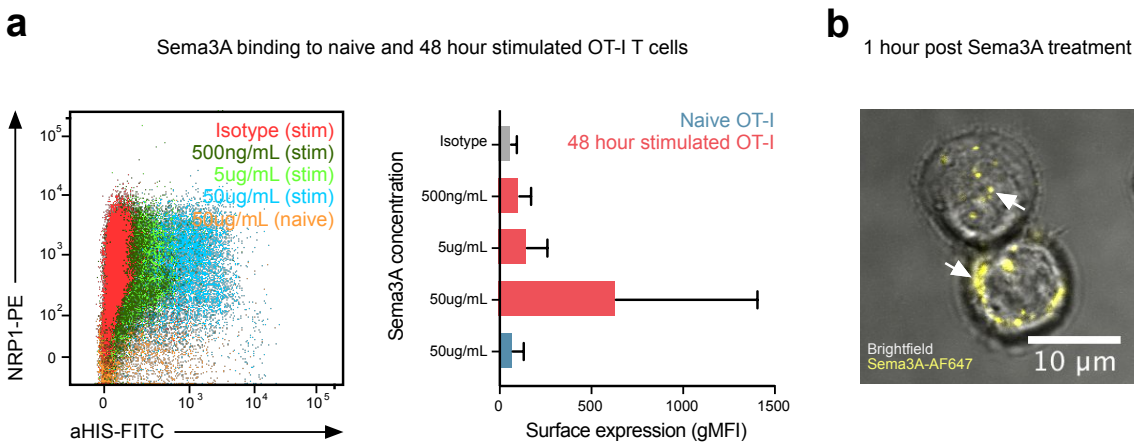


Figure 3.5: **Stimulated, but not naive, OT-I T cells can bind Sema3A. A**. Left: Representative scatter plot. Cells were stained with varying concentrations of Sema3A. While stimulated OT-I T cells showed binding starting at low concentrations of Sema3A, naive T cells did not bind Sema3A even at high concentrations. Cells binding Sema3A can be seen to NRP1 positive. Right: Quantification of surface level expression show that stimulated, but not naive, OT-I T cells bind Sema3A. Cells are gated on CD8 and CD3. Experiment was repeated three times. Data indicate mean ± SD. **B**. Confocal imaging with 48 hour stimulated OT-I T cells stained with AF647-labelled Sema3A show that the protein can bind to the cell membrane (lower white arrow), but punctuate dots in cells indicate that it's also internalized and degraded (upper white arrows). Experiment was performed once.

3.6 Discussion

In this chapter we have explored which Semaphorin receptors are expressed on tumour-specific T cells, using the OT-I-OVA model system. *In silico*, *in vitro* and *in vivo* experiments all point to the receptor pair NRP1 and Plexin-A1 being the major Semaphorin receptors present on CD8+ T cells. Their expression level seem to correlate with level of TCR engagement as shown by our peptide titration experiments and the fact that their expression is retained more long term on OT-I TILs present in antigen-positive tumours, but not in antigen-negative tumours. The upregulation of these receptors al-

lows Sema3A to bind to CD8+ T cells.

A few points from these experiments are worth dwelling on. Primarily, the fact that CD8+ T cells express NRP1 is surprising, as a number of publications claim that NRP1 is not expressed by CD8+ T cells[204, 205]. The receptor has been extensively described on regulatory CD4+CD25+FoxP3+ T cells, but here the receptor is thought to be regulated by TGFβ and identify a special subset of cells[204, 206]. On CD8+ T cells, expression seems to match the level of TCR engagement completely and as such could be thought of as simply an ”activation marker”. As noted above, the effect NRP1 can have on cells is dependent on the availability of co-receptors and their shared ligands. Our experiments show that on CD8+ TILs, Plexin-A1 is the main receptor available for dimerization and downstream signaling. However regulatory T cells found in tumours also express high levels of TGFβRI and TGFβRII, which leaves open the possibility that NRP1 expression could have different effects on different T cell subsets.

Following these initial experiments, we next asked what role NRP1 play on T cells in viral infections and in tumour settings.

Chapter 4

NRP1 Deficiency Enhances Anti-tumour Activity of CD8+ T cells

4.1 Introduction

Following our discovery that NRP1 was expressed on tumour-specific CD8+ T cells, we next wanted to explore what role NRP1 played in T cell—tumour interactions.

Three other groups have explored NRP1's role on T cells using *in vivo* tumour models. These groups have either focused on NRP1's role on regulatory CD4+CD25+FoxP3+ T cells while ignoring CD8+ T cells[175, 204], or explored NRP1's role in T cell tolerance[207]. Little is therefore currently known about the direct role of NRP1 on CD8+ T cells ability to function in the TME. However, a number of *in vitro* studies all point to NRP1 playing important roles in regulating T cell function, although they come to divergent conclusions: Jackson et al[207] claim that NRP1 plays no role in CD8+ T cells cytolytic potential; Wallerius et al[208] that the NRP1-ligand Sema3A enhances CD8+ T

cell responses; while Catalano et al[209], Lepelletier et al[210] and Yamamoto et al[211] find that NRP1 or Sema3A negatively regulates T cell responses. This latter point is supported by autoreactivity studies using the experimental autoimmune encephalitis (EAE) model in NRP1-deficient mice[212].

To explore this further we created T cell conditional NRP1 knockout mice. We first examined their development and ability to react to influenza infection. Next we challenged mice with two different tumour cell-lines, B16.F10 and 3LL, and discovered that mice with NRP1-deficient T cells inhibited the growth of both cell-lines. Examining the tumours closely, we noticed that the main difference between genotypes was the number of infiltrating CD8+ T cells. We tested this hypothesis by first depleting all CD8+ T cells in our NRP1-deficient mice, followed by creation of bone-marrow chimeras and finally by over-expressing the ligand, Sema3A, in B16.F10.Ova cells.

4.2 NRP1-conditional knockout mice develop normally

4.2.1 Generation of T-cell-specific NRP1 knockout mice

In order to interrogate the role of NRP1 on CD8+ T cells, we crossed CD4-Cre mice to $NRP1^{Flox/Flox}$ mice to generate CD4-Cre$\times NRP1^{+/+}$ ($NRP1^{+/+}$), CD4-Cre$\times NRP1^{Flox/+}$ ($NRP1^{Flox/+}$) and CD4-Cre$\times NRP1^{Flox/Flox}$ ($NRP1^{Flox/Flox}$) mice. CD4-Cre and $NRP1^{Flox/Flox}$ mice have been used in published work before[193, 213] and are on a C57BL/6 background.

Since all T cells go through a CD4 and CD8 double-positive phase while developing

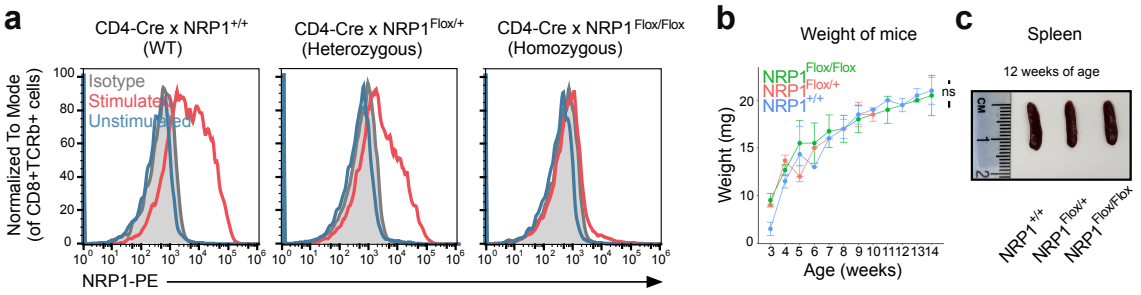


Figure 4.1: **NRP1-conditional knockout mice develop normally.** **A**. Flow cytometric analysis of naive or CD3/CD28 stimulated splenocytes from either NRP1$^{+/+}$, NRP1$^{Flox/+}$ or NRP1$^{Flox/Flox}$ mice. Representative histograms show that NRP1 expression is abrogated in stimulated CD8 T cells in NRP1$^{Flox/Flox}$ mice. Cells are gated on CD8 and TCRβ. Experiment performed more than three times. **B**. The weight of littermates (n=17) were followed for 12 weeks, and revealed no difference between genotypes. Data indicate mean ± SD. **C**. The size of spleens from littermates mice of different genotypes at 12 weeks of age. Experiment performed twice.

in the thymus, this breeding strategy removes NRP1 on all mature T cells, including stimulated CD8+ T cells as can be seen in Figure 4.1A.

4.2.2 NRP1-conditional knockout mice develop normally

We followed the growth and development of NRP1$^{+/+}$, NRP1$^{Flox/+}$ and NRP1$^{Flox/Flox}$ mice. All mice grew at similar rates (Figure 4.1B). We did not detect any splenomegaly, enlarged lymph nodes or other gross anatomical differences when dissecting the mice at 12 weeks of age (Figure 4.1). The mice bred as would be expected and we did not record any unexpected deaths while housing them up till 6 months of age.

4.2.3 NRP1-conditional knockout mice generate similar output and subset of T cells in thymus and spleen

Reports have implicated NRP1 in thymocyte migration[214, 215]. We therefore examined the different thymocyte compartments T cells move through during their development. Thymocytes follow a distinct developmental trajectory as first CD4/CD8 double negative, then double positive, before finally becoming either CD4 or CD8 single positive. If output was stalled at any point, we would expect a high percentage of cells in the previous stage. However, this was not the case, with all genotypes having equal distribution of cells in the different thymocyte groups (Figure 4.2A). We also examined the double negative stage more carefully using the markers CD44 and CD25, but again saw no difference between genotypes.

Additionally, when examining the splenic distribution of CD4+ and CD8+ T cells, we noticed no difference between genotypes. The markers CD44 and CD62L can be used to distinguish between effector subsets of T cells, dividing the cells into naive, effector or memory cells[216]. Using these markers, we found no difference in the percentage of cells in different effector subsets in CD4+ or CD8+ T cells in the spleen (Figure 4.2B).

Hence, in terms of cell numbers, we did not find any differences in thymic and splenic production of CD4+ and CD8+ T cells in $NRP1^{+/+}$, $NRP1^{Flox/+}$ and $NRP1^{Flox/Flox}$ mice.

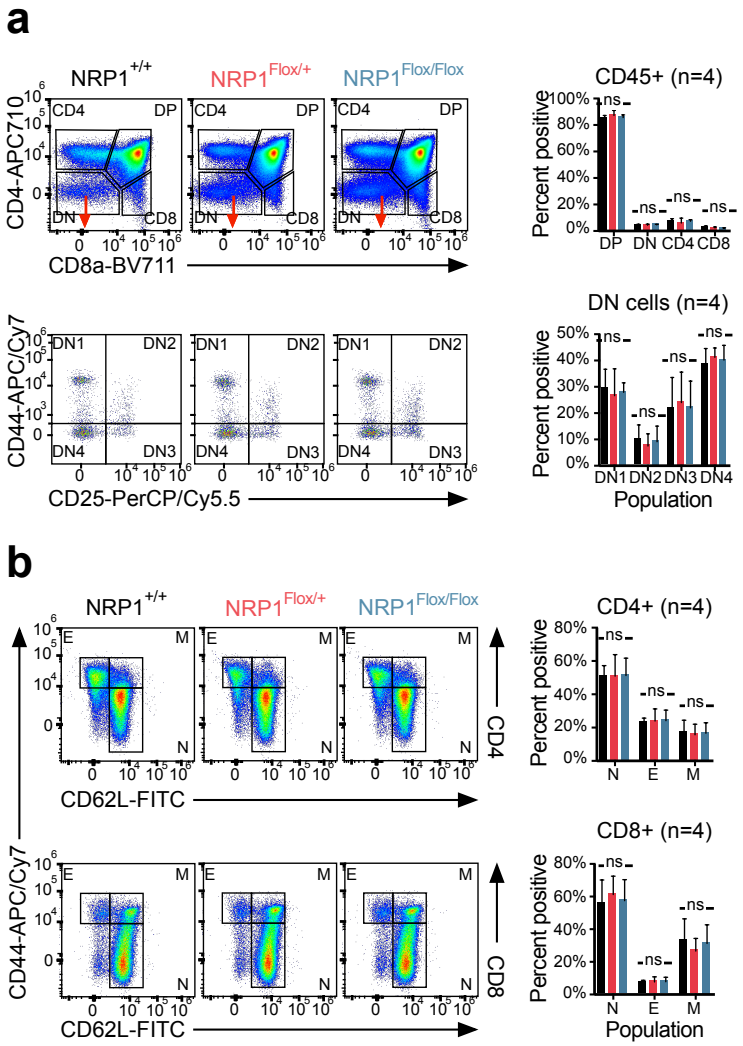


Figure 4.2: **NRP1-conditional knockout mice generate similar output of T cells from thymus and spleen. A**. Upper panel, left: Representative plots showing the distribution of double negative, double positive, CD4 and CD8 T cells in NRP1$^{+/+}$, NRP1$^{Flox/+}$ and NRP1$^{Flox/Flox}$ mice. Cells are gated on CD45.2. Upper panel, right: Quantification-showed no differences between genotypes. Lower panel: No difference was observed in double negative subpopulations. **B**. Upper panel, left: Representative plots showing T cell effector states in splenic CD4+ T cells. Cells are gated on CD45.2 and TCRβ. Upper panel, right: Quantification showed no differences between genotypes. Lower panel: No difference was observed in effector states of CD8+ splenocytes. N=4 mice per group, data combined from two independent experiments. n.s. = not significant by two-way ANOVA.

4.3 NRP1-conditional knockout mice respond similarly to activation

4.3.1 NRP1-conditional knockout CD8+ T cells produce similar levels of effector cytokines

We next asked if there were any functional difference between genotypes. We sorted CD8+ splenocytes from $NRP1^{+/+}$, $NRP1^{Flox/+}$ and $NRP1^{Flox/Flox}$ mice, stimulated them using CD3/CD28 antibodies and analyzed their production of the effector cytokines TNFα, Granzyme B and IFNγ 52 hours post stimulation (Figure 4.3A). As can be seen in Figure 4.3B, following intracellular staining, no difference in effector cytokines could be detected between genotypes.

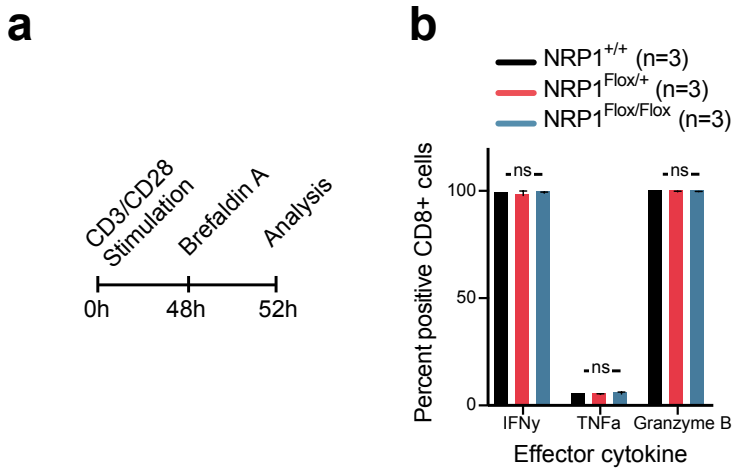


Figure 4.3: **NRP1-conditional knockout CD8+ T cells produce similar levels of effector cytokines. A**. Experimental setup. **B**. Intracellular staining for IFNγ, TNFα and Granzyme B, reveal no difference in the production of these cytokines following stimulation. Cells are gated on TCRβ and CD8. N=3 mice used per group, experiment repeated twice. n.s. = not significant by two-way ANOVA.

4.3.2 NRP1-conditional knockout mice react similarly to challenge with influenza A/PR/8/34 H7N1

We wished to explore T cells ability to be primed and activated *in vivo* and turned to the A/PR/8/34 derived pseudotyped influenza virus H7(Netherlands/2003)-N1(England/2009), here called S-Flu H7N1. S-flu virus particles can readily infect a cell, but since they lack the viral RNA encoding hemagglutinin (HA) they cannot spread from cell to cell[217]. While infection with S-flu H7N1 is excellent at priming and generating T cell-specific response in the lung, they do not generate neutralizing antibodies[217], and so any immune response raised against S-Flu is solely T cell dependent.

We infected $NRP1^{+/+}$, $NRP1^{Flox/+}$ and $NRP1^{Flox/Flox}$ littermates with 10^6 infectious units S-Flu H7N1 intra-nasally and weighed the mice daily till 10 days post infection, where the mice were euthanized and spleen, dLN and lungs harvested for flow cytometric analysis (Figure 4.4A).

C57BL/6 mice generally do not lose weight when infected with S-flu[1], and so we did not expect to see any dramatic changes in mouse weight. Indeed, mice in all groups retained their weight (Figure 4.4A).

The dominant epitope in influenza A/PR/8/34 is the $H\text{-}2D^B$ restricted influenza nuclear protein (NP)[218]. Using $H\text{-}2D^B$ NP-tetramers we first interrogated the ability of S-flu to generate flu-specific T cell response in lung, dLN and spleen. The tetramer stained clearly and strongly in CD8+ T cells in the lungs of infected mice (Figure 4.4B, left). We saw no difference in percentage of NP tetramer positive CD8+ T cells between $NRP1^{+/+}$, $NRP1^{Flox/+}$ and $NRP1^{Flox/Flox}$ mice (Figure 4.4B, right). This indicates that all mice

[1]Personal communication with Dr. Pramila Rijal.

were able to prime and generate a strong T cell influenza response.

Next, we asked if there was any difference in the absolute number of NP tetramer positive CD8+ T cells infiltrating lung, dLN and spleen. This was not the case, with similar number of flu-specific T cells able to infiltrating organs across genotypes (Figure 4.4C).

Finally, we explored the effector phenotype of lung infiltrating CD8+ T cells in $NRP1^{+/+}$, $NRP1^{Flox/+}$ and $NRP1^{Flox/Flox}$ mice using CD44 and CD62L. All infected mice had an expansion of the effector subset and decrease of naive T cells compared to non-infected WT mice, as expected (Figure 4.4D). Again, no difference was observed between genotypes.

Following this characterization of CD8+ T cell ability to be primed, proliferate, migrate to and function in influenza infected lungs, we conclude that there are no intrinsic defects or enhancement in $NRP1^{Flox/Flox}$ CD8+ T cells compared to wild type (WT) T cells.

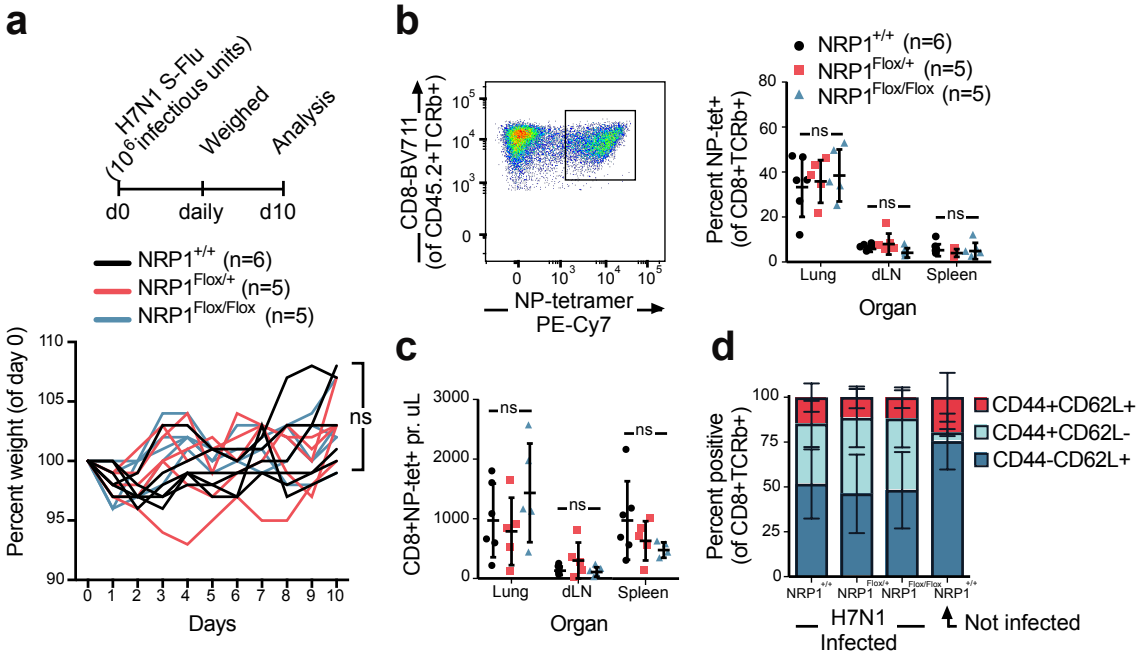


Figure 4.4: **NRP1-conditional knockout mice react similarly to challenge with influenza A/PR/8/34 H7N1. A**. Upper: Experimental design. Lower: Weight of mice infected with S-Flu H7N1 did not show any difference between $NRP1^{+/+}$, $NRP1^{Flox/+}$ and $NRP1^{Flox/Flox}$ mice. **B**. Left: Example H-$2D^B$-NP tetramer staining in lung of infected mouse. Right: Staining with H-$2D^B$-NP tetramers show strong upregulation of flu-specific CD8+ T cells in lungs in all genotypes, with lower levels in dLN and spleen. Cells are gated on CD45.2, TCRβ and CD8. **C**. Quantification of number of H-$2D^B$-NP tetramer positive T cells in lung, dLN and spleen, revealed no difference in number of infiltrating cells between genotypes. Cells are gated on CD45.2, CD8 and TCRβ. **D**. The effector phenotype of lung infiltrating CD8+ T cells in $NRP1^{+/+}$, $NRP1^{Flox/+}$ and $NRP1^{Flox/Flox}$ and $NRP1^{+/+}$ non-infection mice, show more CD44+CD62L- CD8+ T cells in infection mice, but no difference between genotypes. Cells are gated on CD45.2, CD8 and TCRβ. N=5-6 mice per group, all experiments performed once. n.s. = not significant by two-way ANOVA. Data indicate mean ± SD.

4.3.3 Sema3A is not expressed in lung or dLN before or during S-flu H7N1 infection

We wondered if the reason there was no phenotypical differences between CD4-Cre×NRP1 mice during influenza infection, was a lack of Sema3A in either lung or dLN.

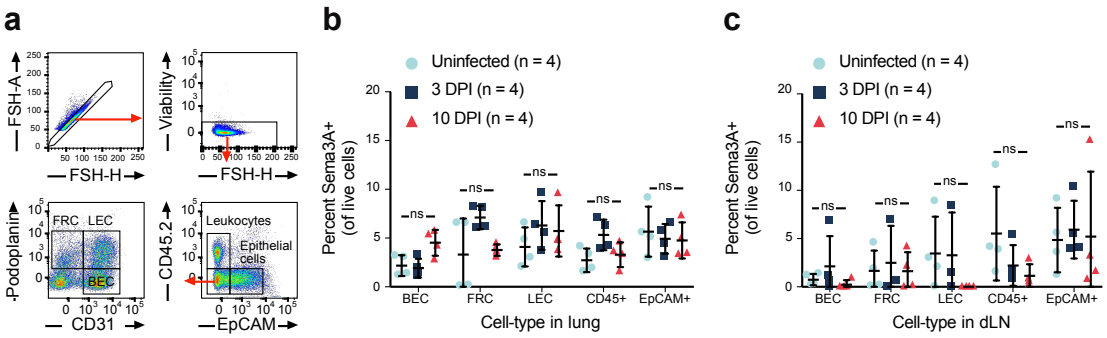


Figure 4.5: **Sema3A is not expressed in lung or dLN before or under S-flu H7N1 infection. A**. Gating strategy for analyzing Sema3A expression among leukocytes, epithelial and endothelial cells in lung and dLN. **B**. Expression of Sema3A across cell types in lung, before, three and ten days post infection with S-Flu H7N1, reveal no upregulation of Sema3A or marked expression of the protein overall. **C**. Expression of Sema3A across cell types in axillary lymph nodes with same time-points and cell-types as in **B**, shows little expression of Sema3A. N=4 mice per group, all experiments performed once. n.s. = not significant by two-way ANOVA. Data indicate mean ± SD.

To explore this, we examined the epithelial and endothelial cells in lung and dLN in uninfected and infected $NRP1^{+/+}$ mice, 3 and 10 days post infection. Using the markers CD45, EpCAM, CD31 and podoplanin, we subdivded all cells into either leukocytes (CD45+ cells), epithelial cells (CD45-EpCAM+ cells) or endothelial cells (CD45-EpCAM- cells) and stained for intracellular expression of Sema3A. Endothelial cells were further subdivided into either fibroblastic reticular cells (FRC), blood endothelial cells (BEC) or lymphatic endothelial cells (LEC) cells (Figure 4.5A). Examining the cell types in lung (Figure 4.5B) and dLN (Figure 4.5C) reveals little expression of Sema3A in any of these cell-types, both before and after infection with S-Flu H7N1.

4.4 Tumour growth is stunted in mice with NRP1-deficient T cells

4.4.1 Sema3A is expressed by B16.F10 cells under varying conditions

We next wanted to challenge the CD4-Cre×NRP1 mice with the B16.F10 cell-line. However, following our analysis of Sema3A expression in the lungs of influenza-infected mice, we decided to explore if Sema3A was expressed by the B16.F10 tumour cell line first.

Preliminary experiments determined that the B16.F10 cell-line expressed varying levels of Sema3A *in vitro*. To understand this further we conducted three different experiments. First we plated cells at varying densities, because expression seemed dependent on confluency of the cell-line, and analyzed Sema3A by flow cytometry. Counter-intuitively, we repeatedly found that B16.F10 cells that were initially plated at low densities expressed higher levels of Sema3A after 72 hours of culture (Figure 4.6A). Perhaps this is a consequence of these cells being in log-phase longer than more confluent cells.

As the TME is often hypoxic, especially in fast growing tumours such as B16.F10[219], we next performed reverse transcription quantitative polymerase chain reaction (RT-qPCR) on B16.F10 cells cultured in either normoxic or hypoxic conditions (1% O_2) for 48 hours. As expected, culturing cells in hypoxic conditions lead to upregulation of a number of known hypoxic response genes, including *PDK1, BINP3* and *VEGFA*, thereby confirming that our experimental setup had worked. We found that *Sema3A*, but not *PDL1*, was upregulated (2.4 fold) in hypoxic cells, as compared to cells cultured

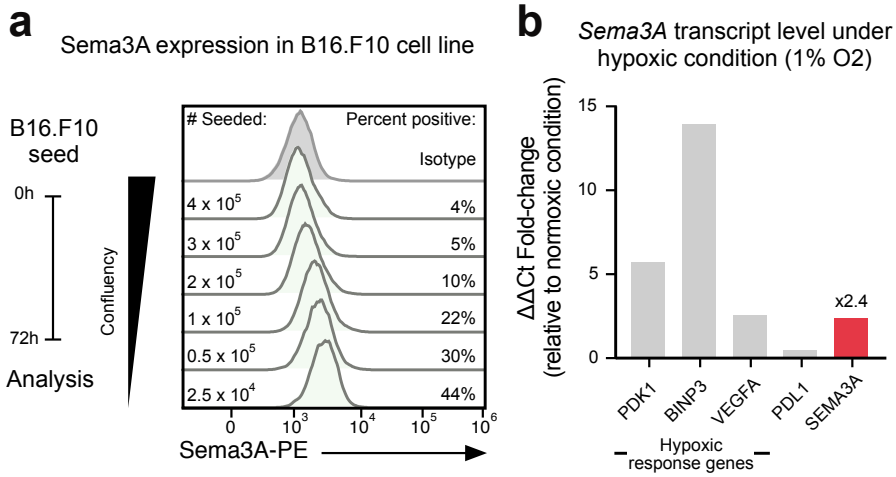


Figure 4.6: **Sema3A is expressed by B16.F10 cells under different conditions. A**. Level of confluency at seeding determines level of Sema3A expression 72 hours later in B16.F10 cells. Representative histograms, experiment repeated three times. **B**. RT-qPCR shows that Sema3A is upregulated 2.4 fold in B16.F10 cells cultured in hypoxic conditions. Experiment performed once.

in normoxic conditions (Figure 4.6B).

Finally, we tested whether TGFβ could induce Sema3A production in B16.F10 cells. TGFβ treatment has been shown to be able to induce epithelial-mesenchymal transition (EMT) and hence increased metastatic ability in this cell-line[220], and it has been suggested that Sema3A can increase the metastatic potential of B16.F10 cells[221]. We therefore wondered if TGFβ-induced EMT could increase Sema3A expression. However, disperse results made it hard to draw any conclusion from this line of inquiry (data not shown).

We conclude that expression of Sema3A in B16.F10 cells can vary substantially, but that the cell-line can express Sema3A, especially under hypoxic conditions.

4.4.2 Tumour growth is stunted in mice with NRP1-deficient T cells

We challenged our mice with two different cancer cell-lines, B16.F10 and 3LL, in order to see what effect T cell NRP1-deficiency would have on tumour growth. Both the 3LL and B16.F10 cell line has been shown to be weakly immunogenic in C57BL/6 mice[222, 223].

In $NRP1^{Flox/Flox}$ mice challenged with B16.F10, tumour growth was severely inhibited (Figure 4.7A), not growing for several weeks, similarly to the effects described in Hansen et al[204] and in Delgoffe et al[175] when they use NRP1 blocking antibodies. In 3LL challenged mice, the effect was similar but not as strong, with tumour cells mainly growing at a slower rate in $NRP1^{Flox/Flox}$ mice than in $NRP1^{+/+}$ or $NRP1^{Flox/+}$ mice (Figure 4.7B). In both B16.F10 and 3LL challenged $NRP1^{Flox/Flox}$ mice, there were some tumours that grew at normal rate, showing some stochasticity in the otherwise very strong phenotype.

When dissecting B16.F10 challenged mice we noticed that the tumour in $NRP1^{Flox/Flox}$ mice, while substantially smaller, was still present (Figure 4.7C).

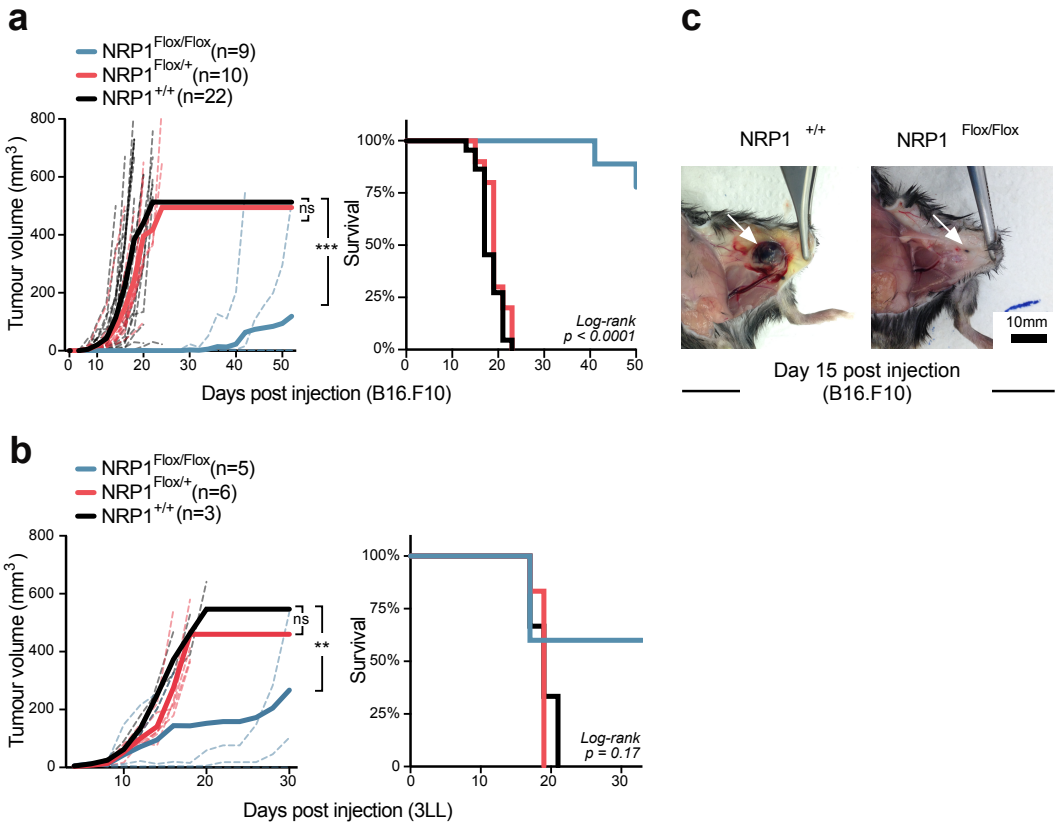


Figure 4.7: **B16.F10 and 3LL cancer growth is stunted in NRP1$^{Flox/Flox}$ mice. A**. Tumour growth in NRP1$^{+/+}$, NRP1$^{Flox/+}$ and NRP1$^{Flox/Flox}$ mice reveal long-term suppression of growth of B16.F10 cells in NRP1$^{Flox/Flox}$ mice. Left: growth curve. Right: Kaplan-Meier survival curve. Combined data from 4 independent experiments with 3-6 mice per group. **B**. Tumour growth in NRP1$^{+/+}$, NRP1$^{Flox/+}$ and NRP1$^{Flox/Flox}$ show stunted growth of 3LL cells in NRP1$^{Flox/Flox}$ mice. Left: growth curve. Right: Kaplan-Meier survival curve. N=3-6 mice per group, experiment performed once. **C**. Dissection of mice show that B16.F10 cells survive in NRP1$^{Flox/Flox}$ mice, but that their growth is much better controlled as compared to NRP1$^{+/+}$ mice. ** = P $<$ 0.001, n.s. = not significant by two-way ANOVA.

4.5 Tumour growth is unaffected in NRP1-deficient mice with depleted CD8+ cells

A number of groups have examined the role of NRP1 on regulatory T cells[175, 204]. However, since we had found that NRP1 was expressed on CD8+ T cells as well, we

wanted to see what effect this T cell compartment had on the stunted growth phenotype we observed.

To this end, we treated littermate $NRP1^{Flox/+}$ and $NRP1^{Flox/Flox}$ mice with either an anti-CD8 antibody or an IgG isotype control antibody at -2, 0, 4, 7 and 10 days after B16.F10 tumour injection. This treatment completely removed CD8 T cells in the anti-CD8 treated groups (Figure 4.8A). We followed the growth of tumours in the four groups for 17 days and noticed that while isotype treated $NRP1^{Flox/Flox}$ mice had stunted growth (light blue line), anti-CD8 treated $NRP1^{Flox/Flox}$ mice (red line) had tumour growth similar to that seen in anti-CD8 $NRP1^{Flox/+}$ treated mice (grey line). Both anti-CD8 treated groups had faster growth than isotype treated $NRP1^{Flox/+}$ mice (black line), indicating that there are intrinsic anti-tumour effects by endogenous CD8 T cells against the B16.F10 cell line (Figure 4.8B).

We conclude that NRP1-deficiency allows T cells to significantly better control B16.F10 and 3LL tumours *in vivo*. Our anti-CD8 experiments additionally show that the major driver of this effect in B16.F10 bearing mice are CD8+ T cells.

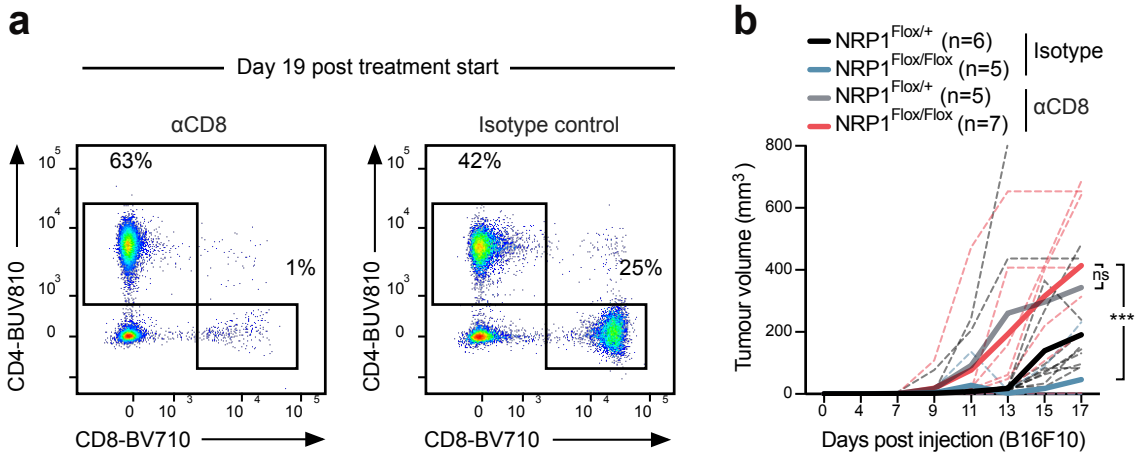


Figure 4.8: **Tumour growth is not stunted in NRP1-deficient mice with depleted CD8+ cells. A**. Representative scatterplot of CD4 and CD8 T cells in spleens of either anti-CD8 or isotype control treated mice, show that anti-CD8 treatment effectively removes CD8 T cells in mice up till 19 days after treatment. Cells gated on TCRβand CD45.2. **B**. Tumour growth shows that isotype treated NRP1$^{Flox/Flox}$ mice (light blue line) have stunted growth, while anti-CD8 treated NRP1$^{Flox/Flox}$ mice (red line) have similar growth as NRP1$^{Flox/+}$ mice (black line). N = 5-7 mice per group, data combined from two independent experiments. *** = $P < 0.0001$, n.s. = not significant by two-way ANOVA.

4.6 NRP1-deficient CD8+ cells infiltrate tumours more readily

In order to explore how NRP1-deficient CD8+ T cells were able to control the growth of B16.F10 cells, we phenotyped CD8+ TILs. B16.F10 cells were injected into NRP1$^{+/+}$, NRP1$^{Flox/+}$ and NRP1$^{Flox/Flox}$ mice (Figure 4.9A), and 15 days later tumours were harvested and analyzed by flow cytometry (Figure 4.9B). There was no difference in number of CD25 or CD69 positive CD8+ T cells between genotypes (Figure 4.9C), indicating little difference in activation state. However significantly more CD8+ T cells, but not CD4+ T cells, had infiltrated into the tumours in NRP1$^{Flox/Flox}$ mice, compared to NRP1$^{+/+}$.

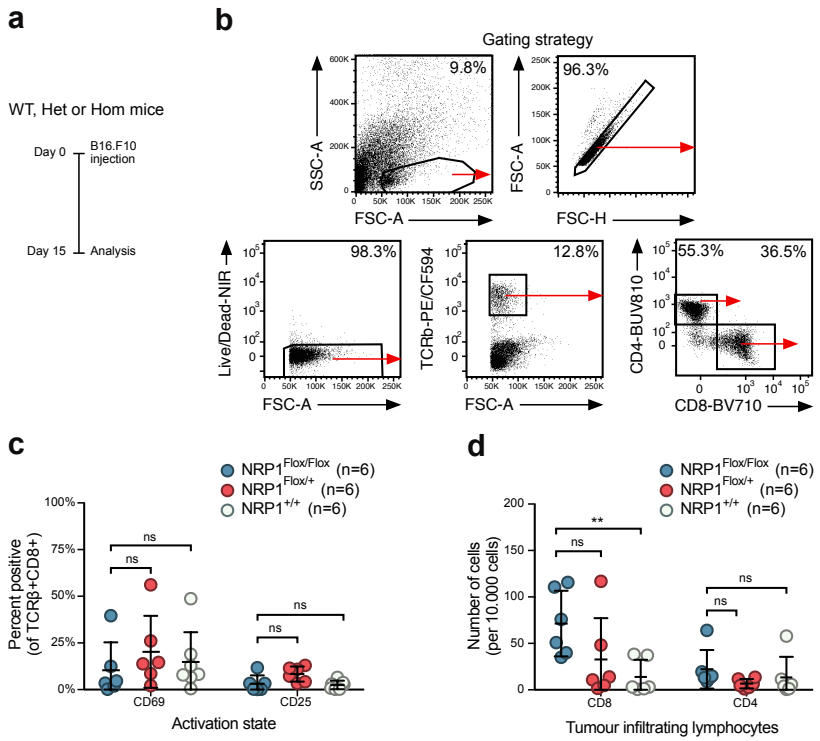


Figure 4.9: **NRP1-deficient CD8+ cells infiltrate into tumours more readily. A**. Experimental design. **B**. Gating strategy for assessing T cell phenotype and numbers in tumours. **C**. Analysis of activation state of CD8+ TILs in $NRP1^{+/+}$, $NRP1^{Flox/+}$ and $NRP1^{Flox/Flox}$ mice. Cells gated as outlined in B. **D**. Analysis of CD4 and CD8 T cell numbers in tumours in $NRP1^{+/+}$, $NRP1^{Flox/+}$ and $NRP1^{Flox/Flox}$ mice. Cells gated as outlined in B. N = 6 mice per group, experiment performed once. Data indicate mean ± SD. ** = $P < 0.001$, n.s. = not significant by two-way ANOVA.

4.7 Generation of Sema3A knockout and over-expressing B16.F10.Ova cell lines

We wanted to be able to more thoroughly investigate the interactions between Sema3A and NRP1, and therefore created Sema3A knockout and over-expression B16.F10.Ova cell lines.

Sema3A was removed from the B16.F10.Ova cells using clustered, regularly interspaced, short palindromic repeats (CRISPR)/Cas9 directed edits across exon 2 in the Sema3A gene. Exon 2 encodes parts of the Sema-domain necessary for binding to Plexin-A1:NRP1 receptors and is furthermore a good target region as any frameshifts upstream in the gene are more likely to introduce stop codons further down. B16.F10.Ova cells were edited and single-cell sorted. Approximately 100 clones were generated and 30 deep-sequenced. One clone had a disrupted target region, with either 4 base-pair deletions or an insertion, both causing frameshifts in the gene (Figure 4.10A). This clone will be called Sema3A KO here. A minority of reads in this clone were identical to the reference sequence, but the low number of reads meant these were most likely contaminations from other clones[2].

A Sema3A overexpressing B16.F10.Ova clone was constructed by constructing a murine cDNA plasmid that was inserted into the cell line using lentiviral transduction. This clone will be called Sema3A OE here.

RT-qPCR confirmed both knockdown and overexpression of Sema3A in the cell-lines (Figure 4.10B). In Sema3A KO cells, the Sema3A transcript was suppressed but did give a signal at cycle 36 of the qPCR. Assuming this is a true signal, it should be noted that nonsense mediated decay of transcript would not happen before the transcript was produced by the cells, and so the fact that we see some transcript does not mean it will be translated into a functioning protein. Indeed, Sema3A could not be detected at the protein level in our Sema3A KO cell's, but was uniformly up-regulated in the Sema3A OE cell's (Figure 4.10C).

Because we had selected and expanded single cell clones, we wanted to ensure that

[2]Personal communication with Professor Tudor A Fulga.

the two cell-lines grew at similar rates. We measured growth in either normal media or media with IFNγ or TNFα to phenocopy growth in an inflamed environment. No difference in growth could be detected *in vitro*. Next we injected mice with Sema3A KO and Sema3A OE in opposing flanks of C57BL/6 mice and measured their growth over 17 days. No difference could be detected with tumours growing at similar rates (Figure 4.10E).

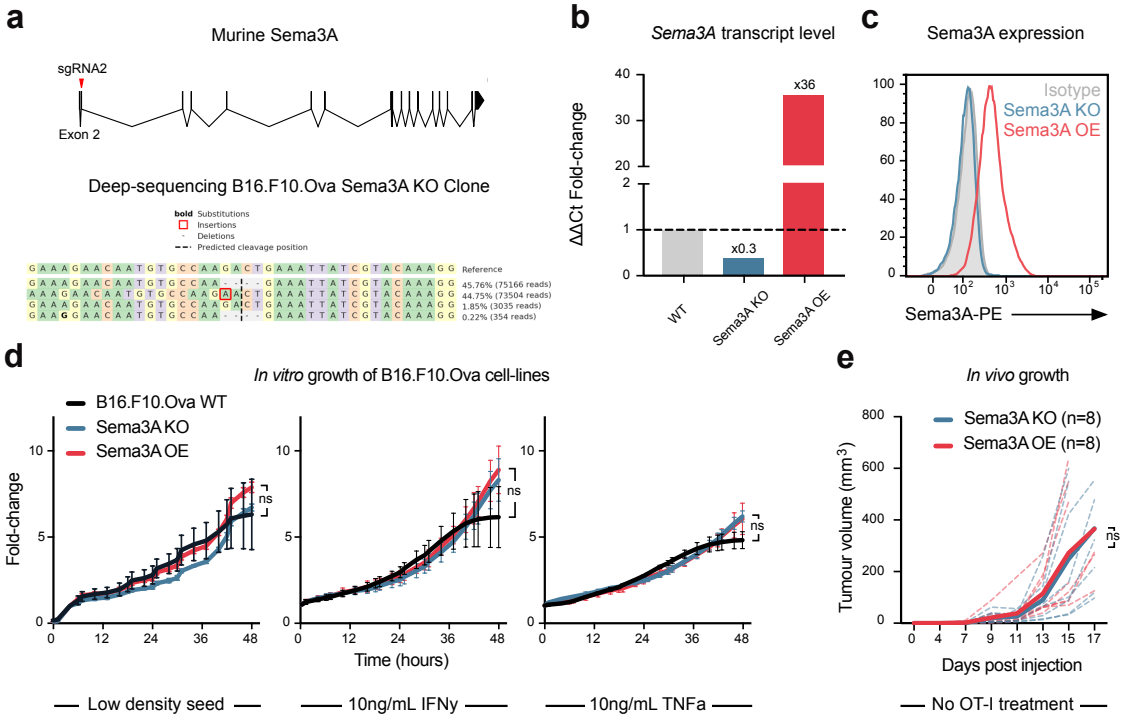


Figure 4.10: **Generation of Sema3A knockout (KO) and over-expression (OE) B16.F10.Ova cell lines.** **A**. Upper: Genomic organization of murine Sema3A, with CRISPR guide sgRNA target indicted with red arrow. Lower: MiSEQ sequence results for chosen KO clone showing 4 base deletion in two alleles (46% of all reads), a frameshift in one allele (45% of all reads) and WT reads in 2% of all reads. **B**. RT-qPCR analysis show down- and up-regulation of Sema3A in Sema3A KO and OE cell lines, respectively. Normalized to *Hprt*. Experiment performed once. **C**. Intracellular staining show no detectable expression of Sema3A in Sema3A KO cells, and expression in Sema3A OE cells, as expected. Experiment performed once, at low seeding density. **D**. No difference in *in vitro* growth between WT, Sema3A KO and Sema3A OE B16.F10.Ova cell lines in untreated, IFNγor TNFαrich media. Experiment performed once. Data indicate mean ± SD. **E**. No difference in *in vivo* growth between Sema3A KO and Sema3A OE in C57BL/6 mice. N = 8 mice per group, experiment performed once. n.s. = not significant by one-way ANOVA.

4.8 Mixed chimera mice with NRP1$^{Flox/+}$ and NRP1$^{Flox/Flox}$ bone-marrows have same phenotype as conditional NRP1-knockout mice

We wanted to test if the phenotype of increased CD8+ T cell infiltration was truly an effect of NRP1-deficiency on T cells themselves or caused by more broad changes in the CD4-Cre×NRP1 mice. We therefore created mixed bone-marrow chimeras in which a 1:1 mix of congenically labelled NRP1$^{Flox/+}$ (CD45.1) and NRP1$^{Flox/Flox}$ (CD45.1+CD45.2) bone-marrows were injected into irradiated male C57BL/6 mice. The bone-marrows were allowed to reconstitute for 10 weeks, after which Sema3A OE cells were injected into the flanks of mice and allowed to grow for 9 days (Figure 4.11A). Tumours were then harvested and the activation state (Figure 4.11B) and effector state (Figure 4.11C) of CD8 T cells analyzed by flow cytometry. No difference could be seen in either activation state or effector state of CD8+ T cells from the two bone-marrows, reflecting the result we saw in NRP1$^{+/+}$ and NRP1$^{Flox/Flox}$ mice (Figure 4.9C).

We also quantified the number of CD8+ TILs (Figure 4.11D). In all mice, there were significantly more CD8+ T cells from the NRP1$^{Flox/Flox}$ bone-marrow than from NRP1$^{Flox/+}$ bone-marrow in the tumours, with approximately 1.4 times as many CD8+ T cells present.

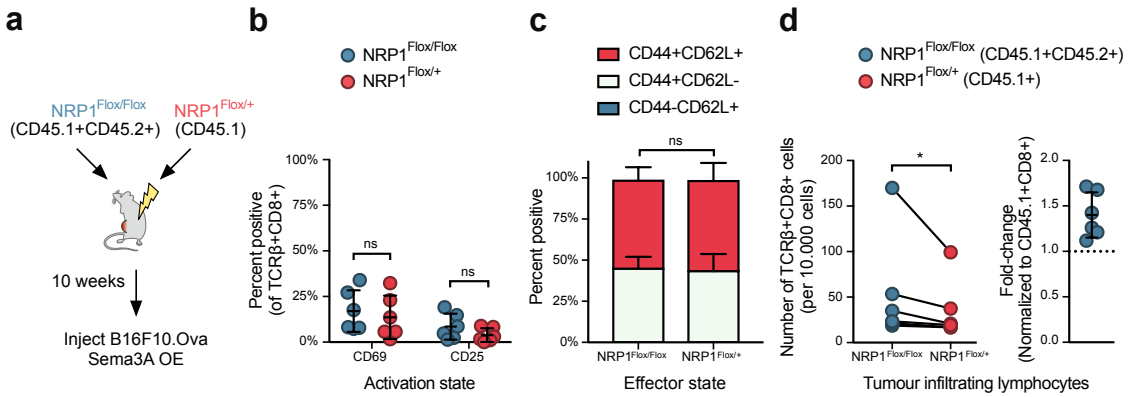


Figure 4.11: **Mixed bone-marrow chimeras have same phenotype as NRP1-knockout mice.** **A**. Experimental design. Irradiated mice were injected with a 1:1 mix of CD4-Cre×NRP1$^{Flox/+}$ and CD4-Cre×NRP1$^{Flox/Flox}$ bone-marrows. After 10 weeks B16.F10.Ova Sema3A OE cells were injected, and analyzed 9 days later. **B**. CD8+ TILs were analyzed for CD25 and CD69 expression. No difference between cells could be seen. Cells are gated in CD45.1, CD45.2, TCRβ, CD8. **C**. CD8+ TILs were analyzed for CD44 and CD62L expression. No difference between cells could be seen. Gated as in B. **D**. Quantification of total CD8+ T cells. In all mice more NRP1$^{Flox/Flox}$ than NRP1$^{Flox/+}$ CD8+ T cells infiltrated the tumour. Right: the ratio of CD8+ T cells from NRP1$^{Flox/Flox}$ to NRP1$^{Flox/+}$ bone-marrow is approximately 1.4. N = 6 mice per group, experiment performed once. Data indicate mean ± SD. * = $P < 0.05$, n.s. = not significant by one-way (B and D) or two-way ANOVA (C).

4.9 Tumour-specific T cells are inhibited from entering Sema3A-rich tumours

We next examined what effects Sema3A had on tumour-specific T cells. We therefore injected Sema3A KO and Sema3A OE B16.F10.Ova cells in opposing flanks in C57BL/6 mice, followed by adoptive transfer of OT-I T cells seven days later (Figure 4.12A).

We measured tumour growth on alternative days and noticed that Sema3A OE tumours grew significantly faster than Sema3A KO tumours in all mice.

15 days post tumour injection, tumours were harvested and analyzed by flow cytom-

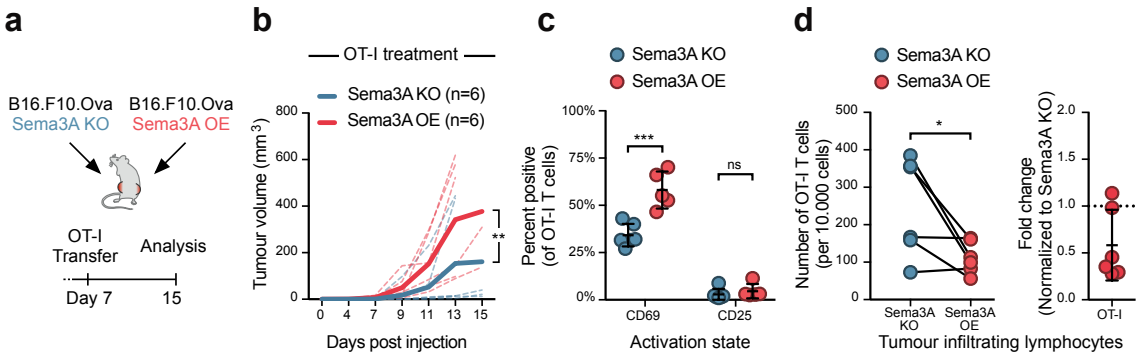


Figure 4.12: **Tumour-specific T cells are inhibited from entering Sema3A-rich tumours. A**. Experimental design. Sema3A KO and Sema3A OE cell lines were injected in opposing flanks of C57BL/6 mice. 7 days later OT-I T cells were adoptively transferred into the mice, and tumour measured on alternate days. 15 days post injection, tumours were harvested and analyzed. **B**. Growth curve of tumours. Sema3A OE tumour grew significantly faster than Sema3A KO tumours. **C**. Tumour-specific OT-I T cells were analyzed for CD25 and CD69 expression. TILs in Sema3A OE tumours were more CD69 positive, and expressed equal levels of CD25. **D**. Left: Quantification of total OT-I T cells. In 4 out of 6 mice, there were more OT-I T cells in the Sema3A KO tumour compared to the Sema3A OE tumour. Right: the ratio of OT-I TILs in Sema3A OE against Sema3A KO tumours is approximately 0.6. N=6 mice per group, all experiments performed once. ** = $P < 0.001$, n.s. = not significant by one-way ANOVA. Data indicate mean ± SD.

etry. OT-I TILs were examining for their expression of the activation markers CD25 and CD69. We found that OT-I T cells in both tumours expressed similar levels of CD25, but that there was significantly more CD69+ OT-I T cells in Sema3A OE tumours (Figure 4.12C). Next we quantified the number of OT-I T cells in each tumour. In 4 out of 6 mice more OT-I T cells had infiltrated into the Sema3A KO tumours (Figure 4.12D).

Taken together, these data show that the Sema3A—NRP1 axis controls CD8+ T cell infiltration into tumours.

4.10 Discussion

We found that mice with NRP1-deficient T cells were significantly better at controlling growth of the B16.F10 and 3LL cell lines (Figure 4.7). Conversely, overexpression of the NRP1-ligand Sema3A lead to faster tumour growth compared to Sema3A KO cells in mice treated with NRP1 positive OT-I T cells (Figure 4.12). Taken together, we conclude that Sema3A — NRP1 signaling can significantly affect growth of tumour cells.

This is partially in line with other published data, although these reports do not describe any CD8+ T cell-intrinsic effects. In Hansen et al[204], the authors also use a CD4-Cre×NRP1 mouse model similar to the one we describe here, while Delgoffe et al[175] use a combination of FoxP3-Cre×NRP1 mice and anti-NRP1 blocking antibodies. Both groups report strong anti-tumour effects of either genetically removing or therapeutically blocking NRP1 but attribute this effect to regulatory CD4+CD25+FoxP3+ T cells, because they do not believe CD8+ T cells express the receptor.

Here, we present four lines of evidence pointing to this effect being mediated by increased infiltration of CD8+ T cells into tumours. First, we detected more CD8+ T cells in tumours in our $NRP1^{Flox/Flox}$ mice compared to $NRP1^{+/+}$ mice (Figure 4.9). This was confirmed using bone-marrow chimeras (Figure 4.11). When we removed CD8+ T cells using anti-CD8 antibodies, B16.F10 tumour growth was no longer inhibited in $NRP1^{Flox/Flox}$ mice (Figure 4.8). Finally, when comparing the number of OT-I TILs in Sema3A KO and Sema3A OE tumours, we saw a lower ratio of tumour-specific T cells in the latter (Figure 4.12).

Additional experiments could strengthen this argument further. For example, we attempted to generate OT-I×CD4-Cre×$NRP1^{Flox/Flox}$ mice, but unfortunately did not suc-

ceed with this before submission of this thesis.

We have tried to ensure that there were no inherent defects or enhancements in the CD4-Cre×NRP1 mouse model we developed and used here. The strongest evidence to this end was our analysis of mice infected with S-Flu H7N1, which resulted in similar levels of T cell response (Figure 4.4). This was most likely due to the simple fact that there was little to no expression of Sema3A in the lung or axillary lymph nodes. Unlike what other groups have reported[214], we did not see any defect in thymocyte development in our CD4×NRP1 mice (Figure 4.2).

One intriguing finding that does not intuitively fit our other data or my interpretation here, is the fact that more OT-I T cells were CD69 positive in Sema3A OE tumours as compared to OT-I T cells in Sema3A KO tumours (Figure 4.12C). I have used CD69 as an activation marker here, because it is quickly up-regulated on activated T cells, but it is worth noting that CD69's function is to retain T cells in tissues[224]. One could speculate that the reason we see more CD69+ OT-I T cells in Sema3A-rich tumours is because these tumours selected for T cells that cannot egress from the tumour easily.

While our final experiment did show a significant difference in number of infiltrating OT-I T cells, the effect in isolation was not as clear as I would have initially guessed. One reason for this could be that there is an endogenous sources of Sema3A in the TME, which I will explore in the next chapter.

Chapter 5

Sema3A is Expressed by Vasculature and Lymphatics in Tumours

5.1 Introduction

Despite having been first described in 1993, the exact expression pattern of Sema3A outside the nervous system and postnatally, is not well explored. Perhaps due to the fact that Sema3A is a secreted protein, expression has mainly been described in terms of tissue type, not individual cell types.

The Immunological Genome Project database shows very low to nil transcript expression of Sema3A in any immune cell at all. However, three reports claim that Sema3A is expressed by cells in the immune system: Lepelletier et al[210] found expression of Sema3A by activated T cells and DC after *in vitro* culture, while Ji et al[225] found Sema3A expressed by macrophages, also following *in vitro* activation. Additionally, in patients with inflammatory bowl disease, Vadasz et al found Sema3A expressed by reg-

ulatory CD4+CD25+FoxP3+ cells[226]. Since any source of Sema3A could potentially affect NRP1+ tumour-specific T cells, we decided to test for expression of Sema3A in these different immune cell populations.

It is becoming increasingly clear that T cell responses against tumours are not only regulated by interactions between cancer cells and T cells, or between T cells and other immune cells, but also their shared interplay with the stromal compartment in both the tumour and surrounding lymphoid organs[227]. We therefore also set out to explore what Sema3A expression we could find in the TME in both cancer and draining lymph nodes, as effects here might affect T cell migration.

5.2 Sema3A is not expressed by CD4+ or CD8+ effector T cells

Following the report by Lepelletier et al[210] that activated T cells could express Sema3A, we assayed CD4+ and CD8+ splenocytes and used the markers CD44 and CD62L to distinguish naive, effector and memory T cells (Figure 5.1A). Intracellular staining for Sema3A in CD4 or CD8 T cell subsets, including effector cells (Figure 5.1B), did not reveal any expression in these cells.

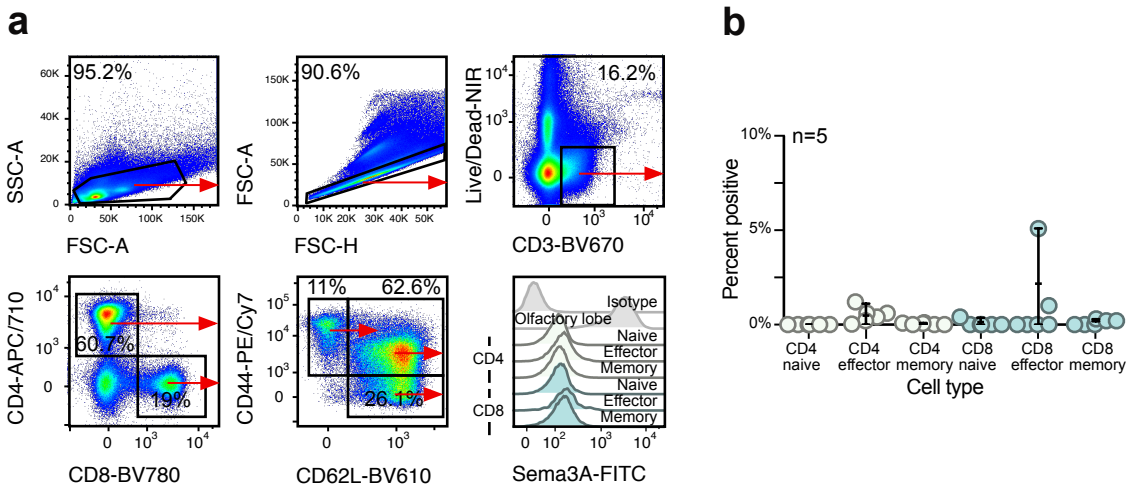


Figure 5.1: **Sema3A is not expressed by CD4+ or CD8+ effector T cells. A**. Gating strategy used to interrogate splenocytes in C57BL/6 mice. Olfactory lobe used as positive control. **B**. Quantification of Sema3A expression in naive, effector or memory CD4+ or CD8+ T cells show no expression in these cells *in vivo*. N = 5 mice, experiment performed once. Data indicate mean ± SD.

5.3 Sema3A is weakly expressed by regulatory CD4+CD25+FoxP3+ T cells

Next we tested expression by regulatory CD4+CD25+FoxP3+ T cells in spleen and lymph nodes (Figure 5.2A). Low expression could be detected in regulatory T cells in spleen, but not in lymph nodes (Figure 5.2B).

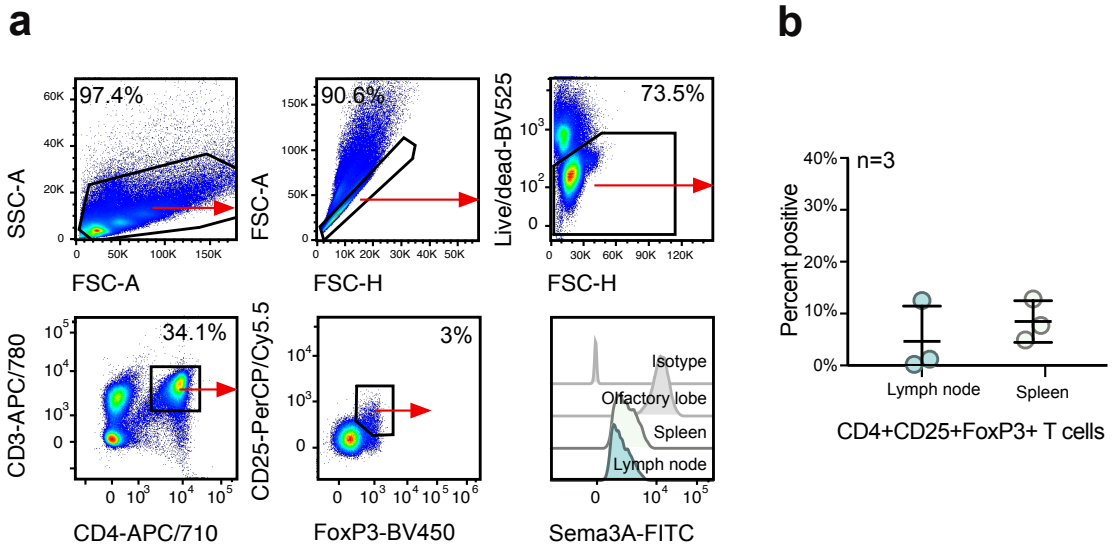


Figure 5.2: **Sema3A is weakly expressed by regulatory CD4+CD25+FoxP3+ T cells A**. Gating strategy used to interrogate regulatory T cells in C57BL/6 mice. Olfactory lobe used as positive control. **B**. Quantification of Sema3A expression in regulatory CD4+CD25+FoxP3+ T cells show weak expression in the spleen. N = 3 mice, experiment performed once. Data indicate mean ± SD.

5.4 Sema3A is not expressed by B cells, monocytes, DC's or macrophages

Because Ji et al[225] had found Sema3A expression in macrophages and Lepelletier et al[210] in DCs, we decided to examining these cell-types as they can regulate CD8+ T cells. However we did not detect in expression in either CD11b+ or CD103+ DC's, in macrophages, monocytes or B cells.

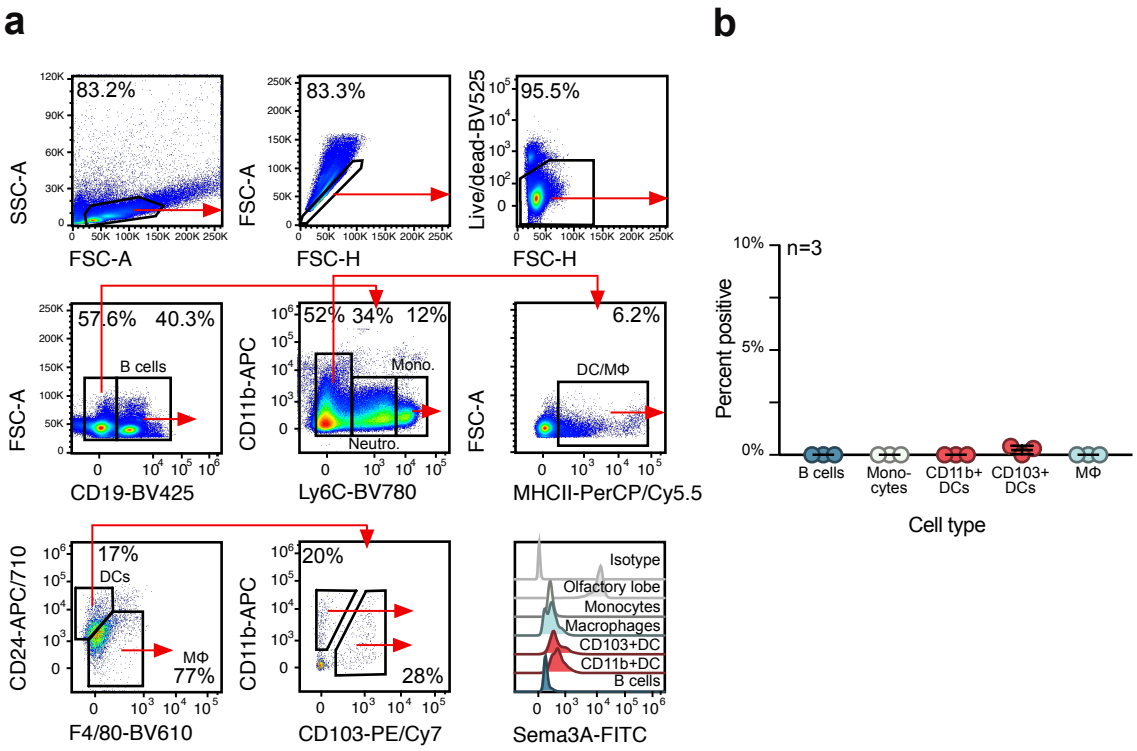


Figure 5.3: **Sema3A is not expressed by B cells, monocytes, DC's or macrophages A**. Gating strategy, based on Broz et al[76], used to examine B cells, monocytes, DCs and macrophages in splenocytes. Olfactory lobe used as positive control. **B**. Quantification of Sema3A expression in show little to no expression among cell types. N = 3 mice, experiment performed once. Data indicate mean ± SD.

5.5 Sema3A is expressed by vasculature and lymphatics in tumours but not in lymph nodes

Finally, we decided to explore what expression could be found among the endothelial cells in tumours, dLN and non-draining lymph node (ndLN), as it is becoming clear that endothelial cells can control CD8+ T cell anti-tumour activity[227] and level of T cell infiltration[131]. Using the markers CD45.2 and CD105 to gate out hematopoetic and

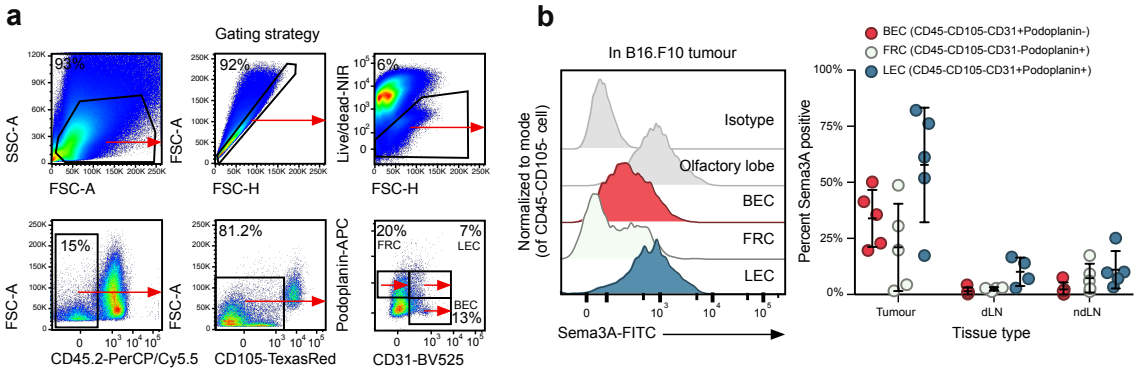


Figure 5.4: **Sema3A is expressed by vasculature and lymphatics in tumours A**. Gating strategy to investigate endothelial cells in tumours, dLN and ndLN. Hematopoetic (CD45.2+) and tumour cells (CD105) were gated out, and endothelial cell subsets defined using Podoplanin and CD31. Olfactory lobe used as positive control. **B**. Left: Histogram showing representative expression in B16.F10 tumour of Sema3A. Olfactory lobe used as positive control. Right: Quantification in 5 mice show upregulation of Sema3A in endothelial cells in tumours, but not dLN or ndLN. N = 5 mice, data combined from two independent experiments. Data indicate mean ± SD.

B16.F10 cancer cells, we subdivided endothelial cells into FRC, BEC and LEC (Figure 5.4A) using the markers CD31 and Podoplanin. We found that all endothelial subsets express moderate to high levels of Sema3A in tumours, but not in dLN or ndLN (Figure 5.4B).

5.6 Discussion

Here we explored Sema3A expression in a number of immune cell subsets in healthy mice. We could not replicate findings by other groups that DC's and T cells should express Sema3A.

Our analysis could be expanded: primarily, we could look at the immune cells that specifically infiltrate tumours. Secondly, by only looking *in vivo* at DCs and

macrophages, our assay might not be sensitive enough to detect up-regulation like that described following activation *in vitro*[210, 225]. However, our data is in line with data from the Immunological Genome Project.

Our investigation shows that endothelial cells in the TME is a major source of Sema3A (Figure 5.4). This is perhaps not surprising: as tumours grow they secrete growth factors that cause neoangiogensis and lymphogenesis. During vascular development endothelial cells have been shown to generate gradients of Sema3A in order to ensure proper spatial organizations of blood vessels[228]. It is not unrealistic that the same programs that are active during development are re-activated in endothelial cells during neoangiogenesis in tumours. Indeed others have found that a subset of MECA32 (a pan-endothelial cell marker) positive cells in other murine cancer models express Sema3A[229], in line with our findings here.

In terms of T cell migration, Sema3A expression on endothelial cells is interesting for several reasons. For example it has been shown that Sema3A elevates permeability of endothelial cells[230, 231]. Vascular leakiness and poor perfusion has been associated with poor infiltration of immune cells[130, 232, 233]. More long-term expression of Sema3A however has also been reported to normalize tumour vasculature[24, 229] and so the indirect consequence on T cell migration via endothelial cells are not immediately clear.

Since Sema3A is known to affect other cell types strongly, we next set out to explore what direct effect, if any, Sema3A would have on CD8+ T cells.

Chapter 6

Sema3A is a Negative Regulator of T cell Adhesion and Migration

6.1 Introduction

After determining that Sema3A was expressed by both the B16.F10 cell line and a subset of endothelial cells in tumours, we wanted to explore what effects Sema3A had on activated CD8+ T cells. In this chapter I will focus on T cell adhesion and migration, while the next chapter will be dedicated to Sema3A's effect on the immunological synapse and consequences of Sema3A-signaling.

T cells constantly circulate between lymph nodes via blood and lymphatic vessels. In both lymph nodes and in tumours, T cells mainly enter the parenchyma through specialized endothelial cells called HEVs[99]. This transmigration is conducted in a sequential and coordinated manner that involves binding via two major adhesion protein families, selectins and integrins. In inflamed tissue, such as cancers, HEVs up-

regulate expression of P- and E-selectins and secretion of chemokines such as CC-chemokine ligand 21 (CCL21), which can be found immobilized on the luminal surface by heparan sulphate[99]. This results in increased rolling of T cells across the endothelium, through binding of P-selectin glycoprotein ligand-1 (PSGL-1) (CD162) on T cells, followed by chemokine-induced activation of T cell integrins, most importantly LFA-1 ($\alpha_L\beta_2$, CD11a:CD18), through CCR7[101] and C-X-C chemokine receptor type 4 (CXCR4)[234]. LFA-1 is maintained in a closed conformational state on circulating T cells, but kinks open following activation, a structural change which increases its affinity to its ligands such as ICAM-1[235]. LFA-1's conformational state is modulated by the small GTPase Rap1[234, 236, 237]. This allows for firm adhesion between the T cell and the endothelial cells, better T cell motility on the endothelium and finally transmigration into the underlying tissue[99].

Like chemokines, Sema3A can bind to cell-surfaces through heparan sulphate[238]. However, instead of promoting integrin activity, Sema3A has been shown to inhibit it in endothelial cells[228] and axonal growth cones, an effect that is dependent on myosin II activity[239]. Studies, examining NRP1 and Plexin-A signalling, suggest that this effect is mediated by Rap1: following Sema3A binding, Plexin-A and NRP1 complexes oligomerize[171], leading to conformational changes in the cytoplasmic domain of Plexin-As which exposes a GAP-domain. This structural re-orientation allows for the GAP-domain to directly convert the small GTPase Rap1, from its activated, GTP-bound state, to its inactive, GDP-bound state[179, 180]. Rap1 itself has been implicated in controlling T cell motility, adhesion and polarity[240, 241] by regulating myosin II activity[242] and coordinating LFA-1 expression and affinity[234, 236, 237]. It is there-

fore tempting to speculate that Sema3A regulates integrin binding through hydrolysis of Rap1-GTP to Rap1-GDP. Surprisingly, the only study that has explored Sema3A's effect on Rap1 directly in T cells, comes to the opposite conclusion: that Sema3A increases the activity of Rap1[209].

Here we examine Sema3A's effect on T cells. We find that in tumours, T cells are in close proximity to Sema3A-rich areas. *In vitro*, T cells round up following contact with Sema3A. Although Sema3A does not change the level of integrin-receptors on T cell surfaces, we find that Sema3A negatively regulates T cell adhesion and migration, an effect that can be inhibited by using blocking anti-NRP1 antibodies.

6.2 T cells are in close proximity to Sema3A rich areas in tumours

Following our investigation of Sema3A expression by tumour cells and endothelial cells in the TME, we performed immunofluorescence (IF) studies to determine the spatial relationship between Sema3A and T cells in B16.F10 tumours.

Clusters of Sema3A could be seen in the tumours, indicating that Sema3A can bind to the cell surface of certain cells, possibly through heparan sulphate[238]. Interestingly most TCRβ positive cells were in close proximity to these areas, although not completely co-localized.

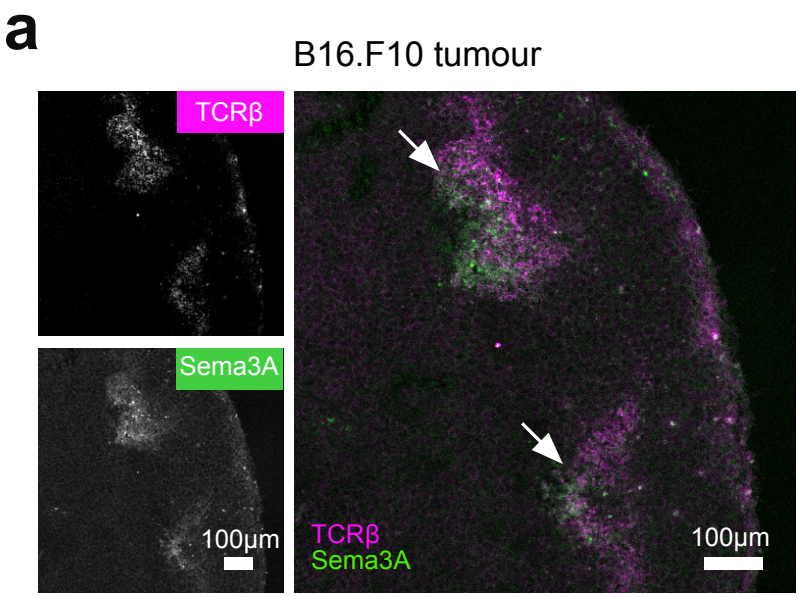


Figure 6.1: **T cells are in close proximity to Sema3A rich areas in tumours**. **A**. Representative IF image of B16.F10 tumour 11 days post injection, stained with anti-TCRβ and anti-Sema3A antibodies. T cells are in close proximity to the Sema3A-rich areas. Experiment performed once.

6.3 Sema3A is a negative regulator of integrin-mediated adhesion

In order to explore why T cells might be located in close proximity to Sema3A-rich areas in tumours, we decided to examine what effects soluble Sema3A had on selectins and integrins known to be involved in transmigration and motility, including PSGL-1 (CD162), integrin alpha-3 (VLA-3, CD49d) and CD11a (α_L part of LFA-1). We stimulated T cells for 48 hours to upregulate NRP1, followed by treatment with either control IgG or Sema3A at varying time-intervals (1-30 minutes), before cells were fixed and assayed by flow cytometry (Figure 6.2A).

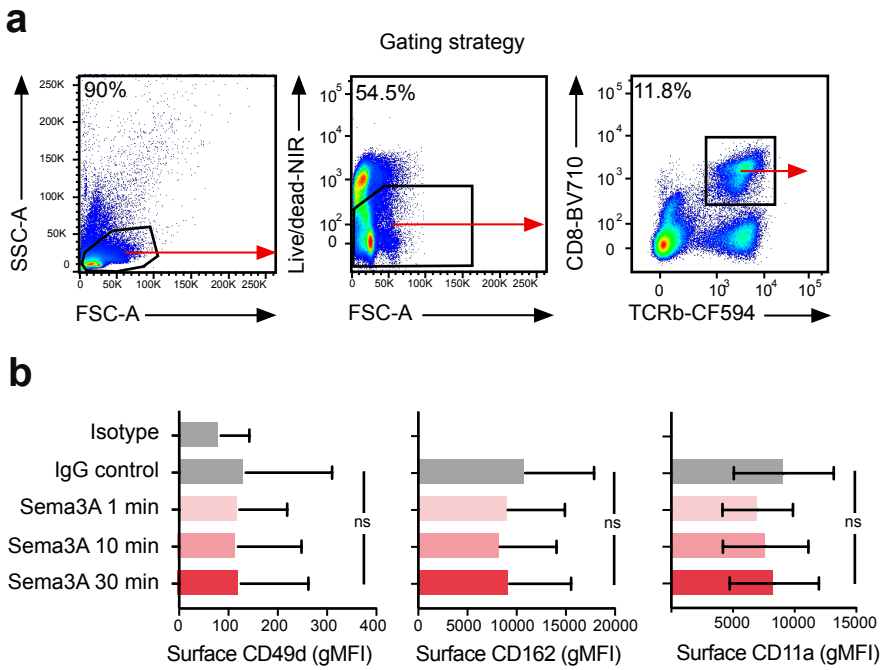


Figure 6.2: **Sema3A does not affect integrin-receptor levels on stimulated T cells**. **A**. Gating strategy for assaying PSGL-1 (CD162), integrin alpha-3 (VLA-3, CD49d) and CD11a (α_L part of LFA-1) on stimulated T cells. **B**. Analysis of surface expression (gMFI) of CD162, CD49d and CD11a following Sema3A treatment at varying time-intervals. Experiment performed once in technical triplicates. Data indicate mean ± SD. n.s. = not significant by one-way ANOVA.

Neither the expression level of CD49d, CD162 or CD11a changed significantly following treatment with Sema3A (Figure 6.2B). For human LFA-1, antibodies exist that can distinguish between LFA-1's open and closed conformational states, but unfortunately no similar reagents are available for murine LFA-1, and so this assay only gives an indication that similar levels of LFA-1 is available for binding immediately after Sema3A treatment, not the affinity of the protein.

Still, we wondered if Sema3A could affect T cell adhesion and migration. To explore this, we first conducted live-cell imaging of T cell migration on plates with immobilized

ICAM-1, CXCL12 and either Sema3A or control IgG. Cells were allowed to settle for 10 minutes, after which we followed individual cells for an additional 10 minutes.

We used interference reflection microscopy (IRM) as a method to assess T cell contact area and adhesion. As can be seen in Figure 6.3A, T cells allowed to adhere to Sema3A-plates formed considerably fewer and smaller contact zones with the plate. This effect was constant, with little change over time (Figure 6.3A).

We noticed that T cells on Sema3A plates were more round than on control IgG plates (Figure 6.3A). We quantified their shape and indeed T cells in contact with Sema3A were less polarized (Figure 6.3B).

These experiments suggest that immobilized Sema3A negatively affects T cell ability to bind ICAM-1, although the effect is most likely not caused by down-regulation of LFA-1.

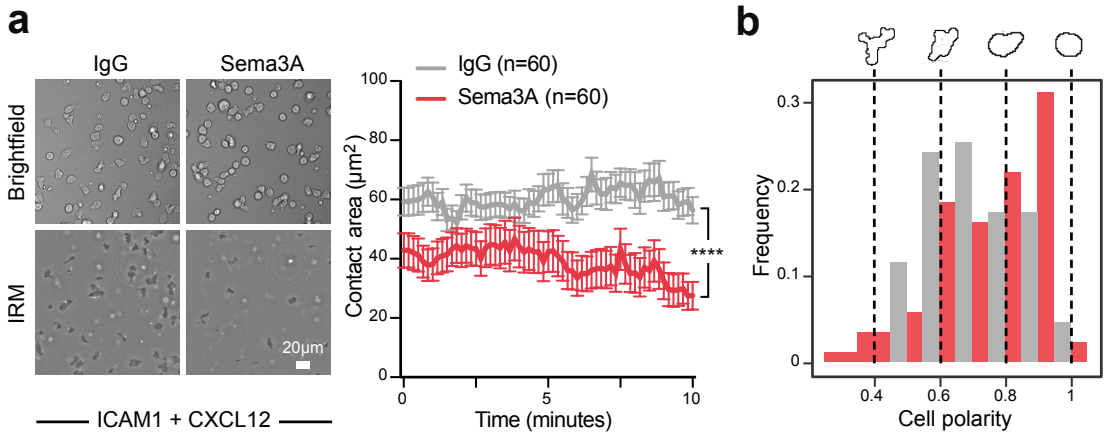


Figure 6.3: **Sema3A is a negative regulator of integrin-mediated adhesion**. **A**. Left: IRM and brightfield images of 48 hour-stimulated T cells on ICAM-1, CXCL12 plates with either Sema3A or IgG immobilized. T cells form smaller contact areas on Sema3A coated plates, as can be seen by smaller IRM shadows and are more round. Right: Quantification of contact area pr. single cells 10 minutes after T cell added to plate using live-cell microscopy show same phenotype over time. Data combined from three independent experiments. Data indicate mean ± SEM. **** = $P < 0.0001$ by students *t* test. **B**. Relative frequency of cell polarity from brightfield images. A polarity of 1 indicates a shape of a perfect circle, 0 a rectangular shape. Example images of T cells illustrated above graph. Significantly more T cells had rounded up on ICAM-1, CXCL12, Sema3A-plate.

6.4 Sema3A negatively affects T cell migration through NRP1

Plating T cells on ICAM-1 and CXCL12 coated plates also allowed us to assess their ability to move in a two-dimensional plane[243]. To this end we again stimulated T cells for 48 hours, sorted CD8+ T cells and visualized them using live-cell microscopy. Additionally, before adding cells to the plate, they were pretreated with either a blocking anti-NRP1 antibody or an isotype control antibody.

We first analyzed the migratory path cells took on control IgG or Sema3A immo-

bilized plates (Figure 6.4A, upper row). In order to maximize their search for antigen, activated T cells have been described as moving in a mix of long trajectories and short, random movements in a specific area, which resembled a generalized Levy walk[244].In our control condition, T cells moved freely around, often in long periods in a single direction, followed by kinks and turns in a single spot (Figure 6.4A, upper left). When Sema3A was immobilized on the plate however, their motility was severely stunted, and the cells did not move very far or not at all (Figure 6.4A, upper right). This effect was mediated through NRP1, because we could rescue T cell migration when pre-treating the cells with a NRP1-blocking antibody (Figure 6.4A, lower right). Not surprisingly, T cells on Sema3A-coated plates moved shorter distances (Figure 6.4B) and significantly slower (Figure 6.4C).

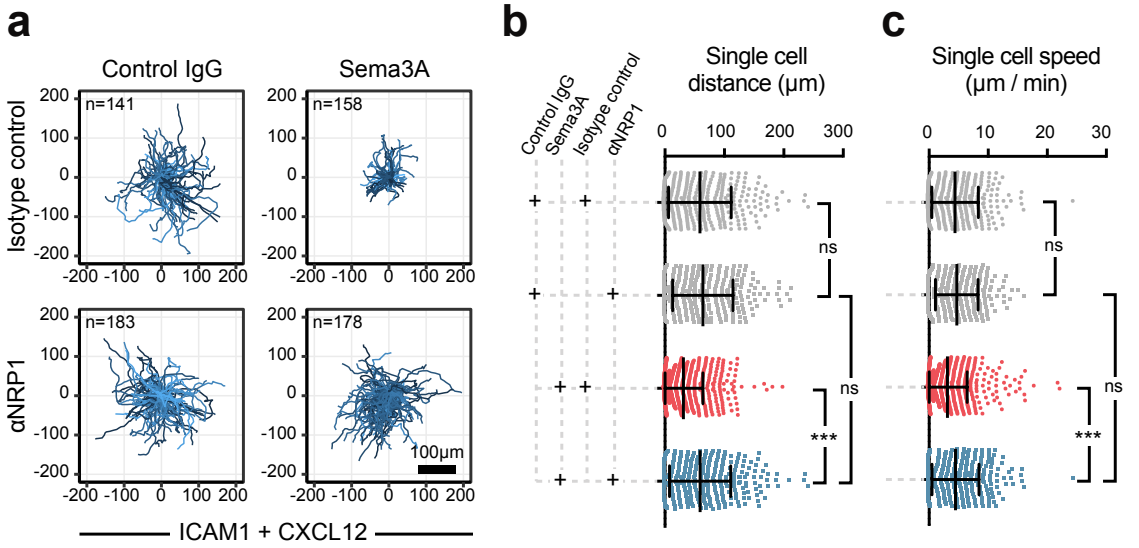


Figure 6.4: **Sema3A negatively affects T cell migration through NRP1**. **A**. Representative spider plots showing the migration paths of individual cells in conditions with either immobilized Sema3A or IgG, and pretreatment with either a block NRP1 antibody or an isotype control. T cells on Sema3A plates move significantly less. Experiment performed independently five times. **B**. Data from all experiments combined. Single cell distance of cells is significantly less on Sema3A coated plates. **C**. Data from all experiments combined. Single cell speed of cells is significantly less on Sema3A coated plates. N=314-744 cells per group. Data indicate mean ± SD. *** = $P < 0.001$, n.s. = not significant by Kruskal-Wallis test.

6.5 Sema3A decreases T cell ability to adhere under physiological levels of flow

We next tested how easily T cells could adhere under levels of flow expected to be found in capillaries[245]. 48 hour stimulated and sorted CD8+ T cells were loaded into a syringe and perfused through a closed chamber with immobilized ICAM1 + CXCL12 and either control IgG or Sema3A (Figure 6.5A). In order not to skew the results, cells were first allowed to settle, before flow was started and visualized for a maximum of

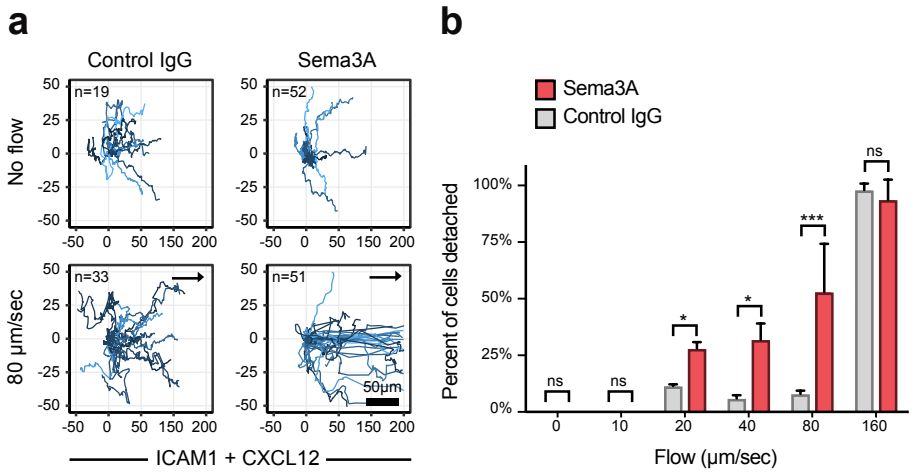


Figure 6.5: **Sema3A decreases T cells ability to adhere under physiological levels of flow**. **A**. Representative spider plots showing the migration paths of individual cells on either control IgG or Sema3A, and with flow or not. Cells on plates with Sema3A immobilized and flow are seen to have a laminar movement in direction of flow. **B**. Quantification of percent of cells that detach in either condition. Data combined from two independent experiments with 4 biological replicates in total. N=20-73 cells per condition and group. * = $P < 0.05$, *** = $P < 0.001$, n.s. = not significant by two-way ANOVA. Data indicate mean ± SEM.

10 minutes. With no flow, T cells displayed the same phenotype as seen before, with little T cell movement on the Sema3A coated plate (Figure 6.5A, upper right). However, under increasing levels of flow, T cells consistently detached more on Sema3A coated plates (Figure 6.5A, lower right and B). Some cells floated, re-attached, and detached again, but most cells simply had a laminar flow pattern, indicating little to no ability to adhere (Figure 6.5A, lower right). We quantified the percentage of cells with a speed above physiological levels ($>13\,\mu m$/second), and found that significantly more T cells on Sema3A-coated plates detached (Figure 6.5B).

6.6 Sema3A negatively affects T cells chemotaxis through NRP1

The final step in T cell extravasation is movement into the underlying parenchyma and migration herein, which is mainly chemokine dependent[101]. Because of the effects of Sema3A on T cell infiltration in our *in vivo* tumour model and motility in our *in vitro* experiments, we wondered if this final step of T cell infiltration was also affected. In tumours, the chemokine CXCL10 has been shown to play a major role in attracting tumour-specific CD8+ T cells[152, 246, 247], and we therefore used this as a chemoattractant in a trans-well assay. We used $3\,\mu m$ Boyden chambers, loaded with the chemokine CXCL10 in the lower chamber and 48 hour stimulated T cells, pretreated with either IgG control or blocking NRP1 antibodies, in the top chamber. 4 hours later cell numbers were enumerated, which showed that Sema3A completely inhibited T cell migration into the bottom well (Figure 6.6A).

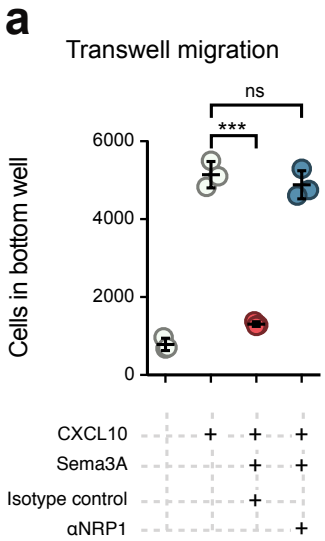


Figure 6.6: **Sema3A negatively affects T cells chemotaxis through NRP1**. **A**. 48 hour activated T cells allowed to migrate through $3\,\mu m$ Boyden chamber with CXCL10 in bottom well. Sema3A in the top chamber completely inhibited chemotaxis, an effect that could be blocked by pre-treating T cells with blocking NRP1 antibodies. Experiment perform with biological triplicates and repeated twice. *** = $P < 0.001$, n.s. = not significant, by two-way ANOVA. Data indicate mean ± SD.

6.7 Discussion

In this chapter we explored the effects of Sema3A on T cell migration and motility. IF experiments indicated that T cells were predominantly found in Sema3A-rich areas in B16.F10 tumours (Figure 6.1). We decided to more closely explore Sema3A's role in migration, specifically on the interaction between LFA-1 and ICAM-1, as T cells are highly dependent on binding between this integrin-ligand pair for both adhesion and transmigration into the underlying tissue.

Flow cytometry experiments indicate that LFA-1 is not down-regulated following interaction with Sema3A (Figure 6.2). Still, data from our adhesion assays clearly showed that T cells formed smaller adhesion area and rounder cells, when Sema3A was immo-

bilized on the plate (Figure 6.3). This also translated into poor motility on 2D surfaces (Figure 6.4) and a severely reduced ability to transmigrate in chemotaxis experiments (Figure 6.5).

Taken together our experiments suggest that Sema3A inhibit T cell motility. Possibly, T cells get stuck in areas that are especially enriched in Sema3A and this is the reason they are in close contact within Sema3A in the tumours. This would be in line with a report by Casazza et al, that find NRP1-dependent entrapment of macrophages in Sema3A-rich areas[248]. For T cells, little has been published on Sema3A's effect on migration: in an exploration of the collapsin response mediator protein 2 (CRMP2) gene, Vincent et al noticed an inhibition of T cells in chemotaxis experiments with Sema3A, although this effect was independent of CRMP2[249]. Studies interrogating Sema3E and Sema3F, ligands for Plexin-D1, have shown they inhibit thymocyte[215] and neutrophil[250] migration, respectively. In dendritic cells however, Sema3A, 3E and 3F have all been associated with increased migration[251, 252], indicating that the downstream effects of semaphorin signaling might be different in different cell types.

We unfortunately only scratch the surface with our assays here. To truly show a Sema3A-dependent effect on LFA-1, we need to conduct ICAM-1-binding assays on T cells. Another obvious follow-up to these experiments would be to quantify Rap1-GTP in Sema3A treated cells, as our results make it seem counter-intuitive that Sema3A should activate, rather than inhibit, Rap1 as suggested by Catalano et al[209]. Indeed Ueda et al, found that Sema3E inhibited Rap1-GTP in thymocytes[215], in line with the effects seen on other cell types following Sema3A treatment[179]. Finally it would be useful to visualize the exact location of both LFA-1, Rap1 and NRP1 to gain a better understanding

of their spatial organization in cells.

Since much of the same cytoskeletal machinery needed for migration is important in organizing the immunological synapse, we next explored how Sema3A affected T cells ability to bind to and kill cancer cells.

Chapter 7

Sema3A Inhibits T cell Synapse Formation by Affecting Actin Dynamics Through Actomyosin II Activity

7.1 Introduction

T cells become activated or can kill target cells when their TCRs recognize cognate antigens in the form of peptides loaded into MHC on antigen-presenting cells (APCs). T cells scan the surface of cells using actin-rich microvilli[253] which push into the target cell to survey it. This serves two purposes: firstly, it enables the close contact (approximately $14\,\mathrm{nm}$)[254] needed for TCR:pMHC interaction to occur[255, 256]. Secondly, it excludes larger molecules such as CD45, which, due to their phosphatase activity, would otherwise inhibit TCR signaling[257, 258]. These microvilli protrusions have half-lives in seconds, but upon antigen recognition they stabilize, form microclusters that last for

minutes, resulting in sustained TCR triggering[253, 256]. Following these initial signaling events T cells form in a immunological synapse, a highly organized cellular architecture[259, 260], which function to stabilize cell—cell contact[260] and direct cytotoxic secretion onto the target cell[109]. The immunological synapse consists of ring domains known as supramolecular activation clusters (SMACs)[259, 260]. The inner domain is rich in pMHC:TCR and CD80:CD28 interactions, and called the central supramolecular activation cluster (c-SMAC)), while ICAM-1:LFA-1 interactions form the periphery, and create a peripheral supramolecular activation cluster (p-SMAC).

In activated T cells, TCR-triggering not only affects proteins at the interphase between T cells and APCs, it also results in a complete morphological rearrangement of the cell, resulting in actin reorganization, uropod retraction and re-positioning of its centrosome towards the center of the emerging immunological synapse[261]. This cytoskeletal rearrangement happens actively during the formation of the immunological synapse and organizes it by forming a symmetrical inward flow of F-actin and a stiffening actin network, which stabilizes the contact[262, 263], increases binding to the target cell[264] and controls the secretion of cytotoxic granules[265, 266]. Following initial contact with an APC, T cells contract their uropod, round up and form a symmetrical contact zone over the course of minutes. Actin in the c-SMAC is depleted[261], while generation of an outer actin-rich ring, referred to as the distal supramolecular activation cluster (d-SMAC)[267], forms a lamellopodium that undulates across the APC[263, 268] and is thought to transport TCR microclusters towards the c-SMAC[269, 270]. *In vitro*, this contact lasts approximately 10 minutes and is then terminated[263], F-actin structure in the c-SMAC is restored[265] and the T cells polarizes and starts to migrate

again.

Although the role of myosin IIA in synapse formation has been controversial[271], it is now becoming clear that this actin-contracting protein-complex plays an important role in directing the inward flow of actin during the lamellopodia/undulating phase of contact[272, 273], helps to clear F-actin in the center of synapse to allow degranulation[266] and ultimately helps terminate the cell—cell contact[263]. High resolution 3D imaging has shown that myosin IIA, the only isoform found in T cells[274], forms bona fide arcs above the p-SMAC[272, 275] in the lamellopodia phase of contact, but then moves inwards and contracts, thereby pinching the T cell away from the APC during termination of the immunological synapse [263]. This last isotropic contraction of the actomyosin ring is reminiscent of myosin's role during cytokinesis[276].

Sema3A's role in the immunological synapse is not well explored. Lepelletier et al[210] found that Sema3A treatment inhibited Zap-70 phosphorylation in T cells and inhibited their contact with DC's. This is in line with work by Catalano et al, who found that Sema3A inhibited cytokine production in T cells[209, 277]. More recently Ueda et al, found that Sema3E, a protein structurally similar to Sema3A, inhibited synapse formation in thymocytes[215]. Importantly, this effect was mediated by inhibition of Rap1-GTP, which is known to be activated during TCR-triggering[278].

Here we explored what effect Sema3A has on the immunological synapse using supported bilayer experiments as well as cell-cell conjugation and killing assays. We find that activated T cells form fewer structured synapses when Sema3A is present and that Sema3A has profound effects on the F-actin cytoskeleton, most likely by over-activating myosin II.

7.2 Sema3A decreases cell adhesion and spreading on an activating surface

We wished to explore what effects Sema3A could have on T cell synapse formation but first wanted to test T cell ability to adhere to an activating surface with immobilized ICAM-1 and CD3. To mimick an environment in which Sema3A has been secreted, medium containing either Sema3A or control IgG were added to wells before T cells were allowed to form contact. Using IRM as a readout for adhesion, we measured the size and spreading speed of the contact areas. T cells in Sema3A-rich media formed fewer and smaller contact zones (Figure 7.1A, left). We noticed that cells in Sema3A-rich media did not spread as much and were slower to adhere (Figure 7.1A, right). We measured the size of contact zone over time. Many cells in Sema3A-rich media could not form large contact areas (Figure 7.1B), while the ones that could, generally spread at a slower speed (Figure 7.1C).

These results were reminiscent of the effects seen when T cells were added to plates with ICAM-1, CXCL12 and Sema3A and indicated that T cells ability to form immunological synapses could be compromised as well.

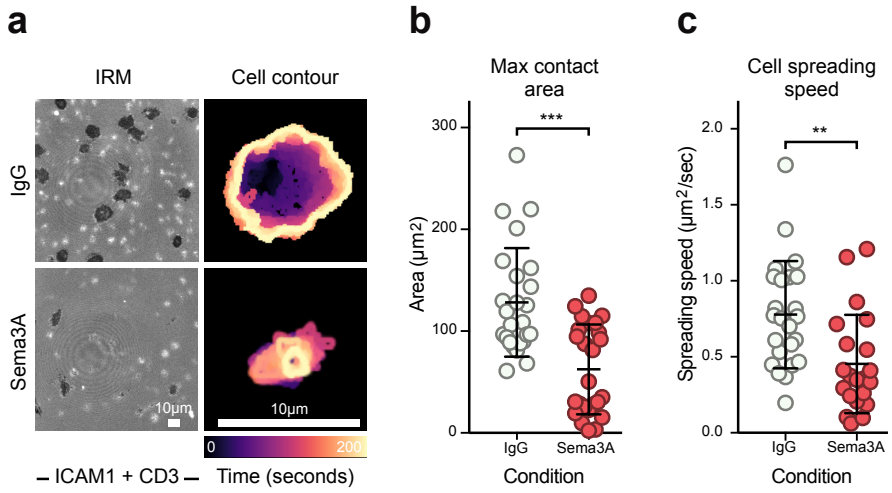


Figure 7.1: **Sema3A decreases cell adhesion and spreading**. **A**. Live-cell imaging of IRM of activated CD8+ T cells as they are dropped on an activating surface with immobilized ICAM-1 and CD3 and either Sema3A or IgG present in media. Cell contour of representative cell from either condition show smaller contact area with Sema3A present in media. **B**. The maximum size of cells contact area. With Sema3A present, a large population of cells never form average sized contact zones. **C**. The speed whereby cells spread from initial contact to the maximum contact area. Cells in Sema3A rich media spread slower. Data representative of three independent experiments. N = 25 cells per group. ** = $P < 0.01$, *** = $P < 0.001$, by Mann-Whitney test. Data indicate mean ± SD.

7.3 Sema3A-bound CD8+ T cells form poor immunological synapses on supported lipid bilayers

In order to examine T cell synapse formation in more detail, we changed two parameters in our setup: first, we modified our T cell stimulation protocol slightly. Tumour-infiltrating T cells engage targets repeatedly and over a prolonged period of time. In order to better mimic this, we repeatedly activated OT-I T cells for a total of three times over four days. All T cells expressed NRP1 following these extra activation steps (data

not shown). Secondly, we turned to supported lipid bilayers for more precise imaging of synapse dynamics and better recapitulation of the interaction between T cells and target cells. In this system we used labelled ICAM-1 and CD80 together with H-2K^b-SIINFEKL loaded monomers to generate a stimulating surface on which OT-I T cells could interact. Because Sema3A has intrinsic nickel-binding propensity (data not shown), we opted to pretreat OT-I T cells with Sema3A for 5 minutes, before washing and adding them to the bilayer, instead of simply having Sema3A in the medium. This was done in order to ensure that Sema3A did not interfere with ICAM-1, which was bound to the bilayer through a HIS-tag[1].

We first used labelled Sema3A and time-lapse total internal reflection fluorescence (TIRF) microscopy, in order to precisely see how T cells with bound Sema3A would interact with the bilayer. Most T cells with bound Sema3A did not form immunological synapses with characteristic SMACs, as indicated by a lack of a peripheral ICAM-1 ring surrounding central CD80 clustering (Figure 7.2, white arrows).

We noticed that a number of cells with bound Sema3A on them, had a roughened and uneven surface as seen by brightfield (top, left image in Figure 7.2. See also Figure 7.7A). We therefore worried that cells that bound Sema3A, were dead or dying cells. However, there are several reasons this was unlikely: almost all cells used in these experiments were alive following sorting 1-2 hours before analysis; Sema3A treatment acutely (within 15 minutes) and longterm (over 48 hours) does not kill T cells as assayed by Annexin V and PI staining (data not shown); finally, Sema3A-bound cells had some movement on the bilayer in resemblance to other T cells on the bilayer. More likely the phenotype is due to Sema3A's effect on the cytoskeleton, which we explore in more

[1]Personal communication with Michael L. Dustin.

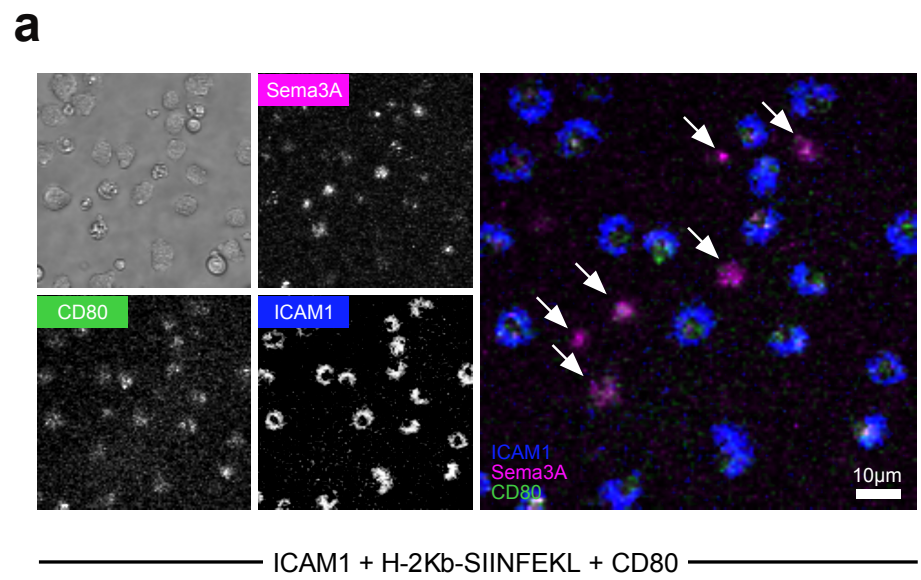


Figure 7.2: **Sema3A-bound CD8+ T cells do not form immunological synapses on supported lipid bilayers**. **A**. Live-cell imaging of activated T cells pretreated with Sema3A-AF647 and allowed to form synapses on supported lipid bilayers with ICAM-1, CD80 and H-2K^{b}-SIINFEKL. Arrows in merged image point to cells that have bound Sema3A and do not form immunological synapses. Experiment performed once.

detail below.

While TIRF microscopy is excellent at interrogating temporal characteristics at the cell—bilayer interphase, the number of cells that can be analyzed is low. We therefore turned to a recently developed high-throughput confocal method[190], which allowed us to assay a large number of immunological synapses (on average 1000 cells per condition).

To validate the method with OT-I T cells, we first made bilayers with an irrelevant peptide loaded into H-2D^{b} MHC monomer, namely the gp33 epitope of lymphocytic choriomeningitis virus (LCMV) and compared OT-I T cell ability to form synapses on it with bilayers made with H-2K^{b}-SIINFEKL. As expected, T cells readily formed identifiable immunological synapses on the H-2K^{b}-SIINFEKL bilayer and almost no synapses on

the H-2D^b-gp33 bilayer (Figure 7.3B). Satisfied that this method worked, we repeated our Sema3A-treatment of OT-I T cells, again for 5 minutes, and confirmed our findings from the initial TIRF experiments across thousands of cells originating from six different mice. In preparing the cells for high-throughput analysis, a washing step was included, and during this step most of the cells pre-treated with Sema3A were washed away (Figure 7.3A, brightfield), again indicating that Sema3A adversely affects adhesion. This resulted in significantly fewer T cells in the Sema3A condition (Figure 7.3A), and fewer identified p-SMACs among the analyzed cells (Figure 7.3C). Even though we had selected for binding T cells via our washing step, the quality of the c-SMAC, as quantified by CD80 intensity, was still poorer when T cells had encountered Sema3A (Figure 7.3C).

Taken together, these experiments strongly indicate that Sema3A affects T cell ability to form immunological synapses, both when Sema3A is present in the media (Figure 7.1) and immediately after T cells have encountered the protein (Figure 7.2 and 7.3).

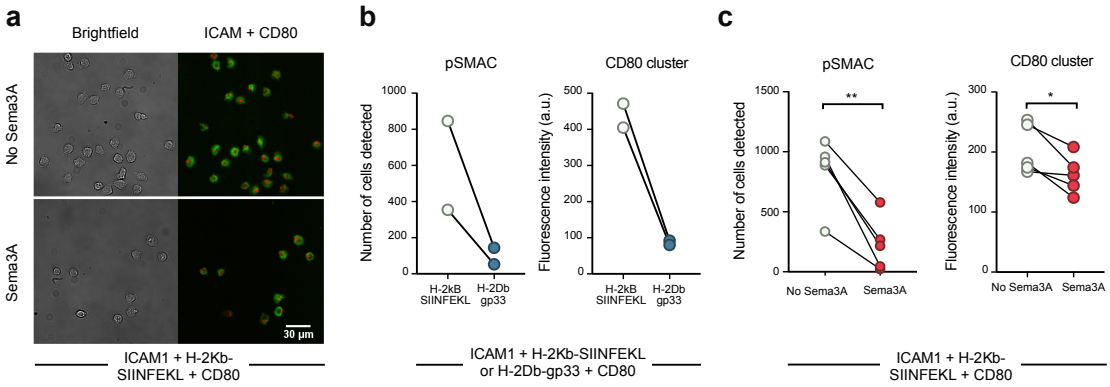


Figure 7.3: **Analysis of thousands of cells show strong effect of Sema3A on adherence and quality of immunological synapses**. **A**. Representative image from high-throughput analysis of immunological synapses with OT-I T cells pre-treated with Sema3A or control IgG. Significantly fewer cells adhere following Sema3A pre-treatment. **B**. Quantification of immunological synapses with a relevant (H-2K^b-SIINFEKL) or irrelevant (H-2D^b-gp33) MHC monomer loaded onto the bilayer. **C**. Quantification of immunological synapses with or without Sema3A pre-treated OT-I T cells. Data representative of six independent experiments. N = 90-1100 cells per mouse per group. * = $P < 0.05$, ** = $P < 0.01$, by paired t test.

7.4 Sema3A negatively affects T cell—cancer cell conjugation

We wanted to test if Sema3A also inhibited T cell binding to live target cells. To this end we utilized a classical cell-cell conjugation assay. Using 48 hour stimulated OT-I T cells, stained with a FarRed dye, and a GFP-positive B16.F10.Ova cell line which had been treated with IFNɣ overnight to up-regulate MHC on the cell surface, cancer cells and T cells were mixed 1:1 in medium containing either control IgG, Sema3A or a Sema3A-mutant protein (which cannot bind NRP1 due to two amino acid changes in the protein sequence[171]). Cells were allowed to conjugate for 15 minutes, fixed and analyzed by flow cytometry (Figure 7.4, left). We noticed an approximately 50% reduction, from

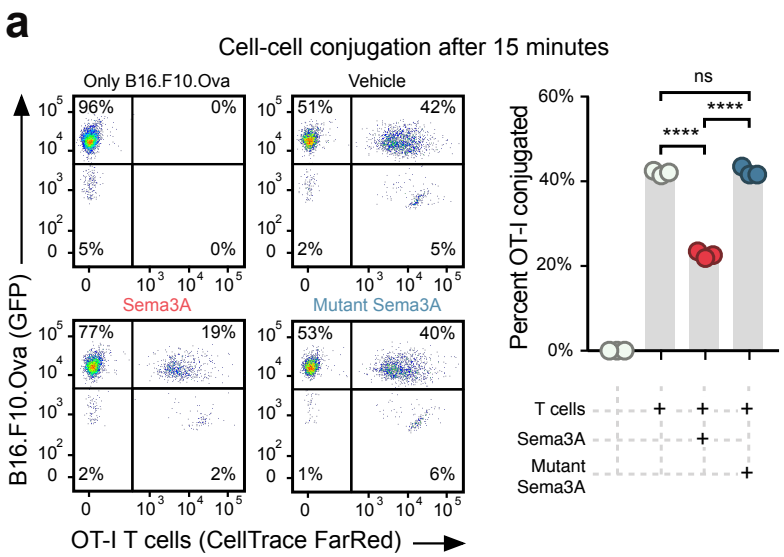


Figure 7.4: **Cell-cell conjugation is inhibited when Sema3A is present**. **A**. Left: Gating strategy and representative images showing number of B16.F10.Ova cells and T cells as either singlets or doublets under four different conditions: cancer cells alone, with normal media, media with Sema3A or with mutant Sema3A. Right: Quantification of 3 biological replicates, showing approximately 50% reduction in cell-cell conjugation when Sema3A is present. Data representative of three independent experiments. **** = $P < 0.0001$, ns = not significant, by two-way ANOVA. Gray bars indicate mean.

40% to 20%, of T cells that were able to form cell-cell conjugates with antigen-positive tumours cells when Sema3A was present in the media (Figure 7.4, right).

7.5 Sema3A decreases tumour-specific T cell cytotoxicity

If Sema3A decreases synapse formation and cell—cell conjugation, we reasoned that tumour-specific killing might be compromised as well. We therefore utilized the B16.F10.Ova Sema3A KO and Sema3A OE cell-lines we had constructed earlier and setup

a co-culture assay to explore this.

T cells were activated for 48 hours, sorted and washed, and allowed to rest for another 48 hours. This resting period was introduced as newly activated T cells killed cancer cells in an antigen-independent manner, most likely because they produce ample amounts of effector cytokines. By resting the cells we circumvented this problem and T cells were able to kill B16.F10.Ova, but not B16.F10 cells (data not shown).

We mixed B16.F10.Ova Sema3A KO and B16.F10.Ova Sema3A OE cells 1:1 and allowed them to rest for two hours, before OT-I T cells were added at various effector/target doses. Twenty-four hours later, cells were removed, and live and dead cancer cells were enumerated by flow cytometry (Figure 7.5, left). We saw no difference in cell numbers with no T cells added and at lower effector/target ratios, but noticed that Sema3A OE cells generally survived better, while the Sema3A KO line died in a dose-dependent manner. At the highest effector/target ratio (18/1), a significant difference in cell numbers was seen, with more Sema3A OE cells surviving.

This result indicates that Sema3A provide some protection against tumour-specific killing by OT-I T cells.

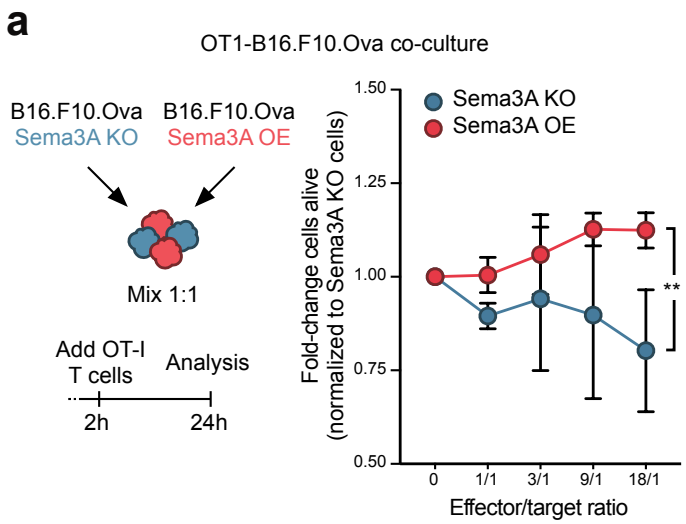


Figure 7.5: **Sema3A decreases tumour-specific T cell cytotoxicity**. **A**. Left: Experimental setup. Right: number of live cells from either Sema3A KO or Sema3A OE cell lines were enumerated following co-culture for 24 hours with OT-I T cells. Data representative of two independent experiments done in technical duplicates. ** = $P < 0.01$, by one-way ANOVA. Data indicate mean ± SD.

7.6 Sema3A immobilizes the F-actin cytoskeleton through actomyosin II activity

How does Sema3A affect T cell ability to adhere, migrate and form immunological synapses? While we had shown that Sema3A treatment initially leads to a decrease in surface expression of LFA-1 (Figure 6.2B), we also noticed that T cells treated with Sema3A underwent distinctive morphological changes. They rounded up (as seen in Figure 6.3B), their surface roughened and took a shape that vaguely resembled that of a a crushed beer can (Figure 7.2A, brightfield image).

Hypothesizing that these morphological changes were caused by Sema3A-induced changes to the F-actin cytoskeleton in T cells, we decided to look more carefully into

how F-actin was affected. Sema3A has been reported to cause either F-actin polymerization[279] or F-actin depolymerization[280, 281] and more generally ”F-actin reorganization”[210], although it is not always clear what authors exactly mean by this phrase.

We generated OT-I×LifeAct-GFP mice and stimulated these using our normal peptide stimulation protocol, after which NRP1 was up-regulated as expected (data not shown). These mice allow for precise interrogation of the F-actin cytoskeleton, as filamentous actin is green fluorescent protein (GFP)-tagged. T cells were allowed to adhere to ICAM-1 and CD3 coated plates, after which we performed live-cell imaging at 1 second per frame to better capture actin dynamics. T cells form stable contacts as judged by IRM and after a few minutes generated lamellopodia that undulated across the surface: while mainly tethered to one spot, cells none the less moved in dynamic ways, with protrusions forming in seemingly random directions as T cells surveyed the surface. These protrusions could be seen by both IRM shadow and LifeAct signal, which overlapped (Figure 7.6A).

We then added Sema3A to the cells. Whereas the cells were highly active before adding Sema3A, almost immediately after the protein was added, cells contracted slightly and displayed a roughened surface (Figure 7.7A, brightfield). This effect was seen approximately 10-30 seconds after Sema3A was added to cells and then progressed over the next 10-30 seconds. The effect of the contraction was dependent on how polarized the cell was beforehand: the more polarized, the more the cells contracted and rounded up. Examining the cell area and F-actin dynamics, as defined by the F-actin outline of the cell, we saw that following this immediate effect, cells simply became immobilized with very little membrane movement (Figure 7.7A, F-actin and cell contour). However,

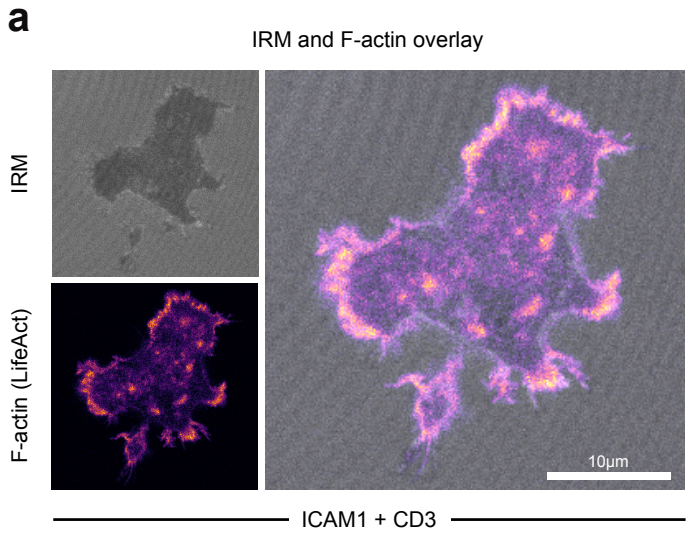


Figure 7.6: **IRM shadow and F-actin signal overlap**. **A**. Images from live-cell imaging of OT-I×LifeAct T cells show good concordance between IRM shadow and F-actin signal.

the F-actin signal did not severely diminish.

We wondered if Sema3A induced F-actin stabilization, similarly to the effect of the endogenous protein CapZ[282] or when cells are treated with the drug Jasplakinolide *in vitro*[283]. These proteins both ”stabilize” F-actin at the barbed end (ie, the polymerizing end). This momentarily freezes F-actin dynamics, but as actin filaments are depolymerized from the opposing end, cells shrink and contract as the cytoskeleton cannot sustain outward force. Using the F-actin contact area as a read-out, we therefore compared the phenotype of Sema3A- or Jasplakinolide-treated T cells. While initially similar, Jasplakinolide treatment continued to lead to contraction of cells (and therefore a small contact area), most likely a consequence of the F-actin treadmilling having been stopped at the barbed end. Sema3A treated cells however did not phenocopy this, and instead retained a certain size after the initial contraction (Figure 7.7B). In some videos the impression of

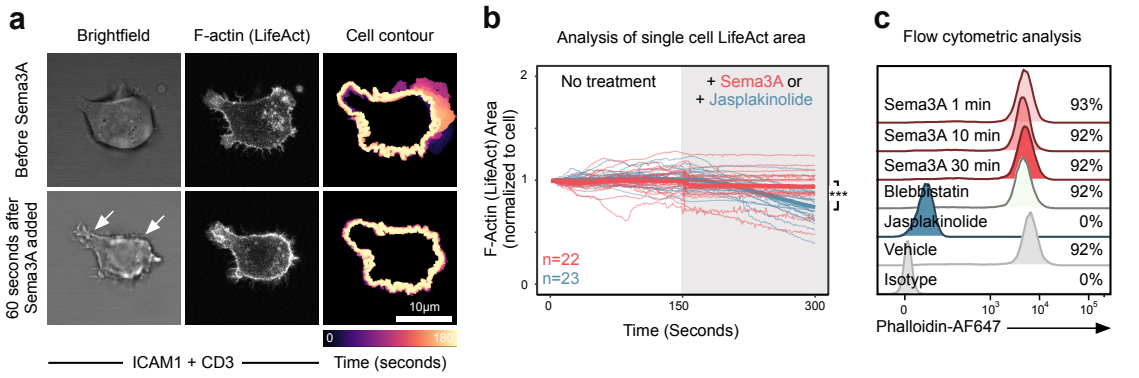


Figure 7.7: **Sema3A immobilizes the F-actin cytoskeleton**. **A**. Brightfield and LifeAct images of a T cell, before and after Sema3A was added to the cell media. Cell contour shows the lamellopodia activity over time. In the Sema3A condition the cell contracts (brightfield) and then becomes immobilized (cell contour). **B**. Analysis of 22-23 single cells before and after treatment with either Sema3A or Jasplakinolide. While cells treated with Jasplakinolide keep contracting, Sema3A treated T cells contact area simply stops moving after initial contraction. **C**. Analysis of F-actin content in cells as judged by Phalloidin-staining. Sema3A does not lead to substantial F-actin depolymerization within 1-30 minutes of treatment. Data combined from four independent experiments. N = 22-23 cells per group (B) or representative of three independent experiments (C). *** = $P < 0.001$ by Mann-Whitney test.

continued F-actin activity could be seen at the cell edges, however protrusions did not emerge.

We then confirmed that Sema3A indeed did not lead to significant F-actin depolymerization by treating OT-I T cells with Sema3A at varying time intervals, or with blebbistatin (a myosin II inhibitor) or Jasplakinolide for 30 minutes, before analyzing Phalloidin signal by flow cytometry (Figure 7.7C). While Jasplakinolide caused almost complete depolymerization after 30 minutes, Sema3A treated cells at 1, 10 or 30 minutes did not seem affected. These results together show that Sema3A does not cause F-actin depolymerization in T cells.

An alternative explanation for the phenotype we observed was that instead of out-

ward F-actin forces becoming weaker, inward forces were becoming stronger. When active, myosin II is known to cross-link F-actin and pull the filaments together, thereby increasing contractility of the cell[249, 284]. In non-muscle cells myosin II is regulated by phosphorylation of the enzyme myosin light chain kinase (MLCK)[284]. In epithelial cells, active Rap1-GTP has been associated with control of myosin II by controlling this phosphorylation[242, 285] and to suppress myosin II activity[286]. Since Sema3A is known to inactivate Rap1, we wondered if this would lead to increased myosin II activity, thereby inhibiting cell motility and immobilizing the F-actin cytoskeleton.

We conducted two versions of an experiment where we treated T cells with Sema3A and blebbistatin in succession: the cells were allowed to form contacts for approximately 3 minutes, after which we visualized their IRM contact area for 3 minutes; Sema3A was then added to cells; 3 minutes later the myosin II-inhibitor blebbistatin was added. The timing was selected in order to stay within the phase in which T cells formed lamellopodia and undulated over the surface. In the other experiment, the same setup was used, but blebbistatin was added before Sema3A (Figure 7.8). Blebbistatin inhibits the power-generating stroke of myosin II, and treating cells with it therefore disables myosin's ability to generate force[287]. As shown earlier, blebbistatin itself did not affect F-actin polymerization (Figure 7.7C). We chose to use IRM area instead of F-actin area as a readout, since blebbistatin is photosensitive and can be inhibited by 488 nm excitation otherwise needed to visualize LifeAct-GFP. When we treated T cells with Sema3A first, the cells contracted and then became immobilized. However, when blebbistatin was added to the cells, lamellopodia formed again, and cells reverted to their former size and activity (Figure 7.8A). In the second experiment, blebbistatin was added first, and in

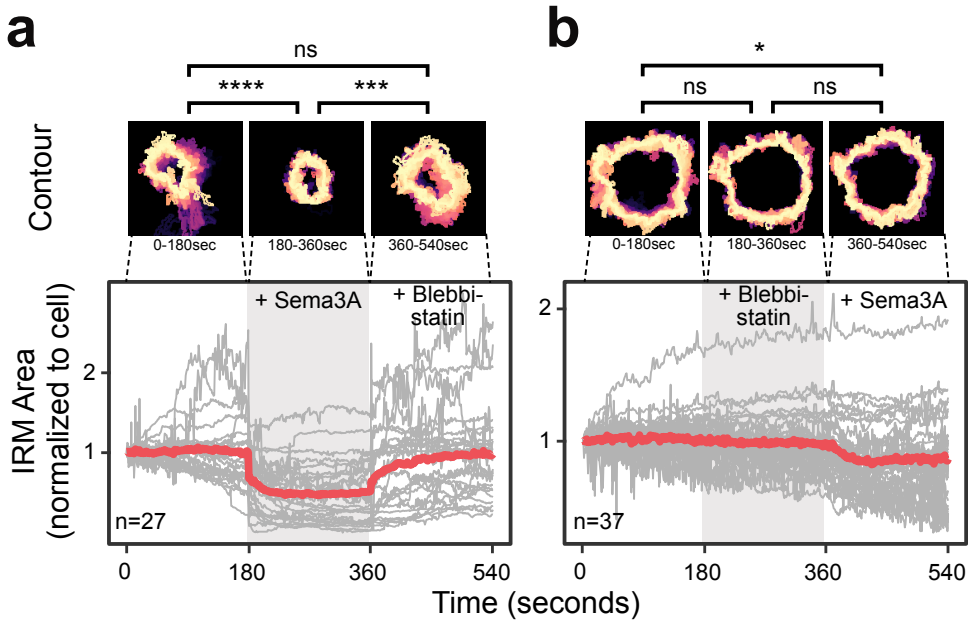


Figure 7.8: **Sema3A increases myosin II activity in activated T cells**. **A**. Activated T cells were added to plates with an activating surface with ICAM-1 and CD3 bound. Cells were allowed to adhere and after approximately 5 minutes, their IRM area visualized every second using time-lapse microscopy for 3 minutes. Sema3A was then added to cells for 3 minutes, followed by blebbistatin. Sema3A treatment lead to smaller contact area, followed by stabilization of IRM dynamics. However, upon blebbistatin treatment, T cells reverted to their former size and activity. **B**. Same experiment as in A, but with blebbistatin added before Sema3A. Here T cells seem immune to Sema3A treatment, although some effect can still be seen. Data combined from three independent experiments. N = 27-37 cells per group. * = $P < 0.05$, *** = $P < 0.001$, **** = $P < 0.0001$, ns = not significant by two-way ANOVA at time-points 90, 270 and 450 seconds.

this condition, most cells were immune to Sema3A treatment, although a few cells still reacted.

Taken together, these two experiments suggest that Sema3A signaling ultimately affects myosin II activity.

7.7 Discussion

In this chapter we explored the effects of Sema3A on immunological synapse formation and CD8+ T cell morphology. Several pieces of evidence point to Sema3A as an inhibitor of immunological synapses: firstly, in two different supported lipid bilayer experiments, we noticed strong negative effects on T cell ability to form properly organized SMACs (Figure 7.2 and 7.3). In our TIRF experiment cells were added to the bilayer after Sema3A treatment, and here Sema3A-bound T cells formed poor or no detectable SMACs (Figure 7.2). In our high-throughput assay, most Sema3A pretreated T cells were likely washed away as we detected significantly fewer cells, but even the ones that did adhere, formed synapses of a poorer quality as judged by CD80 clustering (Figure 7.3). Importantly, we validated this finding using cell-cell conjugation assays, where we noticed a 50% reduction in the number of T cells conjugated to antigen-expressing cancer cells (Figure 7.4), and in a *in vitro* T cell—cancer cell killing assay (Figure 7.5).

Most likely this is a consequence of two downstream effects of Sema3A signaling that may be intertwined: as indicated by our adhesion assay on ICAM-1 and CD3 coated plates in this chapter (Figure 7.1) and on ICAM-1 and CXCL12 coated plates in the previous chapter (Figure 6.3), Sema3A strongly inhibits adhesion, when cells are exposed to Sema3A either in soluble form in the media, immobilized on the plate or when they are pre-treated with the protein. As the small GTPase Rap1 has been shown to control LFA-1 activity[234, 236, 237] and is furthermore influenced by Sema3A signaling[179, 180], this might explain why T cells do not form immunological synapses or cell-cell conjugates at the same rate and quality when Sema3A is present. However, when we add Sema3A to T cells after they have adhered and formed synapses, their morphological

changes, resembling that of a crushed beer can, are not immediately reminiscent of integrin defects. High affinity LFA-1 is not found at T cell protrusions, but mid-center[288]: as cells contract inward towards the middle of the cell after Sema3A treatment, this does not implicate weaker adhesion here. Inspired by the literature on axonal growth cones and their response to Sema3A, we therefore examined F-actin dynamics. We found that while Sema3A does not cause F-actin depolymerization (Figure 7.7), it does immobilize the F-actin cytoskeleton within approximately 30 seconds. We believe this is an effect of myosin II activity becoming stronger when Sema3A is present, since we can both rescue or inhibit Sema3A's effect when treating T cells with blebbistatin (Figure 7.8), a drug that inhibits activated myosin II specifically. There is some credence to this idea in the literature, as Rap1 has also been implicated as a negative regulator of myosin II activity in other cell types[242, 286]. Additionally, in axonal growth cones Sema3A has been shown to increase myosin II activity directly[289].

Our working hypothesis is therefore the following: that active GTP-bound Rap1 tightly controls myosin II activity in T cells, but as Rap1 is converted into its inactive, GDP-bound state, by Sema3A signaling, myosin II becomes a dominant force in T cells leading to premature cell contraction and inhibition of the immunological synapse. This would be in line with reports on Sema3A effects on axonal growth cones[239, 289]. It would also fit with myosin II playing an important role in termination of T cell—APC contact[263].

It is interesting to compare these *in vitro* experiments, to our *in vivo* experiments, in which mice carried Sema3A KO and Sema3A OE tumours on opposing flanks. While they did show a significant difference in tumour growth following OT-I treatment and

increased T cell infiltration, we did not observe less activation of tumour-specific T cells in Sema3A OE tumours (Figure 4.12) as would be expected if Sema3A inhibited synapse formation completely. On the contrary, more OT-I T cells found in Sema3A OE tumours expressed CD69, a surface protein long associated with T cell activation. Perhaps this is a result of the concentrations of Sema3A available in tumours or it's spatial distribution there.

Following this interrogation of Sema3A's effect on murine T cells, we next wanted to test if the Sema3A/NRP1 axis was relevant in human cancers as well. To this end we turned to ccRCC.

Chapter 8

NRP1 and Sema3A Expression in Clear Cell Renal Carcinoma

8.1 Introduction

We wanted to explore whether the Sema3A/NRP1 axis was important in human cancers as well. To this end we utilized access to a ccRCC cohort which is being administered by the Oxford Radcliffe Biobank.

ccRCC is a heterogenous cancer type, which causes the majority of deaths from kidney-related cancers. The VHL tumour supressor gene, which regulates HIF degradation, is mutated in the majority of ccRCC cases, leading to aberrant upregulation of the HIF protein and downstream target genes. The end-result is creation of a tumour-microenvironment rich in lipids and uncontrolled angiogenesis, making the tumours highly vascular, although most of these vessels are immature[290]. Newer therapies have focused on using anti-vascular therapies, such as anti-VEGF antibodies[291] or

VEGF-receptor tyrosine kinase inhibitors[292], which are currently front-line therapies in many settings[290], while complete or partial nephrectomy have been the mainstay in treatment for many years. Interestingly, there are indications that the anti-VEGF therapies alone can ”normalize” the tumour vasculature, and thereby increase the number of TILs in ccRCC tumours[293].

Compared to other tumour types, ccRCC is characterized by having relatively many TILs [294], but most of these display an exhausted phenotype as defined by expression of multiple co-inhibitory receptors[32]. As in metastatic melanoma, interleukin 2 (IL-2) was used as a treatment earlier[295] but fell out of fashion due to poor efficacy and side-effects, when the anti-VEGF therapies were introduced. Currently, a flurry of studies are challenging the current front-line regimes used, with anti-PD1 and anti-PDL1 immunotherapies showing good results as monotherapies or in combination with anti-VEGF therapies[296–299]. Taken together, there is therefore increasing evidence that therapies that modulate the immune system could have beneficial effects in ccRCC.

Here we show that high Sema3A expression is associated with poor survival in ccRCC and using flow cytometry and immunohistochemistry (IHC), confirm our findings from previous chapters, that tumour-specific T cells express NRP1, and are in close contact with Sema3A-rich areas. While descriptive in nature, this chapter reveals that the Sema3A/NRP1 axis is active and important in human cancer.

8.2 Clear cell renal cell carcinoma cohort

We first asked if Sema3A played any role in tumour progression in ccRCC. To this end we analyzed publicly available data from the TCGA using the bioinformatic tool

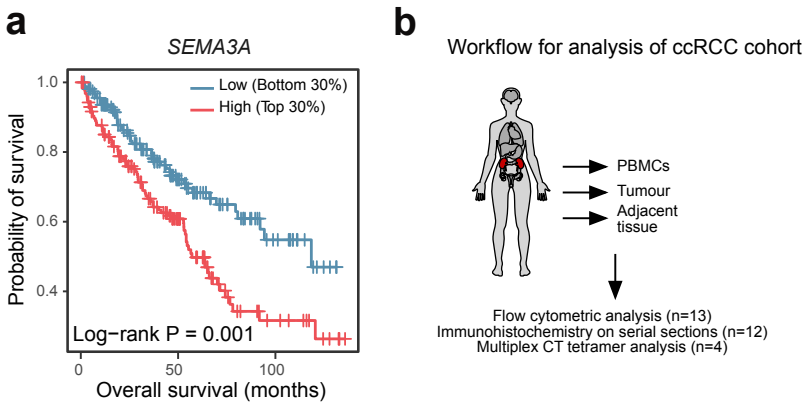


Figure 8.1: **Sema3A expression negatively correlates with survival in ccRCC**. **A**. Analysis of ccRCC data in TCGA dataset, reveals poor prognosis among patients with high expression of Sema3A. N=533 patients. Log-rang P tested used. **B**. Workflow for analysis of Oxford Radcliffe Biobank cohort of ccRCC patients.

TIMER[97]. There was a clear inverse association between Sema3A expression and probability of survival (Figure 8.1A).

To examine this in more detail, we harvested peripheral blood mononuclear cells (PBMCs), tumour and adjacent tissue from patients undergoing radical or partial nephrectomies. All tissue and diagnosis was confirmed by pathologist at the John Radcliffe Hospital in Oxford. The baseline characteristics of the patients are outlined in Table 8.1. In total we collected tissue from 23 patients: 17 were used in flow cytometry studies of T cells for tumour-specificity (n=4) and expression of NRP1 (n=13), while 12 tumours were analysed by IHC for expression of CD31, Sema3A and CD8 (Figure 8.1B).

Table. Baseline characteristics for ccRCC cohort		
Characteristics	Number (range)	Percent
Age		
Mean	64.4 (42-86)	
Gender		
Male	13	56.5%
Female	10	43.5%
Tumour grade (ISUP)		
1	0	0
2	2	8.7%
3	12	52.2%
4	6	26.1%
N/A	3	13%
Tumour location		
Right	14	60.9%
Left	9	39.1%
Type of surgery		
Radical nephrectomy	17	73.9%
Partial nephrectomy	6	26.1%
Tumour stage		
pT1a	1	4.5%
pT1b	5	22.7%
pT2a	1	4.5%
pT3a	14	63.6%
pT3c	1	4.5%
N/A	1	4.5%

Table 8.1: Baseline characteristics for clear cell renal cell carcinoma cohort used in this study.

8.3 Sema3A is located in glomeruli in healthy tissue and on CD31+ cells in ccRCC

We wanted a better understanding of the spatial distribution of Sema3A in ccRCC and therefore stained sections for Sema3A. In adjacent tissue to tumours, we found

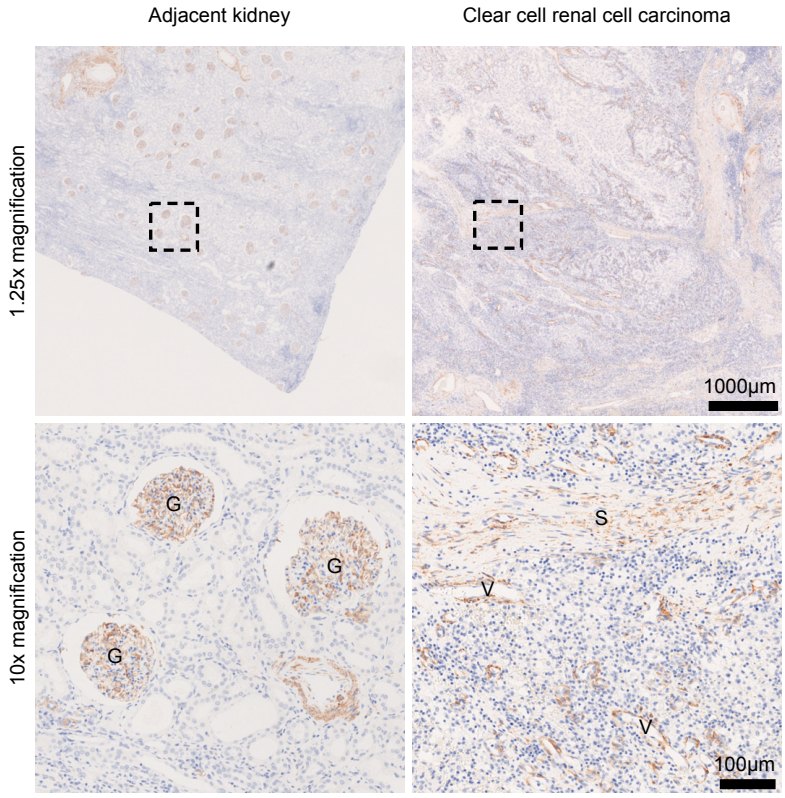


Figure 8.2: **Sema3A expression in healthy and cancerous kidney**. Left column: Staining in adjacent kidney. Sema3A is found in kidney glomeruli (G). Right column: Staining in ccRCC found on vasculature (V) and surrounding smooth muscle as well as some stroma (S).

Sema3A expression restricted to the glomeruli and some smooth muscle (Figure 8.2A). However, in cancerous tissue Sema3A was excessively expressed, mostly on and around blood vessels (Figure 8.2B). This was similar to our findings in B16.F10 tumours in mice. There was also diffuse staining through large areas of the tumour, but it was hard to judge if this was staining on microvessels, from cancer cells or Sema3A binding to extracellular matrix.

In order to closer examine where Sema3A was being expressed and how it related to CD8+ T cells, we stained serial sections of tumour tissue for CD31, Sema3A and CD8 (Figure 8.3). The stains were scanned and computationally aligned, before highly and weakly vascularised regions were selected from each patient (n=12). This was done in a blinded manner, without assessing CD8 and Sema3A staining, in order to ensure that we did not bias our analysis, since it is known that tumour vasculature heavily influenzes T cell infiltration[293, 300]. Analysis of CD31 content in the two groups confirmed that we had indeed correctly identified high and low vascularised regions for our analysis (Figure 8.3B).

In all sections we explored, in both weakly and highly vascularised regions of tumours, Sema3A expression was closely associated with CD31 expression (Figure 8.3A and Figure 8.4A). This indicates that Sema3A is heavily expressed and secreted by endothelial cells and possible surrounding smooth muscle cells in ccRCC, similar to our results using the B16.F10 model in mice. In our mouse model, we saw that T cells were in close contact with Sema3A-rich areas. While this was hard to judge in the highly vascularised regions, simply due to excessive amounts of Sema3A, in the weakly vascularised regions, we found CD8+ T cells and Sema3A were indeed in close contact (Figure 8.3A, white arrow).

We wanted to explore the correlation between Sema3A expression and CD8+ T cell infiltration. Overall, we found there were slightly more CD8+ T cells in the highly vascularised regions (Figure 8.4B), which also had overall higher Sema3A expression (Figure 8.4A). When we correlated CD8+ T cell number to Sema3A expression, we found no correlation in the highly vascularised regions (Figure 8.4C, R^2 = 0.02). However, in the

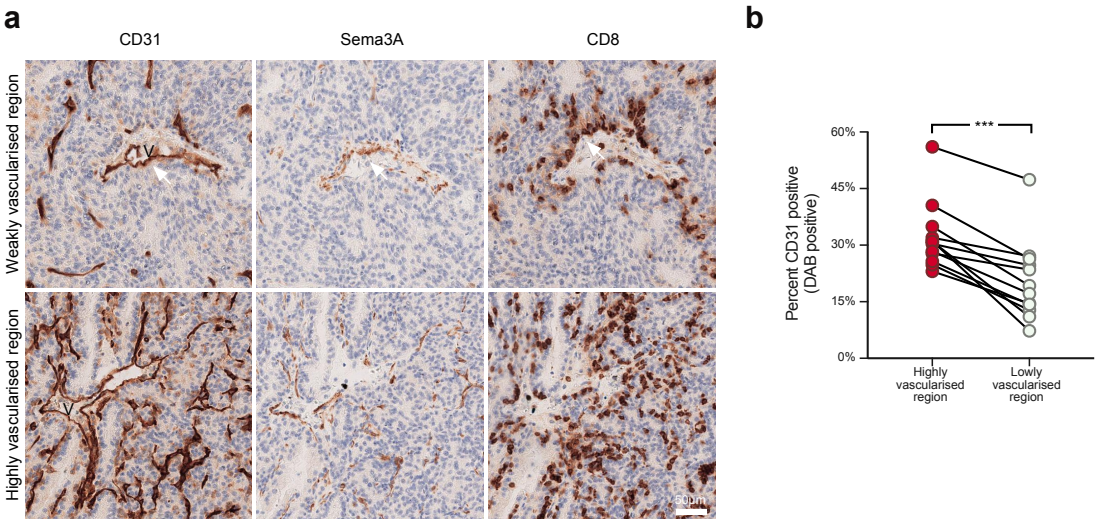


Figure 8.3: **Sema3A and CD31 are co-expressed**. **A**. Serial sections from ccRCC tumours stained for CD31, Sema3A and CD8. Top row: Weakly vascularised region. Bottom row: highly vascularised region. CD31 and Sema3A staining are closely associated. In low vascularised region CD8+ T cells are in close proximity to Sema3A-rich areas. **B**. Analysis of CD31 expression confirm that correct hight and low vascularised regions have been selected. N = 12. *** = $P < 0.001$ by paired t test.

weakly vascularised areas, a moderate inverse correlation between Sema3A and T cell infiltration was seen: the more Sema3A present, the fewer T cells were able to infiltrate into that region (Figure 8.4D, $R^2 = 0.37$). These findings seem to indicate that in areas with amble vessels, T cells more readily infiltrate and Sema3A does not play a major role. In vasculature poor regions, T cells are more often found near Sema3A-rich areas (Figure 8.3A), but here Sema3A is able to repress CD8+ T cell infiltration to a certain extent (Figure 8.3A and 8.4D). It should be noted however, that even our ”weakly” vascularised region contained quite high amounts of vasculature (Figure 8.3B, on average 20.5% of stained area).

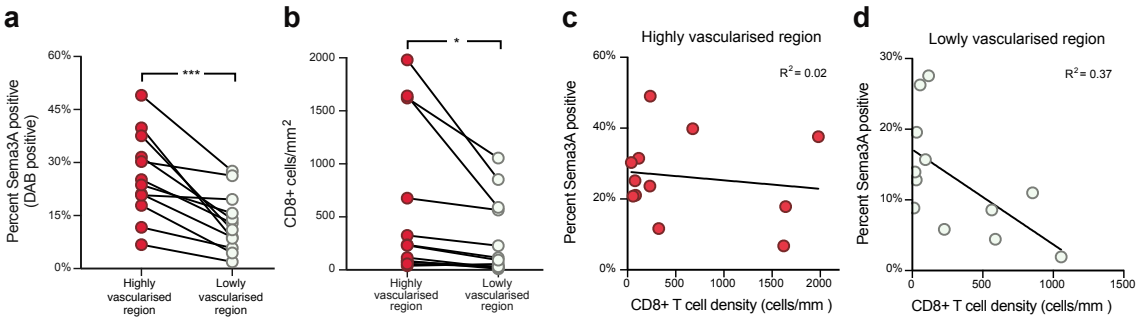


Figure 8.4: **Vasculature and Sema3A are variables in determining T cell infiltration**. **A**. Quantification of Sema3A show that the protein is expressed more in highly vascularised regions. **B**. There are slightly more CD8+ T cells in highly vascularised regions. **C**. There is no correlation between CD8+ T cells infiltration and Sema3A expression in highly vascularised regions. **D**. There is a moderate negative correlation between CD8+ T cell infiltration and Sema3A in weakly vascularised regions. Regression line significantly different from zero. N = 12. * = $P < 0.05$, *** = $P < 0.001$ by paired t test (A and B). Linear regression used in C and D.

8.4 A propotion of tumour-infiltrating T cells are NRP1+

We next wanted to see if CD8+ T cells also expressed the Sema3A-receptor NRP1 in ccRCC tissue. To this end we processed PBMCs, tumour tissue and adjacent kidney from patients. The tissue was processed fresh, meaning on the same or next day following surgery. A pathologist confirmed diagnosis of tissue subtype.

A substantial proportion of CD8+ T cells in tumour and adjacent tissue were NRP1 positive, while most CD8+ T cells in blood did not express the receptor (Figure 8.5A).

Next we screened patient samples for HLA-A2 expression, and in four HLA-A2 positive patients, stained CD8+ TILs with HLA-A2 tetramers loaded with a panel of CT-antigens (see Materials and Methods for complete list). This was done in order to de-

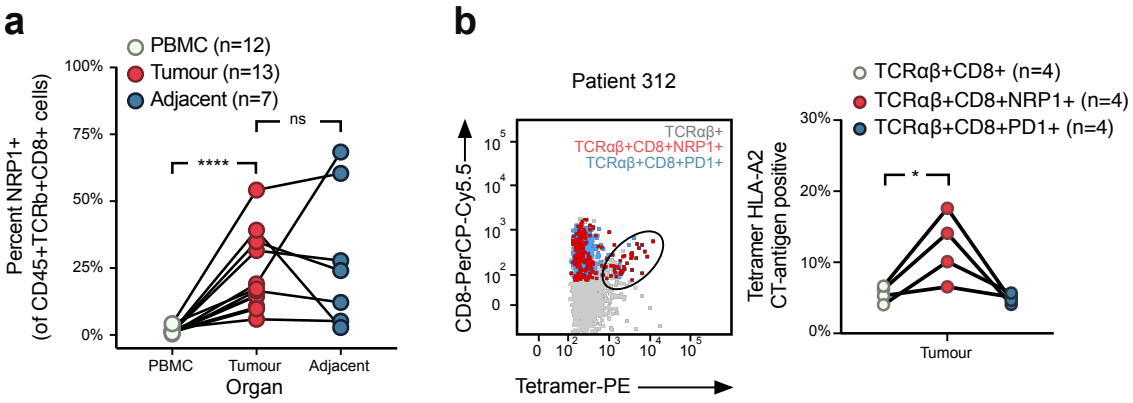


Figure 8.5: **A propotion of tumour-infiltrating T cells are NRP1+.** **A**. Flow cytometric analysis of tumour-infiltrating CD8+ T cells are NRP1+. **B**. HLA-A2-CT-antigen tetramers are to a higher degree found on NRP1+ T cells. N = 7-13. * = P $<$ 0.05, *** = P $<$ 0.001, n.s = not significant by paired t test.

termine whether NRP1+ CD8+ T cells in tumour were specific for known CT-antigens and hence tumour-specific. Overall, we found a significant proportion of CD8+ TILs specific for a CT-antigen (approximately 5%). Importantly though, more NRP1+ CD8+ T cells stained positive for CT-tetramer, indicating that NRP1 also serves as a marker for tumour-specificity in ccRCC.

8.5 Discussion

In this chapter we sought to confirm findings from our work with the murine B16.F10 model in a human cancer. We choose ccRCC as it is an emerging cancer that most likely will benefit from immuno-oncological therapy in the near future, and additionally, is a tumour-type where the neo-vasculature is known to play an important role in tumour progression.

In silico analysis of TCGA data indicated that high Sema3A expression leads to a poor

prognosis among ccRCC patients (Figure 8.1A). This led us to explore the expression pattern of Sema3A in more detail. We found excessive amounts of Sema3A expressed by the tumour vasculature (as defined by the endothelial cell marker CD31) by IHC (Figure 8.3A). In regions with high amounts of vasculaure and Sema3A, we found no difference in CD8+ T cell infiltration, but in regions with more sparse expression, Sema3A had a negative effect on T cell infiltration (Figure 8.4D). IHC images from these lesser vascularised regions were similar to the ones we had seen in our B16.F10 mouse models, where T cells were in close contact with Sema3A-rich areas.

We next determined that a proportion of CD8+ TILs express NRP1 and that NRP1-expression was associated with expression of TCRs specific for a range of CT-antigens. This suggests that, as in mice, NRP1 is a marker for recent activation of human T cells as well.

The close correlation between CD31 expression and Sema3A means that these variables are not independent of each other. Our *in silico* analysis of survival-likelihood and our analysis of CD8+ T cell infiltration are therefore confounded by the fact, that a number of other factors, such as poor perfusion of the vasculature or lack of HEVs, could be impeding survival and T cell infiltration as well. However, following our exploration of Sema3A's effect on murine T cells, the fact that a proportion of CD8+ TILs express NRP1, and that Sema3A is present in ccRCC, gives a strong indication that the same adverse inhibition of major T cell functions could be happening in humans as well.

Chapter 9

Conclusion

9.1 Results from this thesis

The objective of this thesis has been to describe the role of the surface receptor NRP1 on CD8+ T cells in the context of cancer. To this end, a number of animal models and cell-lines were created in order to allow for perturbation of key molecules. Our main findings will be discussed here.

The Sema3A receptors, NRP1 and Plexin-A1, are expressed by tumour-specific T cells

While the effect and expression of NRP1 on CD8+ T cells has been debated[207–211], we here show definitely that CD8+ T cells up-regulate NRP1 expression following TCR-engagement. As NRP1 is a promiscuous receptor, we examined the co-receptor landscape on T cells and identified Plexin-A1 as the main signaling-partner available for NRP1 dimerization on activated CD8+ T cells. T cells expressing both NRP1 and Plexin-

A1 were able to bind recombinant Sema3A. In a model of tumour-specificity, we found that infiltrating T cells retained their expression of both receptors long term in mice. In ccRCC patient samples, we found a large subset of CD8+ T cells that were NRP1 positive and furthermore had the characteristics of being tumour-specific, in the sense that they expressed TCRs for CT-antigens.

Sema3A is a negative regulator of T cell mobility and synapse formation

Other groups have implicated Sema3A as an inhibitor of T cell signaling and proliferation using *in vitro* assays[209, 210]. Here we extend these findings, using both *in vitro* and *in vivo* methods, and validate our findings in a renal cell carcinoma cohort. The work presented here significantly extends our understanding of Sema3A biology in the context of T cell—tumour interactions.

Primarily, we generated several lines of evidence that point to a strong inhibitory effect of Sema3A on T cell migration: in Sema3A-rich tumours, conditional knockout of NRP1 on T cells enabled better infiltration. Conversely, in mice seeded with both over-expressing and Sema3A-deficient tumours, NRP1-positive T cells more readily infiltrate into Sema3A-deficient tumours. *In vitro* experiments recapitulated effects on T cell mobility and transmigration. Importantly, these effects could be inhibited using blocking αNRP1-antibodies. In both our murine model and in ccRCC patients, Sema3A was strongly expressed and associated with endothelial cells. Localized expression along the vasculature might explain why T cells seem to get stuck in close proximity to these areas and explain lack of T cell infiltration deeper into the tumour.

Secondly, multiple experimental assays confirmed strong inhibitory effects of

Sema3A on immunological synapse formation and cell—cell binding. This finding was also reflected in the fact that T cells preferentially killed Sema3A knockout cells, as opposed to Sema3A overexpressing cells.

Most likely both effects are acting synergistically *in vivo*, and explain the remarkable control of tumour growth we saw in our CD4Cre×NRP1 knockout mice.

Sema3A strongly affects T cell F-actin dynamics

How can these multiple effects on T cells be explained? We saw strong effects on T cell ability to adhere to ICAM-1 coated surfaces and characteristic morphological changes when Sema3A was present. Specifically, T cells rounded up, and took a roughened shape that resembled a crushed beer can. Inspired by the literature on Sema3A's effect during embryogenesis, we decided to look at the T cell cytoskeleton during treatment with Sema3A. The effects were striking, with the main consequence being immobilization of membrane dynamics. We believe these effects are caused by hyper-activation of myosin IIA in T cells, as we could block and rescue the effects using the drug Blebbistatin. Although this interpretation is supported by reports in the literature in different cell types[239, 251, 280], much of this signaling pathway still needs to be elucidated in T cells.

Implications for T cell function in cancer

Our study defines a completely novel tumour-escape mechanism, namely inhibition of tumour-specific T cells through inhibitory effects on the T cell cytoskeleton. This is reminiscent of how pox and measles virus escape immune-detection by expressing viral semaphorins[301, 302], and opens new therapeutic avenues, for example by us-

ing blocking αNRP1 antibodies. The fact that recently activated T cells in mice and tumour-specific T cells in ccRCC patients express NRP1, makes this an especially exciting prospect, as these are the exact T cell clones one would want to enable in a tumour.

A number of groups are now utilizing Sema3A as a means to normalize tumour-vasculature and are generating drugs that can be used for this end in humans[23, 24]. Our data suggest careful considerations to timing and usage must be applied, especially if these are combined with checkpoint inhibitors, as exogenous sources of Sema3A most likely will inhibit T cell responses as well.

9.2 Outstanding questions

What is the role of NRP1 on T cells outside tumours?

A question we attempted to address in this thesis, was the role of NRP1 during T cell development. However, we saw no difference in either thymus or splenic T cell numbers or function when comparing NRP1 knockout mice to wild-type mice. This result is at odds with published findings, which claim thymocyte migration is controlled by NRP1[214]. However, unlike Lepelletier et al, we examined this *in vivo*. We also examined whether NRP1 deficiency would impair or enhance anti-viral T cell responses, but saw no defects in priming, migration or effector functions of T cells. Here, I have attributed this lack of an effect, to the fact that very little Sema3A was expressed in the peripheral organs we examined.

Still, it is a mystery why T cells would so strongly up-regulate a protein following activation if it does not play any functional role. Perhaps the function of NRP1 is in

ensuring restriction of migration at certain immune-privileged sites. For example, the placenta is known to express Sema3A[303]. We found that in mice, Sema3A is actively expressed in the prefrontal cortex, an organ that generally has very few T cells. Could NRP1's role be to ensure lack of infiltration into these sensitive organs? Another interesting question is whether NRP1 plays any role in autoimmunity. Unfortunately, we did not have time to address these questions during this work.

Complexity of Semaphorin signaling

The approach taken throughout this thesis has been reductionist: we have attempted to elucidate the functions of NRP1 by removing or over-expressing either it's ligand, Sema3A, or the receptor itself, and then validating our hypothesis in simplistic *in vitro* systems. This approach, while powerful in biological interactions that have a direct, one-to-one causal relationship, can also be deceiving in biological systems with multiple components that can act redundantly, in networks and which exhibit emergent behaviours[304], because unknown confounders can distort one's conclusions.

Is there any indication that NRP1—Sema3A interactions could be confounded in such a way? Yes. Not only is there a Sema3A, there are an additional six Sema3's (Sema3B-G), that could be binding NRP1:Plexin-A1 as well. Other Semaphorin-families also bind to the NRP1:Plexin-A1 receptor complexes. Finally, our understanding of the number of co-receptors available for NRP1 to dimerize to is ever-expanding[305]. In tumour-specific T cells we found some expression of other co-receptors as well, such as TGFβRII, but did not address what effects TGFβ might have in our *in vivo* model. Confounding factors in the TME could also be playing a role: for example, we showed here that Sema3A is

expressed by hypoxic B16.F10 cells. Could the reason we find co-localization of Sema3A and T cells *in vivo* be that these hypoxic regions are simply nutrient-poor and unconducive for T cell migration? Systems biology approaches and single-cell analysis are now attempting to address concerns like these by applying unbiased approaches to biological problems, but we did not utilize any. However, while technical impressive, proponents of these methods often forget that mRNA transcripts are not proteins, and that disruption of the cellular architecture within organs needed to perform these methods, often removes the complexity one set out to explore in the first place. The effects we saw on the F-actin cytoskeleton happened within minutes and at the protein level, and it is uncertain whether many of the transcriptional analysis methods many systems biologists use, would have revealed any effect at this time-scale.

That being said, elucidating the concentration and abundance of semaphorins and their temporal-spatial expression in tumours would be interesting. How they act in concordance with chemokines or other inhibitory secreted proteins is also an interesting avenue to consider. Finally, it is clear that Semaphorins can affect multiple immune cell-types, and if the literature is to be accepted as is, these effects are different from cell to cell. How priming, activation and trafficking of the pan-immune infiltrate within a tumour evolve over time in the context of increasing Semaphorin concentration would also be exciting aspect to explore in a more systems-biology-based approach. Tools are now becoming available for researchers to fine-tune proteins[306]. Combining these tools with quantitative approaches, would perhaps better allow us to construct mechanistic models in the future.

Are Semaphorins chemokine-like molecules?

An intriguing suggestion that is emerging from the growing literature on Semaphorins is whether these proteins should be considered chemokine-like molecules? Although larger and structurally dis-similar to chemokines, Sema3's have now been described to affect the migration of multiple immune cell-types[214, 215, 251]. They are secreted and can be bound to endothelial cells through heparin sulphate; they have known roles during development and angiogenesis; and like chemokines, the semaphorin system is highly redundant. In this thesis, I have described their role as mainly negative in terms of their effects on T cells. However, these effects could also be considered to be "homeostatic", in the sense that they reduce T cell-mediated inflammation.

What is at least clear, is that immunologist need to consider not only chemokines in the future, but also a number of so-called guidance cues, for example Ephrins and Semaphorins, when examining cell migration and synapse formation. Perhaps considering these secreted semaphorins as chemokine-like, would sharpen immunologists' understanding of their function.

9.3 Concluding remarks

Cancer immunotherapy is an incredibly exciting field. The success of checkpoint inhibitors and chimeric-antigen receptor T cells has caught the imagination of both scientists and the general public alike. The extent of this recognition was crystallized with the recent Nobel Prize award to James P. Allison and Tasuku Honjo for their research on CTLA4 and PD-1. The field is now rapidly providing more and more personalized and

advanced treatments for cancer patients. For these therapies to work, fundamental biological questions about the TME and T cell functions still need to be actively explored. Here, I hope, we have provided a small contribution to this thrilling field.

Bibliography

[1] N. McGranahan, and C. Swanton, "Clonal Heterogeneity and Tumor Evolution: Past, Present, and the Future.", Cell **168**, 613–628 (2017).

[2] K. A. Hoadley, C. Yau, T. Hinoue, D. M. Wolf, A. J. Lazar, E. Drill, R. Shen, A. M. Taylor, A. D. Cherniack, V. Thorsson, R. Akbani, R. Bowlby, C. K. Wong, M. Wiznerowicz, F. Sanchez-Vega, A. G. Robertson, B. G. Schneider, M. S. Lawrence, H. Noushmehr, T. M. Malta, Cancer Genome Atlas Network, J. M. Stuart, C. C. Benz, and P. W. Laird, "Cell-of-Origin Patterns Dominate the Molecular Classification of 10,000 Tumors from 33 Types of Cancer.", Cell **173**, 291–304.e6 (2018).

[3] L. Ding, M. H. Bailey, E. Porta-Pardo, V. Thorsson, A. Colaprico, D. Bertrand, D. L. Gibbs, A. Weerasinghe, K.-L. Huang, C. Tokheim, I. Cortés-Ciriano, R. Jayasinghe, F. Chen, L. Yu, S. Sun, C. Olsen, J. Kim, A. M. Taylor, A. D. Cherniack, R. Akbani, C. Suphavilai, N. Nagarajan, J. M. Stuart, G. B. Mills, M. A. Wyczalkowski, B. G. Vincent, C. M. Hutter, J. C. Zenklusen, K. A. Hoadley, M. C. Wendl, l. Shmulevich, A. J. Lazar, D. A. Wheeler, G. Getz, and Cancer Genome Atlas Research Network, "Perspective on Oncogenic Processes at the End of the Beginning of Cancer Genomics.", Cell **173**, 305–320.e10 (2018).

[4] M. H. Bailey, C. Tokheim, E. Porta-Pardo, S. Sengupta, D. Bertrand, A. Weerasinghe, A. Colaprico, M. C. Wendl, J. Kim, B. Reardon, P. K.-S. Ng, K. J. Jeong, S. Cao, Z. Wang, J. Gao, Q. Gao, F. Wang, E. M. Liu, L. Mularoni, C. Rubio-Perez, N. Nagarajan, I. Cortés-Ciriano, D. C. Zhou, W.-W. Liang, J. M. Hess, V. D. Yellapantula, D. Tamborero, A. Gonzalez-Perez, C. Suphavilai, J. Y. Ko, E. Khurana, P. J. Park, E. M. Van Allen, H. Liang, MC3 Working Group, Cancer Genome Atlas Research Network, M. S. Lawrence, A. Godzik, N. Lopez-Bigas, J. Stuart, D. Wheeler, G. Getz, K. Chen, A. J. Lazar, G. B. Mills, R. Karchin, and L. Ding, "Comprehensive Characterization of Cancer Driver Genes and Mutations.", Cell **173**, 371–385.e18 (2018).

[5] D. D. De Carvalho, S. Sharma, J. S. You, S.-F. Su, P. C. Taberlay, T. K. Kelly, X. Yang, G. Liang, and P. A. Jones, "DNA methylation screening identifies driver epigenetic events of cancer cell survival.", Cancer cell **21**, 655–667 (2012).

[6] L. B. Alexandrov, S. Nik-Zainal, D. C. Wedge, S. A. J. R. Aparicio, S. Behjati, A. V. Biankin, G. R. Bignell, N. Bolli, A. Borg, A.-L. Børresen-Dale, S. Boyault, B. Burkhardt, A. P. Butler, C. Caldas, H. R. Davies, C. Desmedt, R. Eils, J. E. Eyfjörd, J. A. Foekens, M. Greaves, F. Hosoda, B. Hutter, T. Ilicic, S. Imbeaud, M. Imielinski, M. Imielinsk, N. Jäger, D. T. W. Jones, D. Jones, S. Knappskog, M. Kool, S. R. Lakhani, C. López-Otín, S. Martin, N. C. Munshi, H. Nakamura, P. A. Northcott, M. Pajic, E. Papaemmanuil, A. Paradiso, J. V. Pearson, X. S. Puente, K. Raine, M. Ramakrishna, A. L. Richardson, J. Richter, P. Rosenstiel, M. Schlesner, T. N. Schumacher, P. N. Span, J. W. Teague, Y. Totoki, A. N. J. Tutt, R. Valdés-Mas, M. M. van Buuren, L. van 't Veer, A. Vincent-Salomon, N. Waddell, L. R. Yates, Aus-

tralian Pancreatic Cancer Genome Initiative, ICGC Breast Cancer Consortium, ICGC MMML-Seq Consortium, ICGC PedBrain, J. Zucman-Rossi, P. A. Futreal, U. McDermott, P. Lichter, M. Meyerson, S. M. Grimmond, R. Siebert, E. Campo, T. Shibata, S. M. Pfister, P. J. Campbell, and M. R. Stratton, "Signatures of mutational processes in human cancer.", Nature **500**, 415–421 (2013).

[7] C. A. Aktipis, and R. M. Nesse, "Evolutionary foundations for cancer biology.", Evolutionary Applications **6**, 144–159 (2013).

[8] D. P. Tabassum, and K. Polyak, "Tumorigenesis: it takes a village.", Nature reviews. Cancer **15**, 473–483 (2015).

[9] M. J. Bissell, and D. Radisky, "Putting tumours in context.", Nature reviews. Cancer **1**, 46–54 (2001).

[10] J. DeGregori, "Connecting cancer to its causes requires incorporation of effects on tissue microenvironments.", Cancer Res. **77**, canres.1207.2017–6068 (2017).

[11] J. Huelsken, and D. Hanahan, "A Subset of Cancer-Associated Fibroblasts Determines Therapy Resistance.", Cell **172**, 643–644 (2018).

[12] L. M. F. Merlo, J. W. Pepper, B. J. Reid, and C. C. Maley, "Cancer as an evolutionary and ecological process.", Nature reviews. Cancer **6**, 924–935 (2006).

[13] M. R. Junttila, and F. J. de Sauvage, "Influence of tumour micro-environment heterogeneity on therapeutic response.", Nature **501**, 346–354 (2013).

[14] M. Gerlinger, A. J. Rowan, S. Horswell, M. Math, J. Larkin, D. Endesfelder, E. Gronroos, P. Martinez, N. Matthews, A. Stewart, P. Tarpey, I. Varela, B. Phillimore, S. Begum, N. Q. McDonald, A. Butler, D. Jones, K. Raine, C. Latimer, C. R. Santos,

M. Nohadani, A. C. Eklund, B. Spencer-Dene, G. Clark, L. Pickering, G. Stamp, M. Gore, Z. Szallasi, J. Downward, P. A. Futreal, and C. Swanton, "Intratumor heterogeneity and branched evolution revealed by multiregion sequencing.", The New England journal of medicine **366**, 883–892 (2012).

[15] P. C. Nowell, "The clonal evolution of tumor cell populations.", Science **194**, 23–28 (1976).

[16] D. Hanahan, and L. M. Coussens, "Accessories to the crime: functions of cells recruited to the tumor microenvironment.", Cancer cell **21**, 309–322 (2012).

[17] K. Polyak, I. Haviv, and I. G. Campbell, "Co-evolution of tumor cells and their microenvironment.", Trends in genetics : TIG **25**, 30–38 (2009).

[18] A. R. A. Anderson, A. M. Weaver, P. T. Cummings, and V. Quaranta, "Tumor morphology and phenotypic evolution driven by selective pressure from the microenvironment.", Cell **127**, 905–915 (2006).

[19] R. Natrajan, H. Sailem, F. K. Mardakheh, M. Arias Garcia, C. J. Tape, M. Dowsett, C. Bakal, and Y. Yuan, "Microenvironmental Heterogeneity Parallels Breast Cancer Progression: A Histology-Genomic Integration Analysis.", PLoS medicine **13**, e1001961 (2016).

[20] D. Lambrechts, E. Wauters, B. Boeckx, S. Aibar, D. Nittner, O. Burton, A. Bassez, H. Decaluwé, A. Pircher, K. Van den Eynde, B. Weynand, E. Verbeken, P. De Leyn, A. Liston, J. Vansteenkiste, P. Carmeliet, S. Aerts, and B. Thienpont, "Phenotype molding of stromal cells in the lung tumor microenvironment.", Nature Medicine **344**, 1396 (2018).

[21] S. Su, J. Chen, H. Yao, J. Liu, S. Yu, L. Lao, M. Wang, M. Luo, Y. Xing, F. Chen, D. Huang, J. Zhao, L. Yang, D. Liao, F. Su, M. Li, Q. Liu, and E. Song, "CD10+GPR77+ Cancer-Associated Fibroblasts Promote Cancer Formation and Chemoresistance by Sustaining Cancer Stemness", Cell **172**, 841–856.e16 (2018).

[22] K. G. Anderson, I. M. Stromnes, and P. D. Greenberg, "Obstacles Posed by the Tumor Microenvironment to T cell Activity: A Case for Synergistic Therapies.", Cancer cell **31**, 311–325 (2017).

[23] N. Lavi, O. Kessler, K. Ziv, I. Nir-Zvi, Y. Mumblat, N. Eiza, Y. Paran, B. Brenner, Z. Vadasz, and G. Neufeld, "Semaphorin-3A inhibits multiple myeloma progression in a mouse model.", Carcinogenesis **2**, a006718 (2018).

[24] N. Gioelli, F. Maione, C. Camillo, M. Ghitti, D. Valdembri, N. Morello, M. Darche, L. Zentilin, G. Cagnoni, Y. Qiu, M. Giacca, M. Giustetto, M. Paques, I. Cascone, G. Musco, L. Tamagnone, E. Giraudo, and G. Serini, "A rationally designed NRP1-independent superagonist SEMA3A mutant is an effective anticancer agent.", Sci Transl Med **10**, eaah4807 (2018).

[25] G. P. Dunn, L. J. Old, and R. D. Schreiber, "The three Es of cancer immunoediting.", Annu. Rev. Immunol. **22**, 329–360 (2004).

[26] G. P. Dunn, L. J. Old, and R. D. Schreiber, "The immunobiology of cancer immunosurveillance and immunoediting.", Immunity **21**, 137–148 (2004).

[27] C. M. Koebel, W. Vermi, J. B. Swann, N. Zerafa, S. J. Rodig, L. J. Old, M. J. Smyth, and R. D. Schreiber, "Adaptive immunity maintains occult cancer in an equilibrium state.", Nature **450**, 903–907 (2007).

[28] S. I. Grivennikov, F. R. Greten, and M. Karin, "Immunity, inflammation, and cancer.", Cell **140**, 883–899 (2010).

[29] M. Binnewies, E. W. Roberts, K. Kersten, V. Chan, D. F. Fearon, M. Merad, L. M. Coussens, D. I. Gabrilovich, S. Ostrand-Rosenberg, C. C. Hedrick, R. H. Vonderheide, M. J. Pittet, R. K. Jain, W. Zou, T. K. Howcroft, E. C. Woodhouse, R. A. Weinberg, and M. F. Krummel, "Understanding the tumor immune microenvironment (TIME) for effective therapy.", Nat. Med. **27**, 450–550 (2018).

[30] V. Thorsson, D. L. Gibbs, S. D. Brown, D. Wolf, D. S. Bortone, T.-H. Ou Yang, E. Porta-Pardo, G. F. Gao, C. L. Plaisier, J. A. Eddy, E. Ziv, A. C. Culhane, E. O. Paull, I. K. A. Sivakumar, A. J. Gentles, R. Malhotra, F. Farshidfar, A. Colaprico, J. S. Parker, L. E. Mose, N. S. Vo, J. Liu, Y. Liu, J. Rader, V. Dhankani, S. M. Reynolds, R. Bowlby, A. Califano, D. Anastassiou, D. Bedognetti, A. Rao, K. Chen, A. Krasnitz, H. Hu, T. M. Malta, C. S. Pedamallu, S. Bullman, A. I. Ojesina, A. Lamb, W. Zhou, H. Shen, T. K. Choueiri, J. N. Weinstein, J. Guinney, J. Saltz, R. A. Holt, C. E. Rabkin, A. J. Lazar, J. S. Serody, E. G. Demicco, M. L. Disis, B. G. Vincent, l. Shmulevich, S. J. Caesar-Johnson, J. A. Demchok, I. Felau, M. Kasapi, M. L. Ferguson, C. M. Hutter, H. J. Sofia, R. Tarnuzzer, Z. Wang, L. Yang, J. C. Zenklusen, J. J. Zhang, S. Chudamani, J. Liu, L. Lolla, R. Naresh, T. Pihl, Q. Sun, Y. Wan, Y. Wu, J. Cho, T. DeFreitas, S. Frazer, N. Gehlenborg, G. Getz, D. I. Heiman, J. Kim, M. S. Lawrence, P. Lin, S. Meier, M. S. Noble, G. Saksena, D. Voet, H. Zhang, B. Bernard, N. Chambwe, V. Dhankani, T. Knijnenburg, R. Kramer, K. Leinonen, Y. Liu, M. Miller, S. Reynolds, I. Shmulevich, W. Zhang, R. Akbani, B. M. Broom, A. M. Hegde, Z. Ju, R. S. Kanchi, A. Korkut, J. Li, H. Liang, S. Ling, W. Liu, Y. Lu,

G. B. Mills, K.-S. Ng, A. Rao, M. Ryan, J. Wang, J. Zhang, A. Abeshouse, J. Armenia, D. Chakravarty, W. K. Chatila, I. de Bruijn, J. Gao, B. E. Gross, Z. J. Heins, R. Kundra, K. La, M. Ladanyi, A. Luna, M. G. Nissan, A. Ochoa, S. M. Phillips, E. Reznik, F. Sanchez-Vega, C. Sander, N. Schultz, R. Sheridan, S. O. Sumer, Y. Sun, B. S. Taylor, J. Wang, H. Zhang, P. Anur, M. Peto, P. Spellman, C. Benz, J. M. Stuart, C. K. Wong, C. Yau, D. N. Hayes, J. S. Parker, M. D. Wilkerson, A. Ally, M. Balasundaram, D. Brooks, R. Carlsen, E. Chuah, N. Dhalla, R. Holt, S. J. M. Jones, K. Kasaian, D. Lee, Y. Ma, M. A. Marra, M. Mayo, R. A. Moore, A. J. Mungall, K. Mungall, A. G. Robertson, S. Sadeghi, J. E. Schein, P. Sipahimalani, A. Tam, N. Thiessen, K. Tse, T. Wong, A. C. Berger, R. Beroukhim, A. D. Cherniack, C. Cibulskis, S. B. Gabriel, G. F. Gao, G. Ha, M. Meyerson, S. E. Schumacher, J. Shih, M. H. Kucherlapati, R. S. Kucherlapati, S. Baylin, L. Cope, L. Danilova, M. S. Bootwalla, P. H. Lai, D. T. Maglinte, D. J. Van Den Berg, D. J. Weisenberger, J. T. Auman, S. Balu, T. Bodenheimer, C. Fan, K. A. Hoadley, A. P. Hoyle, S. R. Jefferys, C. D. Jones, S. Meng, P. A. Mieczkowski, L. E. Mose, A. H. Perou, C. M. Perou, J. Roach, Y. Shi, J. V. Simons, T. Skelly, M. G. Soloway, D. Tan, U. Veluvolu, H. Fan, T. Hinoue, P. W. Laird, H. Shen, W. Zhou, M. Bellair, K. Chang, K. Covington, C. J. Creighton, H. Dinh, H. Doddapaneni, L. A. Donehower, J. Drummond, R. A. Gibbs, R. Glenn, W. Hale, Y. Han, J. Hu, V. Korchina, S. Lee, L. Lewis, W. Li, X. Liu, M. Morgan, D. Morton, D. Muzny, J. Santibanez, M. Sheth, and E. a. Shinbrot, “The Immune Landscape of Cancer”, Immunity (2018).

[31] C. Krieg, M. Nowicka, S. Guglietta, S. Schindler, F. J. Hartmann, L. M. Weber, R. Dummer, M. D. Robinson, M. P. Levesque, and B. Becher, “High-dimensional

single-cell analysis predicts response to anti-PD-1 immunotherapy.", Nat. Med. **9**, 2579–153 (2018).

[32] S. Chevrier, J. H. Levine, V. R. T. Zanotelli, K. Silina, D. Schulz, M. Bacac, C. H. Ries, L. Ailles, M. A. S. Jewett, H. Moch, M. van den Broek, C. Beisel, M. B. Stadler, C. Gedye, B. Reis, D. Pe'er, and B. Bodenmiller, "An Immune Atlas of Clear Cell Renal Cell Carcinoma.", Cell **169**, 736–749.e18 (2017).

[33] Y. Lavin, S. Kobayashi, A. Leader, E.-A. D. Amir, N. Elefant, C. Bigenwald, R. Remark, R. Sweeney, C. D. Becker, J. H. Levine, K. Meinhof, A. Chow, S. Kim-Shulze, A. Wolf, C. Medaglia, H. Li, J. A. Rytlewski, R. O. Emerson, A. Solovyov, B. D. Greenbaum, C. Sanders, M. Vignali, M. B. Beasley, R. Flores, S. Gnjatic, D. Pe'er, A. Rahman, I. Amit, and M. Merad, "Innate Immune Landscape in Early Lung Adenocarcinoma by Paired Single-Cell Analyses.", Cell **169**, 750–765.e17 (2017).

[34] P. G. Coulie, B. J. Van den Eynde, P. van der Bruggen, and T. Boon, "Tumour antigens recognized by T lymphocytes: at the core of cancer immunotherapy.", Nature reviews. Cancer **14**, 135–146 (2014).

[35] S. Tian, R. Maile, E. J. Collins, and J. A. Frelinger, "CD8+ T cell activation is governed by TCR-peptide/MHC affinity, not dissociation rate.", The Journal of Immunology **179**, 2952–2960 (2007).

[36] M. Yarchoan, B. A. Johnson, E. R. Lutz, D. A. Laheru, and E. M. Jaffee, "Targeting neoantigens to augment antitumour immunity.", Nature reviews. Cancer **17**, 209–222 (2017).

[37] T. N. Schumacher, and R. D. Schreiber, "Neoantigens in cancer immunotherapy.", Science **348**, 69–74 (2015).

[38] A. W. Whitehurst, "Cause and consequence of cancer/testis antigen activation in cancer.", Annual review of pharmacology and toxicology **54**, 251–272 (2014).

[39] M. Aleksic, N. Liddy, P. E. Molloy, N. Pumphrey, A. Vuidepot, K.-M. Chang, and B. K. Jakobsen, "Different affinity windows for virus and cancer-specific T-cell receptors: implications for therapeutic strategies.", European journal of immunology **42**, 3174–3179 (2012).

[40] J. Neefjes, and H. Ovaa, "A peptide's perspective on antigen presentation to the immune system.", Nature Chemical Biology **9**, 769–775 (2013).

[41] Z. R. Chalmers, C. F. Connelly, D. Fabrizio, L. Gay, S. M. Ali, R. Ennis, A. Schrock, B. Campbell, A. Shlien, J. Chmielecki, F. Huang, Y. He, J. Sun, U. Tabori, M. Kennedy, D. S. Lieber, S. Roels, J. White, G. A. Otto, J. S. Ross, L. Garraway, V. A. Miller, P. J. Stephens, and G. M. Frampton, "Analysis of 100,000 human cancer genomes reveals the landscape of tumor mutational burden.", Genome medicine **9**, 34 (2017).

[42] B. Li, T. Li, J.-C. Pignon, B. Wang, J. Wang, S. A. Shukla, R. Dou, Q. Chen, F. S. Hodi, T. K. Choueiri, C. Wu, N. Hacohen, S. Signoretti, J. S. Liu, and X. S. Liu, "Landscape of tumor-infiltrating T cell repertoire of human cancers.", Nature genetics **48**, 725–732 (2016).

[43] A. Snyder, V. Makarov, T. Merghoub, J. Yuan, J. M. Zaretsky, A. Desrichard, L. A. Walsh, M. A. Postow, P. Wong, T. S. Ho, T. J. Hollmann, C. Bruggeman, K. Kannan, Y. Li, C. Elipenahli, C. Liu, C. T. Harbison, L. Wang, A. Ribas, J. D. Wol-

chok, and T. A. Chan, “Genetic basis for clinical response to CTLA-4 blockade in melanoma.”, The New England journal of medicine **371**, 2189–2199 (2014).

[44] N. A. Rizvi, M. D. Hellmann, A. Snyder, P. Kvistborg, V. Makarov, J. J. Havel, W. Lee, J. Yuan, P. Wong, T. S. Ho, M. L. Miller, N. Rekhtman, A. L. Moreira, F. Ibrahim, C. Bruggeman, B. Gasmi, R. Zappasodi, Y. Maeda, C. Sander, E. B. Garon, T. Merghoub, J. D. Wolchok, T. N. Schumacher, and T. A. Chan, “Cancer immunology. Mutational landscape determines sensitivity to PD-1 blockade in non-small cell lung cancer.”, Science **348**, 124–128 (2015).

[45] D. S. Chen, and I. Mellman, “Elements of cancer immunity and the cancer-immune set point.”, Nature **541**, 321–330 (2017).

[46] E. M. E. Verdegaal, N. F. C. C. de Miranda, M. Visser, T. Harryvan, M. M. van Buuren, R. S. Andersen, S. R. Hadrup, C. E. van der Minne, R. Schotte, H. Spits, J. B. A. G. Haanen, E. H. W. Kapiteijn, T. N. Schumacher, and S. H. van der Burg, “Neoantigen landscape dynamics during human melanoma-T cell interactions.”, Nature **536**, 91–95 (2016).

[47] V. Anagnostou, K. N. Smith, P. M. Forde, N. Niknafs, R. Bhattacharya, J. White, T. Zhang, V. Adleff, J. Phallen, N. Wali, C. Hruban, V. B. Guthrie, K. Rodgers, J. Naidoo, H. Kang, W. Sharfman, C. Georgiades, F. Verde, P. Illei, Q. K. Li, E. Gabrielson, M. V. Brock, C. A. Zahnow, S. B. Baylin, R. B. Scharpf, J. R. Brahmer, R. Karchin, D. M. Pardoll, and V. E. Velculescu, “Evolution of Neoantigen Landscape during Immune Checkpoint Blockade in Non-Small Cell Lung Cancer.”, Cancer discovery **7**, 264–276 (2017).

[48] A. B. Sharabi, M. Lim, T. L. DeWeese, and C. G. Drake, "Radiation and checkpoint blockade immunotherapy: radiosensitisation and potential mechanisms of synergy.", The Lancet. Oncology **16**, e498–509 (2015).

[49] S. Toraya-Brown, and S. Fiering, "Local tumour hyperthermia as immunotherapy for metastatic cancer.", International journal of hyperthermia : the official journal of European Society for Hyperthermic Oncology, North American Hyperthermia Group **30**, 531–539 (2014).

[50] Y. Min, K. C. Roche, S. Tian, M. J. Eblan, K. P. McKinnon, J. M. Caster, S. Chai, L. E. Herring, L. Zhang, T. Zhang, J. M. DeSimone, J. E. Tepper, B. G. Vincent, J. S. Serody, and A. Z. Wang, "Antigen-capturing nanoparticles improve the abscopal effect and cancer immunotherapy.", Nature nanotechnology **12**, 877–882 (2017).

[51] R. Ramakrishnan, D. Assudani, S. Nagaraj, T. Hunter, H.-I. Cho, S. Antonia, S. Altiok, E. Celis, and D. I. Gabrilovich, "Chemotherapy enhances tumor cell susceptibility to CTL-mediated killing during cancer immunotherapy in mice.", J. Clin. Invest. **120**, 1111–1124 (2010).

[52] S. Mandruzzato, F. Brasseur, G. Andry, T. Boon, and P. van der Bruggen, "A CASP-8 mutation recognized by cytolytic T lymphocytes on a human head and neck carcinoma.", Journal of Experimental Medicine **186**, 785–793 (1997).

[53] B. Fossum, T. Gedde-Dahl, T. Hansen, J. A. Eriksen, E. Thorsby, and G. Gaudernack, "Overlapping epitopes encompassing a point mutation (12 Gly–¿Arg) in p21 ras can be recognized by HLA-DR, -DP and -DQ restricted T cells.", European journal of immunology **23**, 2687–2691 (1993).

[54] T. Wölfel, M. Hauer, J. Schneider, M. Serrano, C. Wölfel, E. Klehmann-Hieb, E. De Plaen, T. Hankeln, K. H. Meyer zum Büschenfelde, and D. Beach, "A p16INK4a-insensitive CDK4 mutant targeted by cytolytic T lymphocytes in a human melanoma.", Science **269**, 1281–1284 (1995).

[55] G. J. Bosch, A. M. Joosten, J. H. Kessler, C. J. Melief, and O. C. Leeksma, "Recognition of BCR-ABL positive leukemic blasts by human CD4+ T cells elicited by primary in vitro immunization with a BCR-ABL breakpoint peptide.", Blood **88**, 3522–3527 (1996).

[56] P. Yotnda, F. Garcia, M. Peuchmaur, B. Grandchamp, M. Duval, F. Lemonnier, E. Vilmer, and P. Langlade-Demoyen, "Cytotoxic T cell response against the chimeric ETV6-AML1 protein in childhood acute lymphoblastic leukemia.", Journal of Clinical Investigation **102**, 455–462 (1998).

[57] L. Chen, M. T. Mizuno, M. C. Singhal, S. L. Hu, D. A. Galloway, I. Hellström, and K. E. Hellström, "Induction of cytotoxic T lymphocytes specific for a syngeneic tumor expressing the E6 oncoprotein of human papillomavirus type 16.", The Journal of Immunology **148**, 2617–2621 (1992).

[58] H. F. Löhr, G. Gerken, H. J. Schlicht, K. H. Meryer zum Büschenfelde, and B. Fleischer, "Low frequency of cytotoxic liver-infiltrating T lymphocytes specific for endogenous processed surface and core proteins in chronic hepatitis B.", The Journal of infectious diseases **168**, 1133–1139 (1993).

[59] E. Jäger, Y. T. Chen, J. W. Drijfhout, J. Karbach, M. Ringhoffer, D. Jäger, M. Arand, H. Wada, Y. Noguchi, E. Stockert, L. J. Old, and A. Knuth, "Simultaneous humoral and cellular immune response against cancer-testis antigen NY-ESO-1: defini-

tion of human histocompatibility leukocyte antigen (HLA)-A2-binding peptide epitopes.", Journal of Experimental Medicine **187**, 265–270 (1998).

[60] P. van der Bruggen, C. Traversari, P. Chomez, C. Lurquin, E. De Plaen, B. Van den Eynde, A. Knuth, and T. Boon, "A gene encoding an antigen recognized by cytolytic T lymphocytes on a human melanoma.", Science **254**, 1643–1647 (1991).

[61] E. S. Kass, J. W. Greiner, J. A. Kantor, K. Y. Tsang, F. Guadagni, Z. Chen, B. Clark, R. De Pascalis, J. Schlom, and C. Van Waes, "Carcinoembryonic antigen as a target for specific antitumor immunotherapy of head and neck cancer.", Cancer Res. **62**, 5049–5057 (2002).

[62] S. K. C. Cheung, P.-K. Chuang, H.-W. Huang, W. W. Hwang-Verslues, C. H.-H. Cho, W.-B. Yang, C.-N. Shen, M. Hsiao, T.-L. Hsu, C.-F. Chang, and C.-H. Wong, "Stage-specific embryonic antigen-3 (SSEA-3) and β3GalT5 are cancer specific and significant markers for breast cancer stem cells.", Proceedings of the National Academy of Sciences of the United States of America **113**, 960–965 (2016).

[63] A. L. Cox, J. Skipper, Y. Chen, R. A. Henderson, T. L. Darrow, J. Shabanowitz, V. H. Engelhard, D. F. Hunt, and C. L. Slingluff, "Identification of a peptide recognized by five melanoma-specific human cytotoxic T cell lines.", Science **264**, 716–719 (1994).

[64] Y. Kawakami, S. Eliyahu, K. Sakaguchi, P. F. Robbins, L. Rivoltini, J. R. Yannelli, E. Appella, and S. A. Rosenberg, "Identification of the immunodominant peptides of the MART-1 human melanoma antigen recognized by the majority of HLA-A2-restricted tumor infiltrating lymphocytes.", Journal of Experimental Medicine **180**, 347–352 (1994).

[65] G. E. Peoples, I. Yoshino, C. C. Douville, J. V. Andrews, P. S. Goedegebuure, and T. J. Eberlein, "TCR V beta 3+ and V beta 6+ CTL recognize tumor-associated antigens related to HER2/neu expression in HLA-A2+ ovarian cancers.", The Journal of Immunology **152**, 4993–4999 (1994).

[66] A. G. Chapuis, G. B. Ragnarsson, H. N. Nguyen, C. N. Chaney, J. S. Pufnock, T. M. Schmitt, N. Duerkopp, I. M. Roberts, G. L. Pogosov, W. Y. Ho, S. Ochsenreither, M. Wölfl, M. Bar, J. P. Radich, C. Yee, and P. D. Greenberg, "Transferred WT1-reactive CD8+ T cells can mediate antileukemic activity and persist in post-transplant patients.", Sci Transl Med **5**, 174ra27–174ra27 (2013).

[67] W. Zou, "Immunosuppressive networks in the tumour environment and their therapeutic relevance.", Nature reviews. Cancer **5**, 263–274 (2005).

[68] L. T. Nguyen, A. R. Elford, K. Murakami, K. M. Garza, S. P. Schoenberger, B. Odermatt, D. E. Speiser, and P. S. Ohashi, "Tumor growth enhances cross-presentation leading to limited T cell activation without tolerance.", Journal of Experimental Medicine **195**, 423–435 (2002).

[69] K. Hildner, B. T. Edelson, W. E. Purtha, M. Diamond, H. Matsushita, M. Kohyama, B. Calderon, B. U. Schraml, E. R. Unanue, M. S. Diamond, R. D. Schreiber, T. L. Murphy, and K. M. Murphy, "Batf3 deficiency reveals a critical role for CD8alpha+ dendritic cells in cytotoxic T cell immunity.", Science **322**, 1097–1100 (2008).

[70] S.-R. Woo, M. B. Fuertes, L. Corrales, S. Spranger, M. J. Furdyna, M. Y. K. Leung, R. Duggan, Y. Wang, G. N. Barber, K. A. Fitzgerald, M.-L. Alegre, and T. F. Gajewski, "STING-dependent cytosolic DNA sensing mediates innate immune recognition of immunogenic tumors.", Immunity **41**, 830–842 (2014).

[71] D.-E. Hu, A. M. Moore, L. L. Thomsen, and K. M. Brindle, "Uric acid promotes tumor immune rejection.", Cancer Res. **64**, 5059–5062 (2004).

[72] S. Somersan, M. Larsson, J. F. Fonteneau, S. Basu, P. Srivastava, and N. Bhardwaj, "Primary tumor tissue lysates are enriched in heat shock proteins and induce the maturation of human dendritic cells.", The Journal of Immunology **167**, 4844–4852 (2001).

[73] M. Schnurr, F. Then, P. Galambos, C. Scholz, B. Siegmund, S. Endres, and A. Eigler, "Extracellular ATP and TNF-alpha synergize in the activation and maturation of human dendritic cells.", The Journal of Immunology **165**, 4704–4709 (2000).

[74] S.-R. Woo, L. Corrales, and T. F. Gajewski, "The STING pathway and the T cell-inflamed tumor microenvironment.", Trends in immunology **36**, 250–256 (2015).

[75] E. W. Roberts, M. L. Broz, M. Binnewies, M. B. Headley, A. E. Nelson, D. M. Wolf, T. Kaisho, D. Bogunovic, N. Bhardwaj, and M. F. Krummel, "Critical Role for CD103(+)/CD141(+) Dendritic Cells Bearing CCR7 for Tumor Antigen Trafficking and Priming of T Cell Immunity in Melanoma.", Cancer cell **30**, 324–336 (2016).

[76] M. L. Broz, M. Binnewies, B. Boldajipour, A. E. Nelson, J. L. Pollack, D. J. Erle, A. Barczak, M. D. Rosenblum, A. Daud, D. L. Barber, S. Amigorena, L. J. Van't Veer, A. I. Sperling, D. M. Wolf, and M. F. Krummel, "Dissecting the tumor myeloid compartment reveals rare activating antigen-presenting cells critical for T cell immunity.", Cancer cell **26**, 638–652 (2014).

[77] P. Bousso, and E. Robey, "Dynamics of CD8+ T cell priming by dendritic cells in intact lymph nodes.", Nature immunology **4**, 579–585 (2003).

[78] A. Boissonnas, F. Licata, L. Poupel, S. Jacquelin, L. Fetler, S. Krumeich, C. Thery, S. Amigorena, and C. Combadiere, "CD8+ tumor-infiltrating T cells are trapped in the tumor-dendritic cell network.", Neoplasia (New York, N.Y.) **15**, 85–94 (2013).

[79] J. J. Engelhardt, B. Boldajipour, P. Beemiller, P. Pandurangi, C. Sorensen, Z. Werb, M. Egeblad, and M. F. Krummel, "Marginating dendritic cells of the tumor microenvironment cross-present tumor antigens and stably engage tumor-specific T cells.", Cancer cell **21**, 402–417 (2012).

[80] R. Arens, and S. P. Schoenberger, "Plasticity in programming of effector and memory CD8 T-cell formation.", Immunological reviews **235**, 190–205 (2010).

[81] H. Tang, Y. Liang, R. A. Anders, J. M. Taube, X. Qiu, A. Mulgaonkar, X. Liu, S. M. Harrington, J. Guo, Y. Xin, Y. Xiong, K. Nham, W. Silvers, G. Hao, X. Sun, M. Chen, R. Hannan, J. Qiao, H. Dong, H. Peng, and Y.-X. Fu, "PD-L1 on host cells is essential for PD-L1 blockade-mediated tumor regression.", J. Clin. Invest. **128**, 580–588 (2018).

[82] H. Lin, S. Wei, E. M. Hurt, M. D. Green, L. Zhao, L. Vatan, W. Szeliga, R. Herbst, P. W. Harms, L. A. Fecher, P. Vats, A. M. Chinnaiyan, C. D. Lao, T. S. Lawrence, M. Wicha, J. Hamanishi, M. Mandai, I. Kryczek, and W. Zou, "Host expression of PD-L1 determines efficacy of PD-L1 pathway blockade-mediated tumor regression.", J. Clin. Invest. **128**, 805–815 (2018).

[83] A. P. Vicari, C. Chiodoni, C. Vaure, S. Aït-Yahia, C. Dercamp, F. Matsos, O. Reynard, C. Taverne, P. Merle, M. P. Colombo, A. O'Garra, G. Trinchieri, and C. Caux, "Reversal of tumor-induced dendritic cell paralysis by CpG immunostimulatory

oligonucleotide and anti-interleukin 10 receptor antibody.", Journal of Experimental Medicine **196**, 541–549 (2002).

[84] J. Borst, T. Ahrends, N. Babala, C. J. M. Melief, and W. Kastenmuller, "CD4 + T cell help in cancer immunology and immunotherapy", Nat Rev Immunol **18**, 635–647 (2018).

[85] J. P. Ridge, F. Di Rosa, and P. Matzinger, "A conditioned dendritic cell can be a temporal bridge between a CD4+ T-helper and a T-killer cell.", Nature **393**, 474–478 (1998).

[86] N. E. Blachère, H. K. Morris, D. Braun, H. Saklani, J. P. Di Santo, R. B. Darnell, and M. L. Albert, "IL-2 is required for the activation of memory CD8+ T cells via antigen cross-presentation.", The Journal of Immunology **176**, 7288–7300 (2006).

[87] T. Ahrends, A. Spanjaard, B. Pilzecker, N. Babala, A. Bovens, Y. Xiao, H. Jacobs, and J. Borst, "CD4 + T Cell Help Confers a Cytotoxic T Cell Effector Program Including Coinhibitory Receptor Downregulation and Increased Tissue Invasiveness", Immunity (2017).

[88] M. Obenaus, C. Leitão, M. Leisegang, X. Chen, I. Gavvovidis, P. van der Bruggen, W. Uckert, D. J. Schendel, and T. Blankenstein, "Identification of human T-cell receptors with optimal affinity to cancer antigens using antigen-negative humanized mice.", Nature biotechnology **33**, 402–407 (2015).

[89] E. Ghorani, R. Rosenthal, N. McGranahan, J. L. Reading, M. Lynch, K. S. Peggs, C. Swanton, and S. A. Quezada, "Differential binding affinity of mutated peptides for MHC class I is a predictor of survival in advanced lung cancer and melanoma.",

Annals of oncology : official journal of the European Society for Medical Oncology **29**, 271–279 (2018).

[90] D. Zehn, S. Y. Lee, and M. J. Bevan, "Complete but curtailed T-cell response to very low-affinity antigen.", Nature **458**, 211–214 (2009).

[91] A. C. Richard, A. T. L. Lun, W. W. Y. Lau, B. Göttgens, J. C. Marioni, and G. M. Griffiths, "T cell cytolytic capacity is independent of initial stimulation strength.", Nat. Immunol. **19**, 849–858 (2018).

[92] M. Shakiba, M. Philip, E. Horste, S. Camara, and A. Schietinger, "Impact of antigen affinity on T cell dysfunction in solid tumors", The Journal of Immunology **198**, 141.1–141.1 (2017).

[93] J. Galon, A. Costes, F. Sanchez-Cabo, A. Kirilovsky, B. Mlecnik, C. Lagorce-Pagès, M. Tosolini, M. Camus, A. Berger, P. Wind, F. Zinzindohoue, P. Bruneval, P.-H. Cugnenc, Z. Trajanoski, W.-H. Fridman, and F. Pagès, "Type, density, and location of immune cells within human colorectal tumors predict clinical outcome.", Science **313**, 1960–1964 (2006).

[94] B. Mlecnik, M. Tosolini, A. Kirilovsky, A. Berger, G. Bindea, T. Meatchi, P. Bruneval, Z. Trajanoski, W.-H. Fridman, F. Pagès, and J. Galon, "Histopathologic-based prognostic factors of colorectal cancers are associated with the state of the local immune reaction.", Journal of Clinical Oncology **29**, 610–618 (2011).

[95] J. Saltz, R. Gupta, L. Hou, T. Kurc, P. Singh, V. Nguyen, D. Samaras, K. R. Shroyer, T. Zhao, R. Batiste, J. Van Arnam, Cancer Genome Atlas Research Network, I. Shmulevich, A. U. K. Rao, A. J. Lazar, A. Sharma, and V. Thorsson, "Spatial Or-

ganization and Molecular Correlation of Tumor-Infiltrating Lymphocytes Using Deep Learning on Pathology Images.", Cell reports **23**, 181–193.e7 (2018).

[96] B. Li, E. Severson, J.-C. Pignon, H. Zhao, T. Li, J. Novak, P. Jiang, H. Shen, J. C. Aster, S. Rodig, S. Signoretti, J. S. Liu, and X. S. Liu, "Comprehensive analyses of tumor immunity: implications for cancer immunotherapy.", Genome biology **17**, 174 (2016).

[97] T. Li, J. Fan, B. Wang, N. Traugh, Q. Chen, J. S. Liu, B. Li, and X. S. Liu, "TIMER: A Web Server for Comprehensive Analysis of Tumor-Infiltrating Immune Cells.", Cancer Res. **77**, e108–e110 (2017).

[98] L. Galluzzi, T. A. Chan, G. Kroemer, J. D. Wolchok, and A. López-Soto, "The hallmarks of successful anticancer immunotherapy.", Sci Transl Med **10**, eaat7807 (2018).

[99] J.-P. Girard, C. Moussion, and R. Förster, "HEVs, lymphatics and homeostatic immune cell trafficking in lymph nodes", Nat Rev Immunol **12**, 762–773 (2012).

[100] C. Y. Slaney, M. H. Kershaw, and P. K. Darcy, "Trafficking of T cells into tumors.", Cancer Res. **74**, 7168–7174 (2014).

[101] S. Nourshargh, and R. Alon, "Leukocyte migration into inflamed tissues.", Immunity **41**, 694–707 (2014).

[102] R. Sackstein, T. Schatton, and S. R. Barthel, "T-lymphocyte homing: an underappreciated yet critical hurdle for successful cancer immunotherapy.", Laboratory investigation; a journal of technical methods and pathology **97**, 669–697 (2017).

[103] H. Harlin, Y. Meng, A. C. Peterson, Y. Zha, M. Tretiakova, C. Slingluff, M. McKee, and T. F. Gajewski, "Chemokine expression in melanoma metastases associated with CD8+ T-cell recruitment.", Cancer Res. **69**, 3077–3085 (2009).

[104] I. M. Mullins, C. L. Slingluff, J. K. Lee, C. F. Garbee, J. Shu, S. G. Anderson, M. E. Mayer, W. A. Knaus, and D. W. Mullins, "CXC chemokine receptor 3 expression by activated CD8+ T cells is associated with survival in melanoma patients with stage III disease.", Cancer Res. **64**, 7697–7701 (2004).

[105] M. E. Mikucki, D. T. Fisher, J. Matsuzaki, J. J. Skitzki, N. B. Gaulin, J. B. Muhitch, A. W. Ku, J. G. Frelinger, K. Odunsi, T. F. Gajewski, A. D. Luster, and S. S. Evans, "Non-redundant requirement for CXCR3 signalling during tumoricidal T-cell trafficking across tumour vascular checkpoints.", Nat Commun **6**, 7458 (2015).

[106] D. L. Woodland, and J. E. Kohlmeier, "Migration, maintenance and recall of memory T cells in peripheral tissues", Nat Rev Immunol **9**, 153–161 (2009).

[107] S. Pabla, J. Conroy, M. Nesline, S. Glenn, B. Burgher, M. Qin, J. Andreas, V. Giamo, F. L. Lenzo, A. Omilian, W. Bshara, A. Papanicolau-Sengos, Y. Wang, M. Ernstoff, M. Gardner, and C. Morrison, "Abstract 5070: Chemokine expression signatures in infiltrated vs non-infiltrated tumors", Cancer Res. **78**, 5070–5070 (2018).

[108] M. F. Krummel, F. Bartumeus, and A. Gérard, "T cell migration, search strategies and mechanisms.", Nat Rev Immunol **16**, 193–201 (2016).

[109] J. C. Stinchcombe, E. Majorovits, G. Bossi, S. Fuller, and G. M. Griffiths, "Centrosome polarization delivers secretory granules to the immunological synapse", Nature **443**, 462–465 (2006).

[110] L. Martínez-Lostao, A. Anel, and J. Pardo, "How Do Cytotoxic Lymphocytes Kill Cancer Cells?", Clin. Cancer Res. **21**, 5047–5056 (2015).

[111] B. Breart, F. Lemaître, S. Celli, and P. Bousso, "Two-photon imaging of intratumoral CD8+ T cell cytotoxic activity during adoptive T cell therapy in mice", Journal of Clinical Investigation **118**, 1390–1397 (2008).

[112] D. H. Kaplan, V. Shankaran, A. S. Dighe, E. Stockert, M. Aguet, L. J. Old, and R. D. Schreiber, "Demonstration of an interferon γ-dependent tumor surveillance system in immunocompetent mice", Proceedings of the National Academy of Sciences **95**, 7556–7561 (1998).

[113] J. S. Weber, and S. A. Rosenberg, "Modulation of murine tumor major histocompatibility antigens by cytokines in vivo and in vitro.", Cancer Res. **48**, 5818–5824 (1988).

[114] A. Sucker, F. Zhao, N. Pieper, C. Heeke, R. Maltaner, N. Stadtler, B. Real, N. Bielefeld, S. Howe, B. Weide, R. Gutzmer, J. Utikal, C. Loquai, H. Gogas, L. Klein-Hitpass, M. Zeschnigk, A. M. Westendorf, M. Trilling, S. Horn, B. Schilling, D. Schadendorf, K. G. Griewank, and A. Paschen, "Acquired IFNγ resistance impairs anti-tumor immunity and gives rise to T-cell-resistant melanoma lesions", Nat Commun **8**, 15440 (2017).

[115] H. T. Khong, and N. P. Restifo, "Natural selection of tumor variants in the generation of \tumor escape" phenotypes", Nat. Immunol. **3**, 999–1005 (2002).

[116] M. Sade-Feldman, Y. J. Jiao, J. H. Chen, M. S. Rooney, M. Barzily-Rokni, J.-P. Eliane, S. L. Bjorgaard, M. R. Hammond, H. Vitzthum, S. M. Blackmon, D. T. Frederick, M. Hazar-Rethinam, B. A. Nadres, E. E. Van Seventer, S. A. Shukla,

K. Yizhak, J. P. Ray, D. Rosebrock, D. Livitz, V. Adalsteinsson, G. Getz, L. M. Duncan, B. Li, R. B. Corcoran, D. P. Lawrence, A. Stemmer-Rachamimov, G. M. Boland, D. A. Landau, K. T. Flaherty, R. J. Sullivan, and N. Hacohen, "Resistance to checkpoint blockade therapy through inactivation of antigen presentation", Nat Commun **8**, 1136 (2017).

[117] M. S. Rooney, S. A. Shukla, C. J. Wu, G. Getz, and N. Hacohen, "Molecular and genetic properties of tumors associated with local immune cytolytic activity.", Cell **160**, 48–61 (2015).

[118] K. Mimura, J. L. Teh, H. Okayama, K. Shiraishi, L. F. Kua, V. Koh, D. T. Smoot, H. Ashktorab, T. Oike, Y. Suzuki, Z. Fazreen, B. R. Asuncion, A. Shabbir, W. P. Yong, J. So, R. Soong, and K. Kono, "PD-L1 expression is mainly regulated by interferon gamma associated with JAK-STAT pathway in gastric cancer", Cancer Science **109**, 43–53 (2018).

[119] A. C. Anderson, N. Joller, and V. K. Kuchroo, "Lag-3, Tim-3, and TIGIT: Co-inhibitory Receptors with Specialized Functions in Immune Regulation.", Immunity **44**, 989–1004 (2016).

[120] A. F. Ochsenbein, "Immunological ignorance of solid tumors", Springer Seminars in Immunopathology **27**, 19–35 (2005).

[121] T. S. Griffith, and T. A. Ferguson, "Cell Death in the Maintenance and Abrogation of Tolerance: The Five Ws of Dying Cells", Immunity **35**, 456–466 (2011).

[122] J. M. T. Janco, P. Lamichhane, L. Karyampudi, and K. L. Knutson, "Tumor-Infiltrating Dendritic Cells in Cancer Pathogenesis", The Journal of Immunology **194**, 2985–2991 (2015).

[123] L. Bezu, L. C. Gomes-de-Silva, H. Dewitte, K. Breckpot, J. Fucikova, R. Spisek, L. Galluzzi, O. Kepp, and G. Kroemer, "Combinatorial strategies for the induction of immunogenic cell death.", Front Immunol **6**, 187 (2015).

[124] L. Zhang, J. R. Conejo-Garcia, D. Katsaros, P. A. Gimotty, M. Massobrio, G. Regnani, A. Makrigiannakis, H. Gray, K. Schlienger, M. N. Liebman, S. C. Rubin, and G. Coukos, "Intratumoral T cells, recurrence, and survival in epithelial ovarian cancer.", The New England journal of medicine **348**, 203–213 (2003).

[125] P. C. Tumeh, C. L. Harview, J. H. Yearley, I. P. Shintaku, E. J. M. Taylor, L. Robert, B. Chmielowski, M. Spasic, G. Henry, V. Ciobanu, A. N. West, M. Carmona, C. Kivork, E. Seja, G. Cherry, A. J. Gutierrez, T. R. Grogan, C. Mateus, G. Tomasic, J. A. Glaspy, R. O. Emerson, H. Robins, R. H. Pierce, D. A. Elashoff, C. Robert, and A. Ribas, "PD-1 blockade induces responses by inhibiting adaptive immune resistance.", Nature **515**, 568–571 (2014).

[126] S. A. Rosenberg, R. M. Sherry, K. E. Morton, W. J. Scharfman, J. C. Yang, S. L. Topalian, R. E. Royal, U. Kammula, N. P. Restifo, M. S. Hughes, D. Schwartzentruber, D. M. Berman, S. L. Schwarz, L. T. Ngo, S. A. Mavroukakis, D. E. White, and S. M. Steinberg, "Tumor Progression Can Occur despite the Induction of Very High Levels of Self/Tumor Antigen-Specific CD8+ T Cells in Patients with Melanoma", The Journal of Immunology **175**, 6169–6176 (2005).

[127] A. Ager, H. A. Watson, S. C. Wehenkel, and R. N. Mohammed, "Homing to solid cancers: a vascular checkpoint in adoptive cell therapy using CAR T-cells", Biochemical Society Transactions **44**, 377–385 (2016).

[128] Y. Huang, S. Goel, D. G. Duda, D. Fukumura, and R. K. Jain, "Vascular normalization as an emerging strategy to enhance cancer immunotherapy.", Cancer Res. **73**, 2943–2948 (2013).

[129] Y. Huang, J. Yuan, E. Righi, W. S. Kamoun, M. Ancukiewicz, J. Nezivar, M. Santosuosso, J. D. Martin, M. R. Martin, F. Vianello, P. Leblanc, L. L. Munn, P. Huang, D. G. Duda, D. Fukumura, R. K. Jain, and M. C. Poznansky, "Vascular normalizing doses of antiangiogenic treatment reprogram the immunosuppressive tumor microenvironment and enhance immunotherapy.", Proceedings of the National Academy of Sciences of the United States of America **109**, 17561–17566 (2012).

[130] A. Johansson, J. Hamzah, C. J. Payne, and R. Ganss, "Tumor-targeted TNFα stabilizes tumor vessels and enhances active immunotherapy.", Proceedings of the National Academy of Sciences of the United States of America **109**, 7841–7846 (2012).

[131] E. Allen, A. Jabouille, L. B. Rivera, I. Lodewijckx, R. Missiaen, V. Steri, K. Feyen, J. Tawney, D. Hanahan, I. P. Michael, and G. Bergers, "Combined antiangiogenic and anti-PD-L1 therapy stimulates tumor immunity through HEV formation.", Sci Transl Med **9**, eaak9679 (2017).

[132] A. W. Griffioen, C. A. Damen, G. H. Blijham, and G. Groenewegen, "Tumor angiogenesis is accompanied by a decreased inflammatory response of tumor-associated endothelium.", Blood **88**, 667–673 (1996).

[133] H. Samaha, A. Pignata, K. Fousek, J. Ren, F. W. Lam, F. Stossi, J. Dubrulle, V. S. Salsman, S. Krishnan, S.-H. Hong, M. L. Baker, A. Shree, A. Z. Gad, T. Shum, D. Fukumura, T. T. Byrd, M. Mukherjee, S. P. Marrelli, J. S. Orange, S. K. Joseph, P. H.

Sorensen, M. D. Taylor, M. Hegde, M. Mamonkin, R. K. Jain, S. El-Naggar, and N. Ahmed, "A homing system targets therapeutic T cells to brain cancer.", Nature **561**, 331–337 (2018).

[134] R. J. Buckanovich, A. Facciabene, S. Kim, F. Benencia, D. Sasaroli, K. Balint, D. Katsaros, A. O'Brien-Jenkins, P. A. Gimotty, and G. Coukos, "Endothelin B receptor mediates the endothelial barrier to T cell homing to tumors and disables immune therapy.", Nature Medicine **14**, 28–36 (2008).

[135] G. T. Motz, S. P. Santoro, L.-P. Wang, T. Garrabrant, R. R. Lastra, I. S. Hagemann, P. Lal, M. D. Feldman, F. Benencia, and G. Coukos, "Tumor endothelium FasL establishes a selective immune barrier promoting tolerance in tumors.", Nature Medicine **20**, 607–615 (2014).

[136] C. Feig, J. O. Jones, M. Kraman, R. J. B. Wells, A. Deonarine, D. S. Chan, C. M. Connell, E. W. Roberts, Q. Zhao, O. L. Caballero, S. A. Teichmann, T. Janowitz, D. I. Jodrell, D. A. Tuveson, and D. T. Fearon, "Targeting CXCL12 from FAP-expressing carcinoma-associated fibroblasts synergizes with anti-PD-L1 immunotherapy in pancreatic cancer.", Proceedings of the National Academy of Sciences of the United States of America **110**, 20212–20217 (2013).

[137] N. Nagarsheth, M. S. Wicha, and W. Zou, "Chemokines in the cancer microenvironment and their relevance in cancer immunotherapy.", Nat Rev Immunol **17**, 559–572 (2017).

[138] S. Mariathasan, S. J. Turley, D. Nickles, A. Castiglioni, K. Yuen, Y. Wang, E. E. Kadel, H. Koeppen, J. L. Astarita, R. Cubas, S. Jhunjhunwala, R. Banchereau, Y. Yang, Y. Guan, C. Chalouni, J. Ziai, Y. Şenbabaoğlu, S. Santoro, D. Sheinson, J.

Hung, J. M. Giltnane, A. A. Pierce, K. Mesh, S. Lianoglou, J. Riegler, R. A. D. Carano, P. Eriksson, M. Höglund, L. Somarriba, D. L. Halligan, M. S. van der Heijden, Y. Loriot, J. E. Rosenberg, L. Fong, I. Mellman, D. S. Chen, M. Green, C. Derleth, G. D. Fine, P. S. Hegde, R. Bourgon, and T. Powles, "TGFβ attenuates tumour response to PD-L1 blockade by contributing to exclusion of T cells.", Nature **554**, 544–548 (2018).

[139] H. S. Hjorthaug, and H. C. Aasheim, "Ephrin-A1 stimulates migration of CD8+CCR7+ T lymphocytes", European journal of immunology **37**, 2326–2336 (2007).

[140] J. Y. Wu, L. Feng, H.-T. Park, N. Havlioglu, L. Wen, H. Tang, K. B. Bacon, Z.-h. Jiang, X.-c. Zhang, and Y. Rao, "The neuronal repellent Slit inhibits leukocyte chemotaxis induced by chemotactic factors", Nature **410**, 948–952 (2001).

[141] A. Prasad, Z. Qamri, J. Wu, and R. K. Ganju, "Slit-2/Robo-1 modulates the CXCL12/CXCR4-induced chemotaxis of T cells", Journal of leukocyte biology **82**, 465–476 (2007).

[142] H. Salmon, K. Franciszkiewicz, D. Damotte, M.-C. Dieu-Nosjean, P. Validire, A. Trautmann, F. Mami-Chouaib, and E. Donnadieu, "Matrix architecture defines the preferential localization and migration of T cells into the stroma of human lung tumors.", J. Clin. Invest. **122**, 899–910 (2012).

[143] E. M. Hanson, V. K. Clements, P. Sinha, D. Ilkovitch, and S. Ostrand-Rosenberg, "Myeloid-derived suppressor cells down-regulate L-selectin expression on CD4+ and CD8+ T cells.", Journal of immunology (Baltimore, Md. : 1950) **183**, 937–944 (2009).

[144] B. Molon, S. Ugel, F. Del Pozzo, C. Soldani, S. Zilio, D. Avella, A. De Palma, P. Mauri, A. Monegal, M. Rescigno, B. Savino, P. Colombo, N. Jonjic, S. Pecanic, L. Lazzarato, R. Fruttero, A. Gasco, V. Bronte, and A. Viola, "Chemokine nitration prevents intratumoral infiltration of antigen-specific T cells.", J. Exp. Med. **208**, 1949–1962 (2011).

[145] M. D. Buck, D. O'Sullivan, and E. L. Pearce, "T cell metabolism drives immunity.", J. Exp. Med. **212**, 1345–1360 (2015).

[146] K. Renner, A. L. Geiselhöringer, M. Fante, C. Bruss, S. Färber, G. Schönhammer, K. Peter, K. Singer, R. Andreesen, P. Hoffmann, P. Oefner, W. Herr, and M. Kreutz, "Metabolic plasticity of human T cells: Preserved cytokine production under glucose deprivation or mitochondrial restriction, but 2-deoxy-glucose affects effector functions.", European journal of immunology **45**, 2504–2516 (2015).

[147] P.-C. Ho, J. D. Bihuniak, A. N. Macintyre, M. Staron, X. Liu, R. Amezquita, Y.-C. Tsui, G. Cui, G. Micevic, J. C. Perales, S. H. Kleinstein, E. D. Abel, K. L. Insogna, S. Feske, J. W. Locasale, M. W. Bosenberg, J. C. Rathmell, and S. M. Kaech, "Phosphoenolpyruvate Is a Metabolic Checkpoint of Anti-tumor T Cell Responses.", Cell **162**, 1217–1228 (2015).

[148] S. R. Jacobs, C. E. Herman, N. J. MacIver, J. A. Wofford, H. L. Wieman, J. J. Hammen, and J. C. Rathmell, "Glucose Uptake Is Limiting in T Cell Activation and Requires CD28-Mediated Akt-Dependent and Independent Pathways", The Journal of Immunology **180**, 4476–4486 (2008).

[149] C.-H. Chang, J. Qiu, D. O'Sullivan, M. D. Buck, T. Noguchi, J. D. Curtis, Q. Chen, M. Gindin, M. M. Gubin, G. J. W. van der Windt, E. Tonc, R. D. Schreiber, E. J.

Pearce, and E. L. Pearce, “Metabolic Competition in the Tumor Microenvironment Is a Driver of Cancer Progression.”, Cell **162**, 1229–1241 (2015).

[150] K. Singer, M. Kastenberger, E. Gottfried, C. G. Hammerschmied, M. Büttner, M. Aigner, B. Seliger, B. Walter, H. Schlösser, A. Hartmann, R. Andreesen, A. Mackensen, and M. Kreutz, “Warburg phenotype in renal cell carcinoma: high expression of glucose-transporter 1 (GLUT-1) correlates with low CD8(+) T-cell infiltration in the tumor.”, Int. J. Cancer **128**, 2085–2095 (2011).

[151] R. B. Holmgaard, D. Zamarin, Y. Li, B. Gasmi, D. H. Munn, J. P. Allison, T. Merghoub, and J. D. Wolchok, “Tumor-Expressed IDO Recruits and Activates MDSCs in a Treg-Dependent Manner.”, Cell reports **13**, 412–424 (2015).

[152] L. L. van der Woude, M. A. J. Gorris, A. Halilovic, C. G. Figdor, and I. J. M. de Vries, “Migrating into the Tumor: a Roadmap for T Cells.”, Trends in cancer **3**, 797–808 (2017).

[153] J. A. Joyce, and D. T. Fearon, “T cell exclusion, immune privilege, and the tumor microenvironment.”, Science **348**, 74–80 (2015).

[154] K. M. Hargadon, J. D. Bishop, J. P. Brandt, Z. C. Hand, Y. T. Ararso, and O. A. Forrest, “Melanoma-derived factors alter the maturation and activation of differentiated tissue-resident dendritic cells.”, Immunology and cell biology **94**, 24–38 (2016).

[155] C. Lu, P. S. Redd, J. R. Lee, N. Savage, and K. Liu, “The expression profiles and regulation of PD-L1 in tumor-induced myeloid-derived suppressor cells.”, OncoImmunology **5**, e1247135 (2016).

[156] M. K. Srivastava, P. Sinha, V. K. Clements, P. Rodriguez, and S. Ostrand-Rosenberg, "Myeloid-derived suppressor cells inhibit T-cell activation by depleting cystine and cysteine.", Cancer Res. **70**, 68–77 (2010).

[157] V. Kumar, S. Patel, E. Tcyganov, and D. I. Gabrilovich, "The Nature of Myeloid-Derived Suppressor Cells in the Tumor Microenvironment.", Trends in immunology **37**, 208–220 (2016).

[158] E. J. Wherry, and M. Kurachi, "Molecular and cellular insights into T cell exhaustion.", Nat Rev Immunol **15**, 486–499 (2015).

[159] L. Baitsch, P. Baumgaertner, E. Devevre, S. K. Raghav, A. Legat, L. Barba, S. Wieckowski, H. Bouzourene, B. Deplancke, P. Romero, N. Rufer, and D. E. Speiser, "Exhaustion of tumor-specific CD8+ T cells in metastases from melanoma patients.", J. Clin. Invest. **121**, 2350–2360 (2011).

[160] A. Gros, P. F. Robbins, X. Yao, Y. F. Li, S. Turcotte, E. Tran, J. R. Wunderlich, A. Mixon, S. Farid, M. E. Dudley, K.-i. Hanada, J. R. Almeida, S. Darko, D. C. Douek, J. C. Yang, and S. A. Rosenberg, "PD-1 identifies the patient-specific CD8+ tumor-reactive repertoire infiltrating human tumors.", J. Clin. Invest. **124**, 2246–2259 (2014).

[161] A. Schietinger, M. Philip, V. E. Krisnawan, E. Y. Chiu, J. J. Delrow, R. S. Basom, P. Lauer, D. G. Brockstedt, S. E. Knoblaugh, G. J. Hammerling, T. D. Schell, N. Garbi, and P. D. Greenberg, "Tumor-Specific T Cell Dysfunction Is a Dynamic Antigen-Driven Differentiation Program Initiated Early during Tumorigenesis.", Immunity **45**, 389–401 (2016).

[162] M. Philip, L. Fairchild, L. Sun, E. L. Horste, S. Camara, M. Shakiba, A. C. Scott, A. Viale, P. Lauer, T. Merghoub, M. D. Hellmann, J. D. Wolchok, C. S. Leslie, and A. Schietinger, "Chromatin states define tumour-specific T cell dysfunction and reprogramming.", Nature **545**, 452–456 (2017).

[163] E. Hui, J. Cheung, J. Zhu, X. Su, M. J. Taylor, H. A. Wallweber, D. K. Sasmal, J. Huang, J. M. Kim, I. Mellman, and R. D. Vale, "T cell costimulatory receptor CD28 is a primary target for PD-1-mediated inhibition.", Science **355**, 1428–1433 (2017).

[164] A. O. Kamphorst, A. Wieland, T. Nasti, S. Yang, R. Zhang, D. L. Barber, B. T. Konieczny, C. Z. Daugherty, L. Koenig, K. Yu, G. L. Sica, A. H. Sharpe, G. J. Freeman, B. R. Blazar, L. A. Turka, T. K. Owonikoko, R. Pillai, S. S. Ramalingam, K. Araki, and R. Ahmed, "Rescue of exhausted CD8 T cells by PD-1-targeted therapies is CD28-dependent.", Science **355**, 1423–1427 (2017).

[165] K. E. Pauken, M. A. Sammons, P. M. Odorizzi, S. Manne, J. Godec, O. Khan, A. M. Drake, Z. Chen, D. R. Sen, M. Kurachi, R. A. Barnitz, C. Bartman, B. Bengsch, A. C. Huang, J. M. Schenkel, G. Vahedi, W. N. Haining, S. L. Berger, and E. J. Wherry, "Epigenetic stability of exhausted T cells limits durability of reinvigoration by PD-1 blockade.", Science **354**, 1160–1165 (2016).

[166] A. Fantin, C. H. Maden, and C. Ruhrberg, "Neuropilin ligands in vascular and neuronal patterning.", Biochemical Society Transactions **37**, 1228–1232 (2009).

[167] A. Kumanogoh, and H. Kikutani, "Immunological functions of the neuropilins and plexins as receptors for semaphorins.", Nat Rev Immunol **13**, 802–814 (2013).

[168] T. Kawasaki, T. Kitsukawa, Y. Bekku, Y. Matsuda, M. Sanbo, T. Yagi, and H. Fujisawa, "A requirement for neuropilin-1 in embryonic vessel formation.", Development (Cambridge, England) **126**, 4895–4902 (1999).

[169] T. Kitsukawa, M. Shimizu, M. Sanbo, T. Hirata, M. Taniguchi, Y. Bekku, T. Yagi, and H. Fujisawa, "Neuropilin-semaphorin III/D-mediated chemorepulsive signals play a crucial role in peripheral nerve projection in mice.", Neuron **19**, 995–1005 (1997).

[170] M. Rossignol, M. L. Gagnon, and M. Klagsbrun, "Genomic organization of human neuropilin-1 and neuropilin-2 genes: identification and distribution of splice variants and soluble isoforms.", Genomics **70**, 211–222 (2000).

[171] B. J. C. Janssen, T. Malinauskas, G. A. Weir, M. Z. Cader, C. Siebold, and E. Y. Jones, "Neuropilins lock secreted semaphorins onto plexins in a ternary signaling complex.", Nature structural & molecular biology **19**, 1293–1299 (2012).

[172] H. Chen, Z. He, A. Bagri, and M. Tessier-Lavigne, "Semaphorin-neuropilin interactions underlying sympathetic axon responses to class III semaphorins.", Neuron **21**, 1283–1290 (1998).

[173] L. Roth, C. Nasarre, S. Dirrig-Grosch, D. Aunis, G. Crémel, P. Hubert, and D. Bagnard, "Transmembrane domain interactions control biological functions of neuropilin-1.", Molecular biology of the cell **19**, 646–654 (2008).

[174] M. Yadav, C. Louvet, D. Davini, J. M. Gardner, M. Martinez-Llordella, S. Bailey-Bucktrout, B. A. Anthony, F. M. Sverdrup, R. Head, D. J. Kuster, P. Ruminski, D. Weiss, D. Von Schack, and J. A. Bluestone, "Neuropilin-1 distinguishes natural

and inducible regulatory T cells among regulatory T cell subsets in vivo.", J. Exp. Med. **209**, 1713–22– S1–19 (2012).

[175] G. M. Delgoffe, S.-R. Woo, M. E. Turnis, D. M. Gravano, C. Guy, A. E. Overacre, M. L. Bettini, P. Vogel, D. Finkelstein, J. Bonnevier, C. J. Workman, and D. A. A. Vignali, "Stability and function of regulatory T cells is maintained by a neuropilin-1-semaphorin-4a axis.", Nature **501**, 252–256 (2013).

[176] R. P. Kruger, J. Aurandt, and K.-L. Guan, "Semaphorins command cells to move", Nature Reviews Molecular Cell Biology **6**, 789–800 (2005).

[177] G. Chen, J. Sima, M. Jin, K.-Y. Wang, X.-J. Xue, W. Zheng, Y.-Q. Ding, and X.-B. Yuan, "Semaphorin-3A guides radial migration of cortical neurons during development.", Nature Neuroscience **11**, 36–44 (2008).

[178] C. H. Bell, A. R. Aricescu, E. Y. Jones, and C. Siebold, "A dual binding mode for RhoGTPases in plexin signalling.", PLoS biology **9**, e1001134 (2011).

[179] Y. Wang, H. He, N. Srivastava, S. Vikarunnessa, Y.-b. Chen, J. Jiang, C. W. Cowan, and X. Zhang, "Plexins Are GTPase-Activating Proteins for Rap and Are Activated by Induced Dimerization", Science signaling **5**, ra6–ra6 (2012).

[180] Y. Wang, H. G. Pascoe, C. A. Brautigam, H. He, and X. Zhang, "Structural basis for activation and non-canonical catalysis of the Rap GTPase activating protein domain of plexin.", Elife **2**, e01279 (2013).

[181] M. A. Wolman, Y. Liu, H. Tawarayama, W. Shoji, and M. C. Halloran, "Repulsion and attraction of axons by semaphorin3D are mediated by different neuropilins

in vivo.", The Journal of neuroscience : the official journal of the Society for Neuroscience **24**, 8428–8435 (2004).

[182] H. Song, G. Ming, Z. He, M. Lehmann, L. McKerracher, M. Tessier-Lavigne, and M. Poo, "Conversion of neuronal growth cone responses from repulsion to attraction by cyclic nucleotides.", Science **281**, 1515–1518 (1998).

[183] D. Bagnard, C. Vaillant, S. T. Khuth, N. Dufay, M. Lohrum, A. W. Puschel, M. F. Belin, J. Bolz, and N. Thomasset, "Semaphorin 3A-vascular endothelial growth factor-165 balance mediates migration and apoptosis of neural progenitor cells by the recruitment of shared receptor.", The Journal of neuroscience : the official journal of the Society for Neuroscience **21**, 3332–3341 (2001).

[184] L. Gautier, L. Cope, B. M. Bolstad, and R. A. Irizarry, "affy–analysis of Affymetrix GeneChip data at the probe level.", Bioinformatics (Oxford, England) **20**, 307–315 (2004).

[185] M. E. Ritchie, B. Phipson, D. Wu, Y. Hu, C. W. Law, W. Shi, and G. K. Smyth, "limma powers differential expression analyses for RNA-sequencing and microarray studies.", Nucleic Acids Research **43**, e47 (2015).

[186] R Core Team, *R: A Language and Environment for Statistical Computing*, R Foundation for Statistical Computing (Vienna, Austria, 2014).

[187] J. Schindelin, I. Arganda-Carreras, E. Frise, V. Kaynig, M. Longair, T. Pietzsch, S. Preibisch, C. Rueden, S. Saalfeld, B. Schmid, J.-Y. Tinevez, D. J. White, V. Hartenstein, K. Eliceiri, P. Tomancak, and A. Cardona, "Fiji: an open-source platform for biological-image analysis.", Nature Methods **9**, 676–682 (2012).

[188] J.-Y. Tinevez, N. Perry, J. Schindelin, G. M. Hoopes, G. D. Reynolds, E. Laplantine, S. Y. Bednarek, S. L. Shorte, and K. W. Eliceiri, "TrackMate: An open and extensible platform for single-particle tracking.", Methods (San Diego, Calif.) **115**, 80–90 (2017).

[189] H. Wickham, *ggplot2: elegant graphics for data analysis* (Springer-Verlag New York).

[190] S. Valvo, V. Mayya, E. Seraia, J. Afrose, H. Novak-Kotzer, D. Ebner, and M. L. Dustin, "Comprehensive Analysis of Immunological Synapse Phenotypes Using Supported Lipid Bilayers", in *The immune synapse* (Springer New York, New York, NY, Mar. 2017), pp. 423–441.

[191] M. Toebes, B. Rodenko, H. Ovaa, and T. N. M. Schumacher, "Generation of peptide MHC class I monomers and multimers through ligand exchange.", Current protocols in immunology **Chapter 18**, Unit 18.16 (2009).

[192] K.-L. Guan, and Y. Rao, "Signalling mechanisms mediating neuronal responses to guidance cues", Nature Reviews Neuroscience **4**, 941–956 (2003).

[193] C. Gu, E. R. Rodriguez, D. V. Reimert, T. Shu, B. Fritzsch, L. J. Richards, A. L. Kolodkin, and D. D. Ginty, "Neuropilin-1 conveys semaphorin and VEGF signaling during neural and cardiovascular development.", Developmental cell **5**, 45–57 (2003).

[194] L. Tamagnone, "Emerging Role of Semaphorins as Major Regulatory Signals and Potential Therapeutic Targets in Cancer", Cancer Cell **22**, 145–152 (2012).

[195] J. A. Best, D. A. Blair, J. Knell, E. Yang, V. Mayya, A. Doedens, M. L. Dustin, T. I. G. P. Consortium, P. Monach, S. A. Shinton, R. R. Hardy, R. Jianu, D. Koller, J. Collins, R. Gazit, B. S. Garrison, D. J. Rossi, K. Narayan, K. Sylvia, J. Kang, A. Fletcher, K. Elpek, A. Bellemare-Pelletier, D. Malhotra, S. Turley, J. A. Best, A. W. Goldrath, V. Jojic, D. Koller, T. Shay, A. Regev, N. Cohen, P. Brennan, M. Brenner, T. Kreslavsky, N. A. Bezman, J. C. Sun, C. C. Kim, L. L. Lanier, J. Miller, B. Brown, M. Merad, E. L. Gautier, C. Jakubzick, G. J. Randolph, F. Kim, T. N. Rao, A. Wagers, T. Heng, M. Painter, J. Ericson, S. Davis, A. Ergun, M. Mingueneau, D. Mathis, and C. Benoist, "Transcriptional insights into the CD8¡sup¿+¡/sup¿ T cell response to infection and memory T cell formation", Nat. Immunol. **14**, 404 (2013).

[196] W. W. Overwijk, and N. P. Restifo, "B16 as a mouse model for human melanoma.", Current protocols in immunology **Chapter 20**, Unit 20.1–20.1.29 (2001).

[197] L. Tamagnone, S. Artigiani, H. Chen, Z. He, G. I. Ming, H. Song, A. Chedotal, M. L. Winberg, C. S. Goodman, M. Poo, M. Tessier-Lavigne, and P. M. Comoglio, "Plexins are a large family of receptors for transmembrane, secreted, and GPI-anchored semaphorins in vertebrates.", Cell **99**, 71–80 (1999).

[198] S. Soker, S. Takashima, H. Q. Miao, G. Neufeld, and M. Klagsbrun, "Neuropilin-1 Is Expressed by Endothelial and Tumor Cells as an Isoform-Specific Receptor for Vascular Endothelial Growth Factor", Cell **92**, 735–745 (1998).

[199] M. V. Gelfand, N. Hagan, A. Tata, W.-J. Oh, B. Lacoste, K.-T. Kang, J. Kopycinska, J. Bischoff, J.-H. Wang, and C. Gu, "Neuropilin-1 functions as a VEGFR2 co-receptor

to guide developmental angiogenesis independent of ligand binding.", Elife **3**, e03720 (2014).

[200] Y. Glinka, S. Stoilova, N. Mohammed, and G. J. Prud'homme, "Neuropilin-1 exerts co-receptor function for TGF-beta-1 on the membrane of cancer cells and enhances responses to both latent and active TGF-beta.", Carcinogenesis **32**, 613–621 (2011).

[201] T. Voron, O. Colussi, E. Marcheteau, S. Pernot, M. Nizard, A.-L. Pointet, S. Latreche, S. Bergaya, N. Benhamouda, C. Tanchot, C. Stockmann, P. Combe, A. Berger, F. Zinzindohoue, H. Yagita, E. Tartour, J. Taieb, and M. Terme, "VEGF-A modulates expression of inhibitory checkpoints on CD8+ T cells in tumors", Journal of Experimental Medicine **212**, 139–148 (2015).

[202] A. Palazon, P. A. Tyrakis, D. Macias, P. Veliça, H. Rundqvist, S. Fitzpatrick, N. Vojnovic, A. T. Phan, N. Loman, I. Hedenfalk, T. Hatschek, J. Lövrot, T. Foukakis, A. W. Goldrath, J. Bergh, and R. S. Johnson, "An HIF-1α/VEGF-A Axis in Cytotoxic T Cells Regulates Tumor Progression.", Cancer cell **32**, 669–683.e5 (2017).

[203] D. A. Thomas, and J. Massagué, "TGF-beta directly targets cytotoxic T cell functions during tumor evasion of immune surveillance.", Cancer Cell **8**, 369–380 (2005).

[204] W. Hansen, M. Hutzler, S. Abel, C. Alter, C. Stockmann, S. Kliche, J. Albert, T. Sparwasser, S. Sakaguchi, A. M. Westendorf, D. Schadendorf, J. Buer, and I. Helfrich, "Neuropilin 1 deficiency on CD4+Foxp3+ regulatory T cells impairs mouse melanoma growth.", J. Exp. Med. **209**, 2001–2016 (2012).

[205] S. Roy, A. K. Bag, R. K. Singh, J. E. Talmadge, S. K. Batra, and K. Datta, "Multifaceted Role of Neuropilins in the Immune System: Potential Targets for Immunotherapy.", Front Immunol **8**, 1228 (2017).

[206] J. M. Weiss, A. M. Bilate, M. Gobert, Y. Ding, M. A. Curotto de Lafaille, C. N. Parkhurst, H. Xiong, J. Dolpady, A. B. Frey, M. G. Ruocco, Y. Yang, S. Floess, J. Huehn, S. Oh, M. O. Li, R. E. Niec, A. Y. Rudensky, M. L. Dustin, D. R. Littman, and J. J. Lafaille, "Neuropilin 1 is expressed on thymus-derived natural regulatory T cells, but not mucosa-generated induced Foxp3+ T reg cells.", J. Exp. Med. **209**, 1723–42–S1 (2012).

[207] S. R. Jackson, M. Berrien-Elliott, J. Yuan, E. C. Hsueh, and R. M. Teague, "Neuropilin-1 expression is induced on tolerant self-reactive CD8+ T cells but is dispensable for the tolerant phenotype.", PloS one **9**, e110707 (2014).

[208] M. Wallerius, T. Wallmann, M. Bartish, J. Östling, A. Mezheyeuski, N. P. Tobin, E. Nygren, P. Pangigadde, P. Pellegrini, M. L. Squadrito, F. Pontén, J. Hartman, J. Bergh, A. De Milito, M. De Palma, A. Östman, J. Andersson, and C. Rolny, "Guidance Molecule SEMA3A Restricts Tumor Growth by Differentially Regulating the Proliferation of Tumor-Associated Macrophages.", Cancer Res. **76**, 3166–3178 (2016).

[209] A. Catalano, P. Caprari, S. Moretti, M. Faronato, L. Tamagnone, and A. Procopio, "Semaphorin-3A is expressed by tumor cells and alters T-cell signal transduction and function.", Blood **107**, 3321–3329 (2006).

[210] Y. Lepelletier, I. C. Moura, R. Hadj-Slimane, A. Renand, S. Fiorentino, C. Baude, A. Shirvan, A. Barzilai, and O. Hermine, "Immunosuppressive role of semaphorin-

3A on T cell proliferation is mediated by inhibition of actin cytoskeleton reorganization.", European journal of immunology **36**, 1782–1793 (2006).

[211] M. Yamamoto, K. Suzuki, T. Okuno, T. Ogata, N. Takegahara, H. Takamatsu, M. Mizui, M. Taniguchi, A. Chédotal, F. Suto, H. Fujisawa, A. Kumanogoh, and H. Kikutani, "Plexin-A4 negatively regulates T lymphocyte responses.", International immunology **20**, 413–420 (2008).

[212] B. D. Solomon, C. Mueller, W.-J. Chae, L. M. Alabanza, and M. S. Bynoe, "Neuropilin-1 attenuates autoreactivity in experimental autoimmune encephalomyelitis.", Proceedings of the National Academy of Sciences of the United States of America **108**, 2040–2045 (2011).

[213] D. J. Puleston, H. Zhang, T. J. Powell, E. Lipina, S. Sims, I. Panse, A. S. Watson, V. Cerundolo, A. R. Townsend, P. Klenerman, and A. K. Simon, "Autophagy is a critical regulator of memory CD8(+) T cell formation.", Elife **3**, 2516 (2014).

[214] Y. Lepelletier, S. Smaniotto, R. Hadj-Slimane, D. M. S. Villa-Verde, A. C. Nogueira, M. Dardenne, O. Hermine, and W. Savino, "Control of human thymocyte migration by Neuropilin-1/Semaphorin-3A-mediated interactions.", Proceedings of the National Academy of Sciences **104**, 5545–5550 (2007).

[215] Y. Ueda, N. Kondo, M. Ozawa, K. Yasuda, T. Tomiyama, and T. Kinashi, "Sema3e/Plexin D1 Modulates Immunological Synapse and Migration of Thymocytes by Rap1 Inhibition.", Journal of immunology (Baltimore, Md. : 1950) **196**, 3019–3031 (2016).

[216] L. Gattinoni, X.-S. Zhong, D. C. Palmer, Y. Ji, C. S. Hinrichs, Z. Yu, C. Wrzesinski, A. Boni, L. Cassard, L. M. Garvin, C. M. Paulos, P. Muranski, and N. P. Restifo,

"Wnt signaling arrests effector T cell differentiation and generates CD8+ memory stem cells.", Nature Medicine **15**, 808–813 (2009).

[217] T. J. Powell, J. D. Silk, J. Sharps, E. Fodor, and A. R. M. Townsend, "Pseudotyped influenza A virus as a vaccine for the induction of heterotypic immunity.", Journal of virology **86**, 13397–13406 (2012).

[218] A. R. Townsend, A. J. McMichael, N. P. Carter, J. A. Huddleston, and G. G. Brownlee, "Cytotoxic T cell recognition of the influenza nucleoprotein and hemagglutinin expressed in transfected mouse L cells.", Cell **39**, 13–25 (1984).

[219] M. Z. Noman, B. Janji, B. Kamińska, K. Van Moer, S. Pierson, P. Przanowski, S. Buart, G. Berchem, P. Romero, F. Mami-Chouaib, and S. Chouaib, "Blocking hypoxia-induced autophagy in tumors restores cytotoxic T-cell activity and promotes regression.", Cancer Res. **71**, 5976–5986 (2011).

[220] C. Kudo-Saito, H. Shirako, T. Takeuchi, and Y. Kawakami, "Cancer Metastasis Is Accelerated through Immunosuppression during Snail-Induced EMT of Cancer Cells", Cancer cell **15**, 195–206 (2009).

[221] L. M. Acevedo, J. Desgrosellier, and D. A. Cheresh, "Abstract 1474: Semaphorin 3A potentiates metastatic disease by binding to endothelial Neuropilin-1 and disrupting vascular barrier function", Cancer Res. **71**, 1474–1474 (2011).

[222] L. Bellelli, M. L. Sezzi, A. Tirabassi, and F. Ippoliti, "Immunogenicity of Lewis lung carcinoma in C57BL/6 mice. I. Tumor-associated antigen(s) in peripheral blood, thymus and spleen of tumor-bearing mice.", Tumori **68**, 373–380 (1982).

[223] J. C. Castle, S. Kreiter, J. Diekmann, M. Löwer, N. van de Roemer, J. de Graaf, A. Selmi, M. Diken, S. Boegel, C. Paret, M. Koslowski, A. N. Kuhn, C. M. Britten, C. Huber, O. Türeci, and U. Sahin, "Exploiting the mutanome for tumor vaccination.", Cancer Res. **72**, 1081–1091 (2012).

[224] L. R. Shiow, D. B. Rosen, N. Brdicková, Y. Xu, J. An, L. L. Lanier, J. G. Cyster, and M. Matloubian, "CD69 acts downstream of interferon-alpha/beta to inhibit S1P1 and lymphocyte egress from lymphoid organs.", Nature **440**, 540–544 (2006).

[225] J.-D. Ji, K.-H. Park-Min, and L. B. Ivashkiv, "Expression and function of semaphorin 3A and its receptors in human monocyte-derived macrophages", Human Immunology **70**, 211–217 (2009).

[226] Z. Vadasz, T. Rainis, A. Nakhleh, T. Haj, J. Bejar, K. Halasz, and E. Toubi, "The Involvement of Immune Semaphorins in the Pathogenesis of Inflammatory Bowel Diseases (IBDs).", PloS one **10**, e0125860 (2015).

[227] A. Riedel, D. Shorthouse, L. Haas, B. A. Hall, and J. Shields, "Tumor-induced stromal reprogramming drives lymph node transformation.", Nat. Immunol. **17**, 1118–1127 (2016).

[228] G. Serini, D. Valdembri, S. Zanivan, G. Morterra, C. Burkhardt, F. Caccavari, L. Zammataro, L. Primo, L. Tamagnone, M. Logan, M. Tessier-Lavigne, M. Taniguchi, A. W. Püschel, and F. Bussolino, "Class 3 semaphorins control vascular morphogenesis by inhibiting integrin function.", Nature **424**, 391–397 (2003).

[229] F. Maione, F. Molla, C. Meda, R. Latini, L. Zentilin, M. Giacca, G. Seano, G. Serini, F. Bussolino, and E. Giraudo, "Semaphorin 3A is an endogenous angiogenesis in-

hibitor that blocks tumor growth and normalizes tumor vasculature in transgenic mouse models.", J. Clin. Invest. **119**, 3356–3372 (2009).

[230] S. T. Hou, L. Nilchi, X. Li, S. Gangaraju, S. X. Jiang, A. Aylsworth, R. Monette, and J. Slinn, "Semaphorin3A elevates vascular permeability and contributes to cerebral ischemia-induced brain damage.", Scientific reports **5**, 7890 (2015).

[231] L. M. Acevedo, S. Barillas, S. M. Weis, J. R. Göthert, and D. A. Cheresh, "Semaphorin 3A suppresses VEGF-mediated angiogenesis yet acts as a vascular permeability factor.", Blood **111**, 2674–2680 (2008).

[232] J. Hamzah, M. Jugold, F. Kiessling, P. Rigby, M. Manzur, H. H. Marti, T. Rabie, S. Kaden, H.-J. Gröne, G. J. Hammerling, B. Arnold, and R. Ganss, "Vascular normalization in Rgs5-deficient tumours promotes immune destruction.", Nature **453**, 410–414 (2008).

[233] A. Calcinotto, M. Grioni, E. Jachetti, F. Curnis, A. Mondino, G. Parmiani, A. Corti, and M. Bellone, "Targeting TNF-α to neoangiogenic vessels enhances lymphocyte infiltration in tumors and increases the therapeutic potential of immunotherapy.", Journal of immunology (Baltimore, Md. : 1950) **188**, 2687–2694 (2012).

[234] H. Ghandour, X. Cullere, A. Alvarez, F. W. Luscinskas, and T. N. Mayadas, "Essential role for Rap1 GTPase and its guanine exchange factor CalDAG-GEFI in LFA-1 but not VLA-4 integrin mediated human T-cell adhesion.", Blood **110**, 3682–3690 (2007).

[235] T. A. Springer, and M. L. Dustin, "Integrin inside-out signaling and the immunological synapse", Current opinion in cell biology **24**, 107–115 (2012).

[236] K. M. T. de Bruyn, S. Rangarajan, K. A. Reedquist, C. G. Figdor, and J. L. Bos, "The small GTPase Rap1 is required for Mn(2+)- and antibody-induced LFA-1- and VLA-4-mediated cell adhesion.", The Journal of Biological Chemistry **277**, 29468–29476 (2002).

[237] K. Katagiri, A. Maeda, M. Shimonaka, and T. Kinashi, "RAPL, a Rap1-binding molecule that mediates Rap1-induced adhesion through spatial regulation of LFA-1", Nat. Immunol. **4**, 741–748 (2003).

[238] M. Corredor, R. Bonet, A. Moure, C. Domingo, J. Bujons, I. Alfonso, Y. Pérez, and À. Messeguer, "Cationic Peptides and Peptidomimetics Bind Glycosaminoglycans as Potential Sema3A Pathway Inhibitors.", Biophysical journal **110**, 1291–1303 (2016).

[239] J. A. Brown, R. B. Wysolmerski, and P. C. Bridgman, "Dorsal root ganglion neurons react to semaphorin 3A application through a biphasic response that requires multiple myosin II isoforms.", Molecular biology of the cell **20**, 1167–1179 (2009).

[240] M. Shimonaka, K. Katagiri, T. Nakayama, N. Fujita, T. Tsuruo, O. Yoshie, and T. Kinashi, "Rap1 translates chemokine signals to integrin activation, cell polarization, and motility across vascular endothelium under flow", The Journal of cell biology **161**, 417–427 (2003).

[241] A. Gérard, A. E. E. Mertens, R. A. van der Kammen, and J. G. Collard, "The Par polarity complex regulates Rap1- and chemokine-induced T cell polarization.", The Journal of cell biology **176**, 863–875 (2007).

[242] T. J. Jeon, D.-J. Lee, S. Merlot, G. Weeks, and R. A. Firtel, “Rap1 controls cell adhesion and cell motility through the regulation of myosin II.”, The Journal of cell biology **176**, 1021–1033 (2007).

[243] X. Liu, E. S. Welf, and J. M. Haugh, “Linking morphodynamics and directional persistence of T lymphocyte migration.”, Journal of the Royal Society, Interface / the Royal Society **12**, 20141412–20141412 (2015).

[244] T. H. Harris, E. J. Banigan, D. A. Christian, C. Konradt, E. D. Tait Wojno, K. Norose, E. H. Wilson, B. John, W. Weninger, A. D. Luster, A. J. Liu, and C. A. Hunter, “Generalized Lévy walks and the role of chemokines in migration of effector CD8+ T cells.”, Nature **486**, 545–548 (2012).

[245] H. N. Mayrovitz, “Skin capillary metrics and hemodynamics in the hairless mouse”, Microvascular research **43**, 46–59 (1992).

[246] H. Harlin, Y. Meng, A. C. Peterson, Y. Zha, M. Tretiakova, C. Slingluff, M. McKee, and T. F. Gajewski, “Chemokine Expression in Melanoma Metastases Associated with CD8+ T-Cell Recruitment”, Cancer Res. **69**, 3077–3085 (2009).

[247] D. Peng, I. Kryczek, N. Nagarsheth, L. Zhao, S. Wei, W. Wang, Y. Sun, E. Zhao, L. Vatan, W. Szeliga, J. Kotarski, R. Tarkowski, Y. Dou, K. Cho, S. Hensley-Alford, A. Munkarah, R. Liu, and W. Zou, “Epigenetic silencing of TH1-type chemokines shapes tumour immunity and immunotherapy.”, Nature **527**, 249–253 (2015).

[248] A. Casazza, D. Laoui, M. Wenes, S. Rizzolio, N. Bassani, M. Mambretti, S. Deschoemaeker, J. A. Van Ginderachter, L. Tamagnone, and M. Mazzone, “Impeding macrophage entry into hypoxic tumor areas by Sema3A/Nrp1 signaling blockade

inhibits angiogenesis and restores antitumor immunity.", Cancer Cell **24**, 695–709 (2013).

[249] P. Vincent, Y. Collette, R. Marignier, C. Vuaillat, V. Rogemond, N. Davoust, C. Malcus, S. Cavagna, A. Gessain, I. Machuca-Gayet, M.-F. Belin, T. Quach, and P. Giraudon, "A role for the neuronal protein collapsin response mediator protein 2 in T lymphocyte polarization and migration.", Journal of immunology (Baltimore, Md. : 1950) **175**, 7650–7660 (2005).

[250] H. Movassagh, A. Saati, S. Nandagopal, A. Mohammed, N. Tatari, L. Shan, J. S. Duke-Cohan, K. R. Fowke, F. Lin, and A. S. Gounni, "Chemorepellent Semaphorin 3E Negatively Regulates Neutrophil Migration In Vitro and In Vivo.", Journal of immunology (Baltimore, Md. : 1950) **198**, 1023–1033 (2016).

[251] H. Takamatsu, N. Takegahara, Y. Nakagawa, M. Tomura, M. Taniguchi, R. H. Friedel, H. Rayburn, M. Tessier-Lavigne, Y. Yoshida, T. Okuno, M. Mizui, S. Kang, S. Nojima, T. Tsujimura, Y. Nakatsuji, I. Katayama, T. Toyofuku, H. Kikutani, and A. Kumanogoh, "Semaphorins guide the entry of dendritic cells into the lymphatics by activating myosin II.", Nat. Immunol. **11**, 594–600 (2010).

[252] S. Curreli, B. S. Wong, O. Latinovic, K. Konstantopoulos, and N. M. Stamatos, "Class 3 semaphorins induce F-actin reorganization in human dendritic cells: Role in cell migration", Journal of leukocyte biology **100**, 1323–1334 (2016).

[253] E. Cai, K. Marchuk, P. Beemiller, C. Beppler, M. G. Rubashkin, V. M. Weaver, A. Gérard, T.-L. Liu, B.-C. Chen, E. Betzig, F. Bartumeus, and M. F. Krummel, "Visualizing dynamic microvillar search and stabilization during ligand detection by T cells.", Science **356**, eaal3118 (2017).

[254] K. C. Garcia, M. Degano, R. L. Stanfield, A. Brunmark, M. R. Jackson, P. A. Peterson, L. Teyton, and I. A. Wilson, "An alphabeta T cell receptor structure at 2.5 A and its orientation in the TCR-MHC complex.", Science **274**, 209–219 (1996).

[255] K. Choudhuri, M. Parker, A. Milicic, D. K. Cole, M. K. Shaw, A. K. Sewell, G. Stewart-Jones, T. Dong, K. G. Gould, and P. A. van der Merwe, "Peptide-major histocompatibility complex dimensions control proximal kinase-phosphatase balance during T cell activation.", The Journal of Biological Chemistry **284**, 26096–26105 (2009).

[256] P. T. Sage, L. M. Varghese, R. Martinelli, T. E. Sciuto, M. Kamei, A. M. Dvorak, T. A. Springer, A. H. Sharpe, and C. V. Carman, "Antigen Recognition Is Facilitated by Invadosome-like Protrusions Formed by Memory/Effector T Cells", The Journal of Immunology **188**, 1102594–3699 (2012).

[257] V. T. Chang, R. A. Fernandes, K. A. Ganzinger, S. F. Lee, C. Siebold, J. McColl, P. Jönsson, M. Palayret, K. Harlos, C. H. Coles, E. Y. Jones, Y. Lui, E. Huang, R. J. C. Gilbert, D. Klenerman, A. R. Aricescu, and S. J. Davis, "Initiation of T cell signaling by CD45 segregation at 'close contacts'.", Nat. Immunol. **17**, 574–582 (2016).

[258] P. A. van der Merwe, and O. Dushek, "Mechanisms for T cell receptor triggering.", Nat Rev Immunol **11**, 47–55 (2011).

[259] C. R. Monks, B. A. Freiberg, H. Kupfer, N. Sciaky, and A. Kupfer, "Three-dimensional segregation of supramolecular activation clusters in T cells.", Nature **395**, 82–86 (1998).

[260] A. Grakoui, S. K. Bromley, C. Sumen, M. M. Davis, A. S. Shaw, P. M. Allen, and M. L. Dustin, "The immunological synapse: a molecular machine controlling T cell activation.", Science **285**, 221–227 (1999).

[261] A. T. Ritter, Y. Asano, J. C. Stinchcombe, N. M. G. Dieckmann, B.-C. Chen, C. Gawden-Bone, S. van Engelenburg, W. Legant, L. Gao, M. W. Davidson, E. Betzig, J. Lippincott-Schwartz, and G. M. Griffiths, "Actin Depletion Initiates Events Leading to Granule Secretion at the Immunological Synapse", Immunity **42**, 864–876 (2015).

[262] B.-R. Na, H.-R. Kim, I. Piragyte, H.-M. Oh, M.-S. Kwon, U. Akber, H.-S. Lee, D.-S. Park, W. K. Song, Z.-Y. Park, S.-H. Im, M.-C. Rho, Y.-M. Hyun, M. Kim, and C.-D. Jun, "TAGLN2 regulates T cell activation by stabilizing the actin cytoskeleton at the immunological synapse", The Journal of cell biology **209**, 143–162 (2015).

[263] M. Fritzsche, R. A. Fernandes, V. T. Chang, H. Colin-York, M. P. Clausen, J. H. Felce, S. Galiani, C. Erlenkämper, A. M. Santos, J. M. Heddleston, I. Pedroza-Pacheco, D. Waithe, J. B. de la Serna, B. C. Lagerholm, T.-L. Liu, T.-L. Chew, E. Betzig, S. J. Davis, and C. Eggeling, "Cytoskeletal actin dynamics shape a ramifying actin network underpinning immunological synapse formation.", Science advances **3**, e1603032 (2017).

[264] W. A. Comrie, A. Babich, and J. K. Burkhardt, "F-actin flow drives affinity maturation and spatial organization of LFA-1 at the immunological synapse.", The Journal of cell biology **208**, 475–491 (2015).

[265] A. T. Ritter, S. M. Kapnick, S. Murugesan, P. L. Schwartzberg, G. M. Griffiths, and J. Lippincott-Schwartz, "Cortical actin recovery at the immunological synapse

leads to termination of lytic granule secretion in cytotoxic T lymphocytes.", Proceedings of the National Academy of Sciences of the United States of America **114**, E6585–E6594 (2017).

[266] A. F. Carisey, E. M. Mace, M. B. Saeed, D. M. Davis, and J. S. Orange, "Nanoscale Dynamism of Actin Enables Secretory Function in Cytolytic Cells", Current Biology (2018).

[267] B. A. Freiberg, H. Kupfer, W. Maslanik, J. Delli, J. Kappler, D. M. Zaller, and A. Kupfer, "Staging and resetting T cell activation in SMACs.", Nature immunology **3**, 911–917 (2002).

[268] M. L. Dustin, "Cell adhesion molecules and actin cytoskeleton at immune synapses and kinapses", Current opinion in cell biology **19**, 529–533 (2007).

[269] Y. Yu, N. C. Fay, A. A. Smoligovets, H.-J. Wu, and J. T. Groves, "Myosin IIA Modulates T Cell Receptor Transport and CasL Phosphorylation during Early Immunological Synapse Formation", PloS one **7**, e30704 (2012).

[270] R. Varma, G. Campi, T. Yokosuka, T. Saito, and M. L. Dustin, "T Cell Receptor-Proximal Signals Are Sustained in Peripheral Microclusters and Terminated in the Central Supramolecular Activation Cluster", Immunity **25**, 117–127 (2006).

[271] J. A. Hammer, and J. K. Burkhardt, "Controversy and consensus regarding myosin II function at the immunological synapse.", Current opinion in immunology **25**, 300–306 (2013).

[272] J. Yi, X. S. Wu, T. Crites, and J. A. Hammer, "Actin retrograde flow and actomyosin II arc contraction drive receptor cluster dynamics at the immunological synapse in Jurkat T cells.", Molecular biology of the cell **23**, 834–852 (2012).

[273] S. Murugesan, J. Hong, J. Yi, D. Li, J. R. Beach, L. Shao, J. Meinhardt, G. Madison, X. Wu, E. Betzig, and J. A. Hammer, "Formin-generated actomyosin arcs propel T cell receptor microcluster movement at the immune synapse.", The Journal of cell biology **215**, 383–399 (2016).

[274] J. Jacobelli, S. A. Chmura, D. B. Buxton, M. M. Davis, and M. F. Krummel, "A single class II myosin modulates T cell motility and stopping, but not synapse formation.", Nature immunology **5**, 531–538 (2004).

[275] J. Hong, S. Murugesan, E. Betzig, and J. A. Hammer, "Contractile actomyosin arcs promote the activation of primary mouse T cells in a ligand-dependent manner.", PloS one **12**, e0183174 (2017).

[276] M. Murrell, P. W. Oakes, M. Lenz, and M. L. Gardel, "Forcing cells into shape: the mechanics of actomyosin contractility.", Nature Reviews Molecular Cell Biology **16**, 486–498 (2015).

[277] A. Catalano, "The Neuroimmune Semaphorin-3A Reduces Inflammation and Progression of Experimental Autoimmune Arthritis", Journal of immunology (Baltimore, Md. : 1950) **185**, 6373–6383 (2010).

[278] K. Katagiri, M. Shimonaka, and T. Kinashi, "Rap1-mediated lymphocyte function-associated antigen-1 activation by the T cell antigen receptor is dependent on phospholipase C-gamma1.", The Journal of Biological Chemistry **279**, 11875–11881 (2004).

[279] T. Takahashi, A. Fournier, F. Nakamura, L.-H. Wang, Y. Murakami, R. G. Kalb, H. Fujisawa, and S. M. Strittmatter, "Plexin-Neuropilin-1 Complexes Form Functional Semaphorin-3A Receptors", Cell **99**, 59–69 (1999).

[280] J. A. Brown, and P. C. Bridgman, "Disruption of the cytoskeleton during Semaphorin 3A induced growth cone collapse correlates with differences in actin organization and associated binding proteins", Developmental Neurobiology **69**, 633–646 (2009).

[281] E. W. Dent, A. M. Barnes, F. Tang, and K. Kalil, "Netrin-1 and Semaphorin 3A Promote or Inhibit Cortical Axon Branching, Respectively, by Reorganization of the Cytoskeleton", The Journal of neuroscience : the official journal of the Society for Neuroscience **24**, 3002–3012 (2004).

[282] J. Xu, J. F. Casella, and T. D. Pollard, "Effect of capping protein, CapZ, on the length of actin filaments and mechanical properties of actin filament networks.", Cell motility and the cytoskeleton **42**, 73–81 (1999).

[283] M. R. Bubb, I. Spector, B. B. Beyer, and K. M. Fosen, "Effects of jasplakinolide on the kinetics of actin polymerization. An explanation for certain in vivo observations.", The Journal of Biological Chemistry **275**, 5163–5170 (2000).

[284] A. J. Ridley, M. A. Schwartz, K. Burridge, R. A. Firtel, M. H. Ginsberg, G. Borisy, J. T. Parsons, and A. R. Horwitz, "Cell migration: integrating signals from front to back.", Science **302**, 1704–1709 (2003).

[285] M. Smutny, H. L. Cox, J. M. Leerberg, E. M. Kovacs, M. A. Conti, C. Ferguson, N. A. Hamilton, R. G. Parton, R. S. Adelstein, and A. S. Yap, "Myosin II isoforms

identify distinct functional modules that support integrity of the epithelial zonula adherens.", Nature Cell Biology **12**, 696–702 (2010).

[286] K. Ando, S. Fukuhara, T. Moriya, Y. Obara, N. Nakahata, and N. Mochizuki, "Rap1 potentiates endothelial cell junctions by spatially controlling myosin II activity and actin organization.", The Journal of cell biology **202**, 901–916 (2013).

[287] J. S. Allingham, R. Smith, and I. Rayment, "The structural basis of blebbistatin inhibition and specificity for myosin II.", Nature structural & molecular biology **12**, 378–379 (2005).

[288] A. Smith, Y. R. Carrasco, P. Stanley, N. Kieffer, F. D. Batista, and N. Hogg, "A talin-dependent LFA-1 focal zone is formed by rapidly migrating T lymphocytes", The Journal of cell biology **170**, 141–151 (2005).

[289] G. Gallo, "RhoA-kinase coordinates F-actin organization and myosin II activity during semaphorin-3A-induced axon retraction.", J Cell Sci **119**, 3413–3423 (2006).

[290] J. J. Hsieh, M. P. Purdue, S. Signoretti, C. Swanton, L. Albiges, M. Schmidinger, D. Y. Heng, J. Larkin, and V. Ficarra, "Renal cell carcinoma", Nature Reviews Disease Primers **3**, 17009 (2017).

[291] B. Escudier, A. Pluzanska, P. Koralewski, A. Ravaud, S. Bracarda, C. Szczylik, C. Chevreau, M. Filipek, B. Melichar, E. Bajetta, V. Gorbunova, J.-O. Bay, I. Bodrogi, A. Jagiello-Gruszfeld, N. Moore, and AVOREN Trial investigators, "Bevacizumab plus interferon alfa-2a for treatment of metastatic renal cell carcinoma: a randomised, double-blind phase III trial.", Lancet (London, England) **370**, 2103–2111 (2007).

[292] R. J. Motzer, B. Escudier, S. Oudard, T. E. Hutson, C. Porta, S. Bracarda, V. Grunwald, J. A. Thompson, R. A. Figlin, N. Hollaender, G. Urbanowitz, W. J. Berg, A. Kay, D. Lebwohl, A. Ravaud, and RECORD-1 Study Group, "Efficacy of everolimus in advanced renal cell carcinoma: a double-blind, randomised, placebo-controlled phase III trial.", Lancet (London, England) **372**, 449–456 (2008).

[293] D. J. Martini, L. Hamieh, R. R. McKay, L. C. Harshman, R. Brandao, C. K. Norton, J. A. Steinharter, K. M. Krajewski, X. Gao, F. A. Schutz, B. McGregor, D. Bossé, A.-K. A. Lalani, G. de Velasco, M. D. Michaelson, D. F. McDermott, and T. K. Choueiri, "Durable Clinical Benefit in Metastatic Renal Cell Carcinoma Patients Who Discontinue PD-1/PD-L1 Therapy for Immune-Related Adverse Events.", Cancer immunology research **6**, 402–408 (2018).

[294] Y. Şenbabaoğlu, R. S. Gejman, A. G. Winer, M. Liu, E. M. Van Allen, G. de Velasco, D. Miao, I. Ostrovnaya, E. Drill, A. Luna, N. Weinhold, W. Lee, B. J. Manley, D. N. Khalil, S. D. Kaffenberger, Y. Chen, L. Danilova, M. H. Voss, J. A. Coleman, P. Russo, V. E. Reuter, T. A. Chan, E. H. Cheng, D. A. Scheinberg, M. O. Li, T. K. Choueiri, J. J. Hsieh, C. Sander, and A. A. Hakimi, "Tumor immune microenvironment characterization in clear cell renal cell carcinoma identifies prognostic and immunotherapeutically relevant messenger RNA signatures.", Genome biology **17**, 231 (2016).

[295] D. F. McDermott, M. M. Regan, J. I. Clark, L. E. Flaherty, G. R. Weiss, T. F. Logan, J. M. Kirkwood, M. S. Gordon, J. A. Sosman, M. S. Ernstoff, C. P. G. Tretter, W. J. Urba, J. W. Smith, K. A. Margolin, J. W. Mier, J. A. Gollob, J. P. Dutcher, and M. B. Atkins, "Randomized phase III trial of high-dose interleukin-2 versus

subcutaneous interleukin-2 and interferon in patients with metastatic renal cell carcinoma.", Journal of Clinical Oncology **23**, 133–141 (2005).

[296] R. J. Motzer, B. Escudier, D. F. McDermott, S. George, H. J. Hammers, S. Srinivas, S. S. Tykodi, J. A. Sosman, G. Procopio, E. R. Plimack, D. Castellano, T. K. Choueiri, H. Gurney, F. Donskov, P. Bono, J. Wagstaff, T. C. Gauler, T. Ueda, Y. Tomita, F. A. Schutz, C. Kollmannsberger, J. Larkin, A. Ravaud, J. S. Simon, L.-A. Xu, I. M. Waxman, and P. Sharma, "Nivolumab versus Everolimus in Advanced Renal-Cell Carcinoma", ezproxy-prd.bodleian.ox.ac.uk **373**, 1803–1813 (2015).

[297] R. J. Motzer, N. M. Tannir, D. F. McDermott, O. Arén Frontera, B. Melichar, T. K. Choueiri, E. R. Plimack, P. Barthélémy, C. Porta, S. George, T. Powles, F. Donskov, V. Neiman, C. K. Kollmannsberger, P. Salman, H. Gurney, R. Hawkins, A. Ravaud, M.-O. Grimm, S. Bracarda, C. H. Barrios, Y. Tomita, D. Castellano, B. I. Rini, A. C. Chen, S. Mekan, M. B. McHenry, M. Wind-Rotolo, J. Doan, P. Sharma, H. J. Hammers, B. Escudier, and CheckMate 214 Investigators, "Nivolumab plus Ipilimumab versus Sunitinib in Advanced Renal-Cell Carcinoma.", The New England journal of medicine **378**, 1277–1290 (2018).

[298] D. F. McDermott, M. A. Huseni, M. B. Atkins, R. J. Motzer, B. I. Rini, B. Escudier, L. Fong, R. W. Joseph, S. K. Pal, J. A. Reeves, M. Sznol, J. Hainsworth, W. K. Rathmell, W. M. Stadler, T. Hutson, M. E. Gore, A. Ravaud, S. Bracarda, C. Suárez, R. Danielli, V. Gruenwald, T. K. Choueiri, D. Nickles, S. Jhunjhunwala, E. Piault-Louis, A. Thobhani, J. Qiu, D. S. Chen, P. S. Hegde, C. Schiff, G. D. Fine, and T. Powles, "Clinical activity and molecular correlates of response to atezolizumab alone or in

combination with bevacizumab versus sunitinib in renal cell carcinoma.", Nature Medicine **24**, 749–757 (2018).

[299] T. K. Choueiri, J. Larkin, M. Oya, F. Thistlethwaite, M. Martignoni, P. Nathan, T. Powles, D. McDermott, P. B. Robbins, D. D. Chism, D. Cho, M. B. Atkins, M. S. Gordon, S. Gupta, H. Uemura, Y. Tomita, A. Compagnoni, C. Fowst, A. di Pietro, and B. I. Rini, "Preliminary results for avelumab plus axitinib as first-line therapy in patients with advanced clear-cell renal-cell carcinoma (JAVELIN Renal 100): an open-label, dose-finding and dose-expansion, phase 1b trial.", The Lancet. Oncology **19**, 451–460 (2018).

[300] J. D. Peske, A. B. Woods, and V. H. Engelhard, "Control of CD8 T-Cell Infiltration into Tumors by Vasculature and Microenvironment", Advances in cancer research **128**, 263–307 (2015).

[301] H. Tran-Van, E. Avota, C. Börtlein, N. Mueller, and S. Schneider-Schaulies, "Measles virus modulates dendritic cell/T-cell communication at the level of plexinA1/neuropilin-1 recruitment and activity.", European journal of immunology **41**, 151–163 (2011).

[302] F. Myster, L. Palmeira, O. Sorel, F. Bouillenne, E. DePauw, I. Schwartz-Cornil, A. Vanderplasschen, and B. G. Dewals, "Viral semaphorin inhibits dendritic cell phagocytosis and migration but is not essential for gammaherpesvirus-induced lymphoproliferation in malignant catarrhal fever.", Journal of virology **89**, 3630–3647 (2015).

[303] D. Marzioni, L. Tamagnone, L. Capparuccia, C. Marchini, A. Amici, T. Todros, P. Bischof, S. Neidhart, G. Grenningloh, and M. Castellucci, "Restricted innervation

of uterus and placenta during pregnancy: evidence for a role of the repelling signal Semaphorin 3A.", Developmental dynamics : an official publication of the American Association of Anatomists **231**, 839–848 (2004).

[304] Y. Lazebnik, "Can a biologist fix a radio?–Or, what I learned while studying apoptosis.", Cancer Cell **2**, 179–182 (2002).

[305] L. Muhl, E. B. Folestad, H. Gladh, Y. Wang, C. Moessinger, L. Jakobsson, and U. Eriksson, "Neuropilin 1 binds PDGF-D and is a co-receptor in PDGF-D-PDGFRβ signaling.", Journal of Cell Science **130**, 1365–1378 (2017).

[306] Y. S. Michaels, M. B. Barnkob, H. Barbosa, T. A. Baeumler, M. K. Thompson, V. Andre, H. Colin-York, M. Fritzsche, U. Gileadi, H. M. Sheppard, D. J. Knapp, T. A. Milne, V. Cerundolo, and T. A. Fulga, "Precise tuning of gene expression output levels in mammalian cells", bioRxiv, 352377 (2018).